Thermal Energy Storage and Management in Water-based Trombe Walls

HARMEET SINGH

A THESIS SUBMITTED TO
THE FACULTY OF GRADUATE STUDIES
IN PARTIAL FULFILLMENT OF THE REQUIREMENTS
FOR THE DEGREE OF
MASTER OF SCIENCE

GRADUATE PROGRAM IN MECHANICAL ENGINEERING
YORK UNIVERSITY
TORONTO, ONTARIO

April 2022

ABSTRACT

Trombe walls use solar energy to reduce energy consumption in buildings. However, Trombe walls can cause overheating during summer. The objective of this thesis is to design aesthetically pleasing Trombe walls that use solar energy for space and water heating more effectively. The water-based Trombe wall design consists of a semi-transparent sheet that absorbs sunlight which is immersed in water. Results from performing simulations and lab-scale experiments show that water-based Trombe walls can reduce building heating loads to the same extent as conventional Trombe walls during winter months. Furthermore, to prevent overheating during summer, heated water extracted from the top of the Trombe wall can be used as pre-heated water and supplied to a hot water tank. Results show the Trombe walls designs proposed in this research can produce 3.5 times more than the amount of heated water required during summer in an average household in Toronto, Canada.

ACKNOWLEDGEMENTS

I would like to express my sincere gratitude and appreciation to my supervisor Prof. O'Brien for his invaluable assistance, dedicated involvement, and guidance. This research would have never been accomplished without his continuous support, motivation, and guidance in every step throughout my master's degree. I would also like to thank Prof. Cooper for providing invaluable inputs and comments as part of my Supervisory Committee. Further, I'm thankful towards Prof. Bashir for taking the time to serve on my Oral Examination Committee. Very special thanks to my fellow lab mates, especially Abdallah Alshantaf for helping and supporting in building the Trombe wall prototype in the lab. Last but not the least, I would like to thank my family for their unconditional love and support throughout the entire thesis process and every day.

TABLE OF CONTENTS

LIST OF TABLES

LIST OF FIGURES

LIST OF SYMBOLS

Symbol		Units	Symbol		Units
A	Area	m^2	ρ	Density	Kg/m^3
T	Time	s	λ	Conductivity	W/m·K
V	Volume	m^3	c_p	Specific heat	J/Kg·K
c	Speed of light	m/s	A_T	Thermal Absorptance (emissivity)	
T	Temperature	°C or K	A_V	Visible absorptance	
H	Planck's constant		A_S	Solar absorptance	
k_B	Boltzman's constant		v	Air velocity	m/s
λ	Wavelength	m	t_o	Operative temperature	
α_s	Solar radiation absorption		t_a	Air temperature	
$R(\lambda)$	Reflectance		t_r	Radiant temperature	
$A(\lambda)$	Absorptance		Δh	Phase change enthalpy	J/g °C
$T(\lambda)$	Transmittance		m	Mass	g or kg
Q	Heat stored in the material	J	ε_t	Thermal infrared radiation emission	
E_s	Total solar energy absorbed by the system		E_w	Total energy absorbed by the water	
E_a	Energy carried by the air		T_M	Maximum temperature	°C
			η	Thermal efficiency	

LIST OF ACRONYMS

CIBSE	Chartered institution of building services engineers
CTF	Conduction transfer function
DHI	Diffuse horizontal irradiance
DNI	Direct normal irradiance
DOE-2	Design of experiments- version 2
DWVG	Delta winglet vortex generators
EC	Electrochromic
GHI	Global hemispherical radiation
HVAC	Heating, ventilation, and air conditioning
Ins	Insulation
IEA	International energy agency
IW	Inner wall
OW	Outer wall
PCM	Phase change material
PV	Photovoltaic
SHGC	Solar heat gain coefficient
TARP	Thermal analysis research program
TES	Thermal energy storage
Tg	Tinted glass
TIM	Translucent insulation material
TMY2	Typical Meteorological Year – 2nd edition
Wat	Water
WYEC2	Weather Year for Energy Calculation – Version 2

CHAPTER 1: INTRODUCTION

The residential sector is one of the key energy consumption sectors amongst all essential energy consumption sectors such as the transportation, industrial, and commercial sectors in most countries worldwide [1]. It has been observed that the residential sector alone attributes 13 % of energy consumption globally, and approximately 50 % of this energy is used in residential space heating [2].

According to the International Energy Agency (IEA), electricity and natural gas are two major energy sources responsible for approximately 50 % of the total global energy demand in the residential sector in 2018 [3]. The significant uses of energy in the residential sector are typically for space and water heating. As reported by the IEA, out of 32.7 EJ of residential energy consumption, globally, a total of 16.2 EJ (50 % of the total energy) is consumed just for space heating purposes [4]. The growing energy demands for space and water heating have resulted in 12 % of the CO_2 emissions worldwide due to the consumption of fossil fuels [5].

In Canada, the residential sector accounted for approximately 17 % of the total energy consumption in 2018 [6]. The primary sources of total energy consumption of approximately 1600 PJ per annum by Canadian households are natural gas, electricity, wood, and fuel oil (Figure 1.1). Natural gas accounts for 46 % and electricity accounts for 38 % of the total site energy consumption in Canada [6].

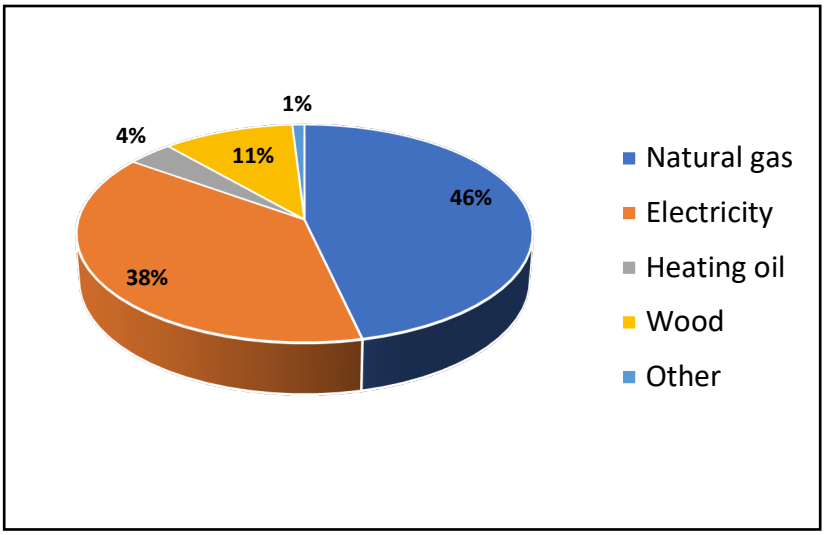

Figure 1.1. Energy consumption by energy sources for the residential sector in Canada (2018) [6]

There was a nearly 8% increase in the energy demand for the residential sector between 2000 and 2018 in Canada. [6] However, there may be slight variations across the regions. For example, electricity is the primary source of energy in Quebec and the Atlantic region, whereas natural gas accounts for the main energy consumption source in all other regions [7]. As reported by Natural Resources Canada in 2018, approximately 64% of energy consumption by end-use is utilized for space heating and 18% is used for water heating in the residential sector in Canada (Figure 1.2) [7]. The monthly demand profile of space and domestic hot water (DHW) heating for an average household during the winter season from September through May in Ontario is shown in Figure 1.3. [8]

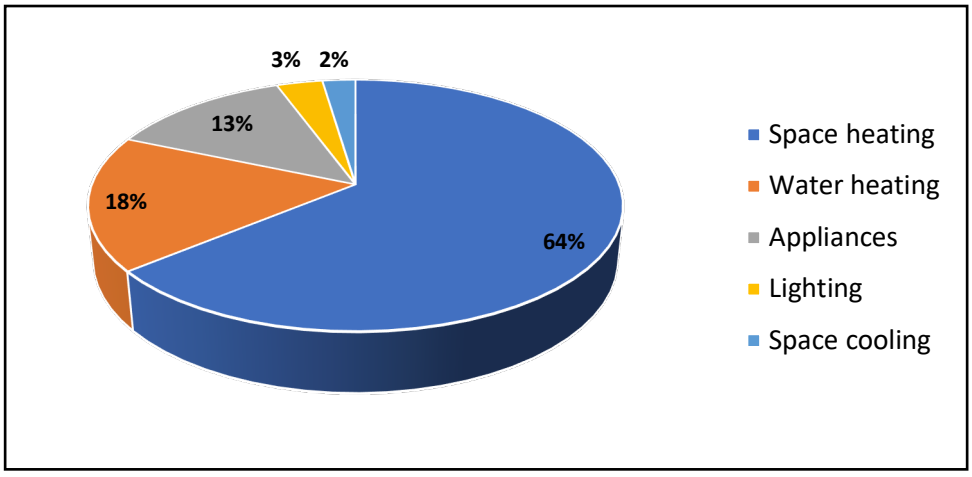

Figure 1.2. Energy consumption by end-use for the residential sector in Canada (2018) [6]

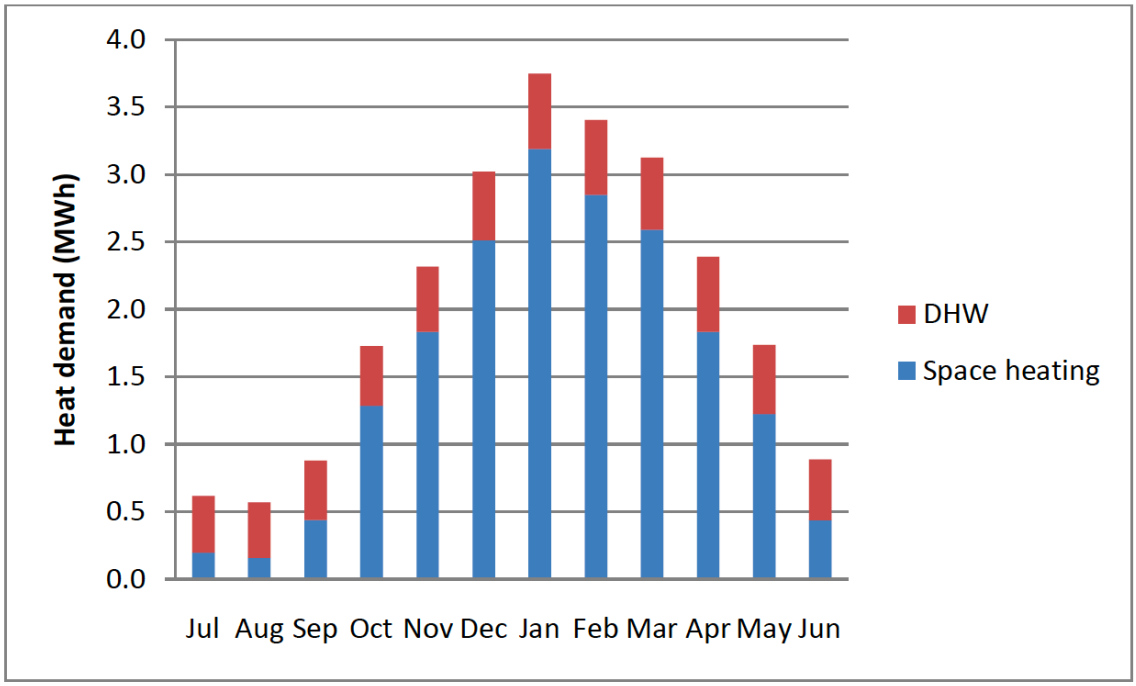

Figure 1.3. Monthly space heating and domestic hot water demand [8]

Since fossil fuels have been used as the primary energy source for space and water heating, they have resulted in ~43 Mt and ~13 Mt of CO_2 emissions in Canada, annually [9]. In Canada, the residential sector was responsible for producing 13 % of the total greenhouse gas emissions related to energy in 2017 [9]**.** This has had a negative impact on global warming, as it has been estimated that CO_2 emissions are responsible for about 80% of the total greenhouse effect in Canada [9]**.** It is desirable to replace fossil fuels with reliable, cost-effective, and renewable energy sources such as hydro, wind, or solar energy that can contribute to space and water heating energy demands to the greatest extent possible [10].

Hydro is the leading renewable energy source in Canada and accounts for 67.6% of electric power usage followed by solid biomass which accounts for approximately 23% of energy use as shown in Figure 1.4 [11]. Wind accounts for 5% of the renewable electricity generation in Canada. In 2017, the total wind power generated in Canada was approximately 29 TWh, and the total capacity of the Canadian industry is 12,817 MW. In 2018, Ontario had the most wind energy capacity with 5,076 MW of power, followed by Quebec with 3,882 MW of power [11].

Solar PV accounts for 0.6 % of the renewable electricity generation and solar thermal only accounts for 0.1 % of total renewable energy production, and is used for space heating, and other industrial processes. Most of the solar capacity in Canada is located in Ontario. In 2018, the capacity of the solar photovoltaic industry in Canada was 3,040 MW.[11]

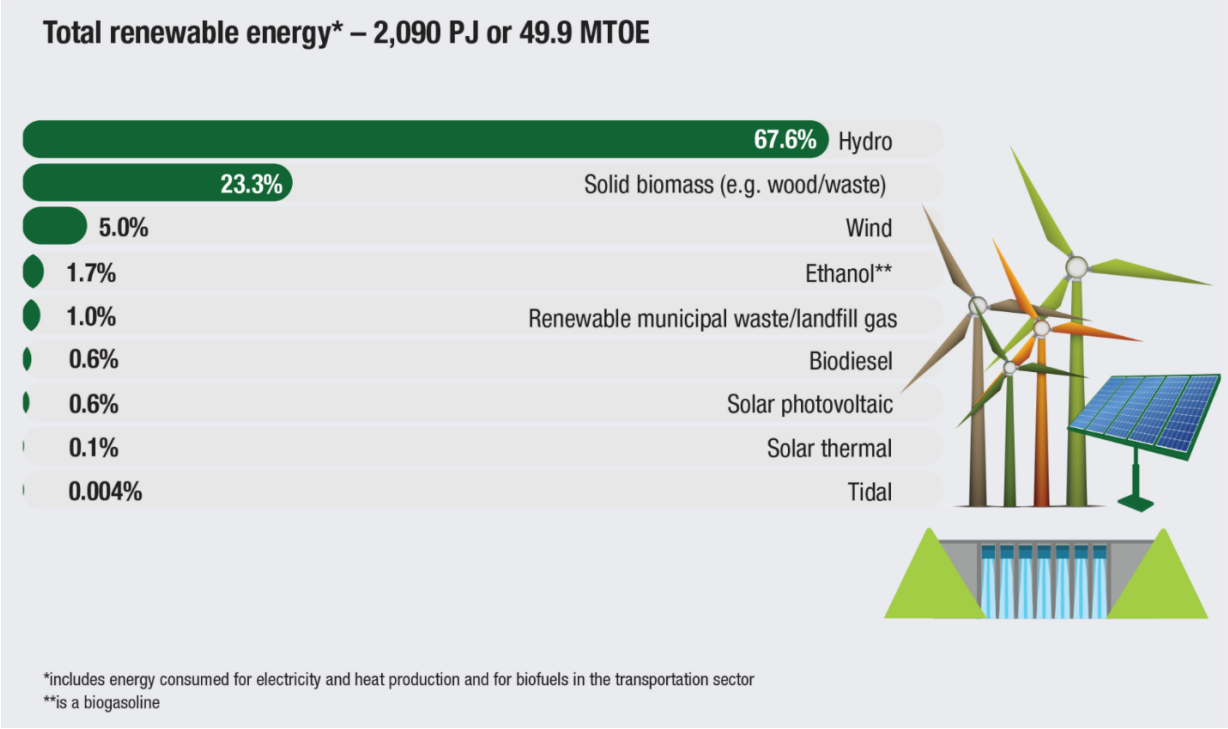

Figure 1.4. Renewable energy sources usage in Canada [11]

Solar thermal energy makes up only 0.1 % of the renewable energy in Canada, which is low, considering its potential. However, solar energy has increasingly been used to generate electricity and heat energy which also helps with reducing CO_2 emissions [12][13]. One of the main reasons for limited use of solar thermal energy is that the availability of solar energy does not optimally match the time profile for the heat demand in typical residential buildings.

For example, the hot water demand profile peaks during the morning hours between 6 - 7 am and during the evening around 6 – 7 pm [14]. Furthermore, it is estimated that the demand for hot water in the winter season is nearly 10% higher than in the summer season, and space heating is actively utilized from September through April [14]. In winter, the on-peak hours for space heating usage are between 6–8 am in the morning and after 5 pm in the evening [15]. However, most solar energy is only available during the later hours of the morning and the earlier hours of

the afternoon.[15]. On the other hand, with regards to Southern Ontario, the mean daily global insolation on a horizontal surface is about 1.5 kWh/m^2 and 5.5 kWh/m^2 during the winter and summer months, respectively [16]. Table 1.1 indicates the mean daily insolation during the summer and winter months on surfaces with different tilt angles in Southern Ontario.

Table 1.1 Mean daily global insolation in Ontario by month (kWh/m^2) [16]

Month	South-facing vertical (tilt=90 degrees)	South-facing (tilt=latitude+15 degrees)
January	2.89	3.01
February	3.66	4.03
March	3.71	4.59
April	3.09	4.61
May	2.72	4.59
June	2.6	4.69
July	2.69	4.78
August	2.94	4.68
September	3.16	4.35
October	3.17	3.82
November	2.31	2.54
December	2.26	2.35
Annual	2.93	4

To help mitigate CO_2 emissions, it is increasingly encouraged to integrate passive solar systems in residential buildings for sustainable development. It has been reported that passive solar systems may contribute to reducing up to 30 % of the heating demand in Toronto, Canada [17]. Several passive solar systems are being studied, nowadays, such as solar chimneys, solar roofs, and Trombe walls [18]. According to research conducted at the Solar Energy Research facility in Zion National Park Visitor Centre, U.S., Trombe walls equipped with a thermal storage medium can be efficiently used to meet approximately 30% of heating demands in buildings [19]. Trombe walls that store solar thermal energy also reduce the temporal mismatch between the availability of solar energy and the demand for heating in the residential sector.

Despite the promising potential to use Trombe walls to reduce energy consumption they have yet to be integrated into buildings on a large scale. This may be a result of the added costs during construction, the fact that Trombe walls can cause excess heating during warm weather conditions if not optimally operated, or an overall lack of awareness of the benefits that a Trombe wall can provide.

The research in this thesis is directed towards the design and development of Trombe walls that use water as a thermal energy storage medium. More specifically, the research question is to what extent the performance of a water Trombe wall can be improved by using the thermal energy stored within the water for other purposes within the building, such as for showering, washing clothes and dishes, and providing pre-heated water for the hot water tank. To date, little research has been done in this area. The objective of this thesis is to design water-based Trombe walls that achieve exceptionally high thermal efficiency. The ability to use the thermal energy stored in water for other applications in the building, especially during the summer months, is assessed. Furthermore, the goal is to perform simulations and experiments to demonstrate the enhanced performance of these water-based Trombe walls. The contents of this thesis are organized as follows:

In Chapter 2, the background of different types of Trombe walls and their thermal efficiency is discussed with focus on water-based Trombe walls. Prior to that, different kinds of solar systems such as active and passive, and thermal energy storage mediums are presented. At the end, the objective and an overview of the research conducted in this thesis is discussed.

Chapter 3 entails the detailed numerical and experimental methods employed to conduct the simulation analysis and experiments in the lab. A three-dimensional simulation base model of a novel water based Trombe wall is built using Design Builder software to investigate the performance of different Trombe wall configurations. The chapter first discusses the properties of materials and model configurations selected in the simulation analysis of different types of Trombe walls. It then explains in detail the experimental model of a Trombe wall prototype setup in the lab and different cases of Trombe walls model considered during experiments are specified.

Chapter 4 includes the results of simulation models and experimental models under summer and winter weather conditions. In the first section, the simulation results of different Trombe walls under winter and summer weather conditions are discussed followed by a comparison of water

walls with a total thickness of 20 cm under summer weather conditions. In the second section, the results of different cases of experimental model are presented and discussed. It also discusses the how thermal energy stored in water-based Trombe walls can be utilized in buildings during summer weather conditions.

Chapter 5 concludes the research work presented in this thesis and provides recommendations for future work.

CHAPTER 2: BACKGROUND

2.1. Solar energy

Solar energy from the sun is emitted to space in the form of visible and near-infrared light which is incident onto the Earth's surface to produce thermal energy or heat energy. It can be stored and converted to other forms of energy for use in various applications. Solar energy is a renewable source of energy and is pollution-free, whereas fossil fuels produce harmful greenhouse gases such as CO_2 [20][21]. The total amount of solar power reaching the top of Earth's surface is approximately 1.73 x 10^{17} W, and the total solar radiation energy received by Earth annually is about 5.46 x 10^{24} J. [22]

It has been reported that solar energy provides 17.3 x 10^4 TWh of energy to Earth in approximately 1 hour, which is more than seven times higher than the global energy demands for the residential sector in 2018 (i.e., 2.4 x 10^4 TWh) [4][5][23]. For instance, the world's annual energy demands can be met easily by building a solar thermal plant on 1% of the Sahara Desert [24]. The sun can be considered as a blackbody with an effective temperature of 5778 K.

Irradiance is expressed in W/m^2 which is defined as the rate at which radiant energy is incident per square meter of surface area [25][26][27]. The total irradiance on an inclined surface, G_i is calculated as:

$$G_i = G_{b,i} + G_{d,i} + G_{r,i} \quad \text{(2.1)}$$

where $G_{b,i}$ is the beam irradiance

$G_{d,i}$ is the diffuse irradiance

$G_{r,i}$ is the reflected irradiance

and, the beam irradiance on an inclined surface, $G_{b,i}$ can be calculated as:

$$G_{b,i} = G_b \frac{\cos\theta_i}{\sin\alpha_s} = R_b G_b \quad \text{(2.2)}$$

where G_b is the horizontal beam irradiance

θ_i is the angle of incidence on the surface

α_s is the solar elevation

R_b is a geometric factor (($R_b \geq 0$), and is defined as the ratio of the beam irradiance on the inclined surface to the horizontal beam irradiance.

The angle of incidence on the surface is calculated as:

$\theta_i = \sin\alpha_s \cos\beta + \cos\alpha_s \sin\beta \cos(\gamma_s - \gamma_i)$ ..... (2.3)

where β is the inclination angle of the surface, γ_s is the azimuth angle of the sun, and γ_i is the azimuth angle of the normal of the surface.

For a case of isotropic sky, the diffuse irradiance on inclined surface $G_{d,i}$ can be defined as:

$G_{d,i} = G_d(1 + \cos\beta)/2$ ..... (2.4)

G_d is the horizontal diffuse irradiance

$G_{r,i} = \rho_g G(1 - \cos\beta)/2$ ..... (2.5)

Where ρ_g is the average reflectance off the ground, and G is the horizontal global irradiance [30].

2.1.1. Solar and thermal radiation

All objects emit electromagnetic radiation. An ideal object that absorbs all radiation falling on it is called a blackbody [29]. The absolute temperature, T, of an object that behaves as a blackbody defines the intensity and wavelength of the electromagnetic radiation it emits [29]. The wavelength distribution of radiation emitted from a blackbody can be calculated by Planck's radiation law:

$I_{b,\lambda}(T) = \frac{2\pi hc^2}{\lambda^5}\left[\frac{1}{e^{hc/\lambda k_B T}-1}\right]$ ..... (2.6)

where,

h is Planck's constant, k_B is Boltzman's constant, c is the speed of light, $I_{b,\lambda}$ is the spectral intensity of the black body radiation, and λ is the wavelength of the radiation emitted by the blackbody surface [29].

As shown in Figure 2.1, solar light is electromagnetic radiation that falls into the spectral range of ~0.3 – ~4 μm and the highest intensity is in the range of 0.4 – 0.7 μm, which corresponds to an effective blackbody temperature of approximately 5800 K [29]. Ultraviolet light has a shorter

wavelength ranging from 0.1 – 0.4 μm. Infrared light falls within the range from 0.7 μm to over 0.001 m. The normalized solar spectrum and normalized blackbody radiation spectrum are shown at three different temperatures of 373 K, 473 K, and 573 K. When the temperature of the radiating object is below 500 °C, the radiation spectra does not strongly overlap with the solar spectrum [29].

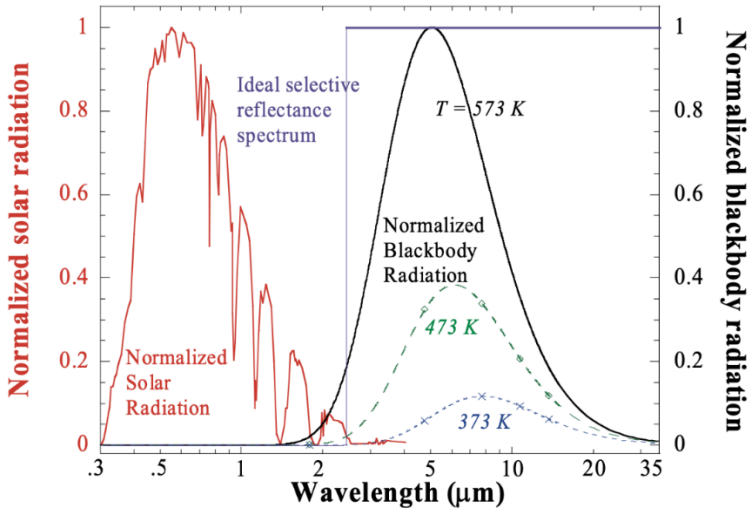

Figure 2.1. The normalized solar radiation spectrum, the blackbody radiation spectra at three different temperatures of 373 K, 473 K, and 573 K, and the ideal selective reflectance spectrum [29]

2.1.2. Absorptance of solar radiation

Solar absorptance is the ratio of the solar irradiance intensity of sunlight absorbed by the material to the intensity of incident solar radiation [31]. For normally incident sunlight, the solar absorptance is calculated as below [28].

$$\alpha_s = \frac{\int_0^\infty (1-\rho(\lambda)) I_{s(\lambda)} d\lambda}{\int_0^\infty I_{s(\lambda)} d\lambda} \quad \text{..... (2.7)}$$

Where $\rho(\lambda)$ is the reflectance at wavelength (λ), and $I_{s(\lambda)}$ is the solar spectral radiation intensity.

2.1.3. Thermal emittance

Thermal emittance is referred as the ratio of radiative heat released by a given surface to that of a blackbody at the same temperature [32]. The thermal emittance ranges from 0 to 1 i.e., $0 \leq \varepsilon_t \leq 1$ [32]. The thermal emittance is calculated as:

$$\varepsilon_t = \frac{\int_0^\infty (1-\rho(\lambda)) I_{b,\lambda}(T) d\lambda}{\int_0^\infty I_{b,\lambda}(T) d\lambda} \quad \ldots\ldots (2.8)$$

where, $I_{b,\lambda}(T)$ is the blackbody radiation intensity at wavelength λ and temperature, T. The peak value of the radiation intensity depends on the temperature of the object, although the limits of integration in Equation 2.8 can be taken as $\lambda = 0$ to $\lambda = \infty$ for all cases [28][32]. It is assumed in Equation 2.8 that the surface is diffuse. In general, the thermal emittance is highly dependent on the temperature of the physical body, chemical properties, surface texture, intrinsic geometric structure, and angle of the emitted energy [32].

2.1.4. Ideal solar spectral selectivity

Solar selectivity can be interpreted as the ratio of solar absorptance (α_s) to thermal emittance (ε_t) [29][32].When solar light is incident on a solid surface, it interacts with the atoms, ions, and electrons in the material, and some portion of the incident light is reflected, some part is absorbed and some of the light energy may be transmitted depending upon the wavelength and incident angle of the light [29][32]. The reflected light at wavelength λ is known as the reflectance, ρ_λ. The absorbed light at wavelength λ is known as the absorptance, α_λ. The transmitted light at wavelength λ is known as the transmittance, τ_λ (Figure 2.2) [32].

Therefore, $$\alpha_\lambda + \rho_\lambda + \tau_\lambda = 1 \quad \ldots\ldots (2.9)$$

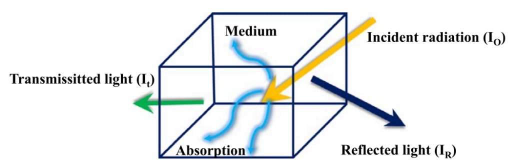

Figure 2.2. Interaction of electromagnetic radiation with matter [32]

According to Kirchhoff's law, spectral emittance is equal to the spectral absorptance and:

$$\varepsilon_\lambda = \alpha_\lambda = 1 - \rho_\lambda - \tau_\lambda \quad \text{(2.10)}$$

For an opaque surface the transmittance becomes zero and:

$$\varepsilon_\lambda = 1 - \rho_\lambda \quad \text{(2.11)}$$

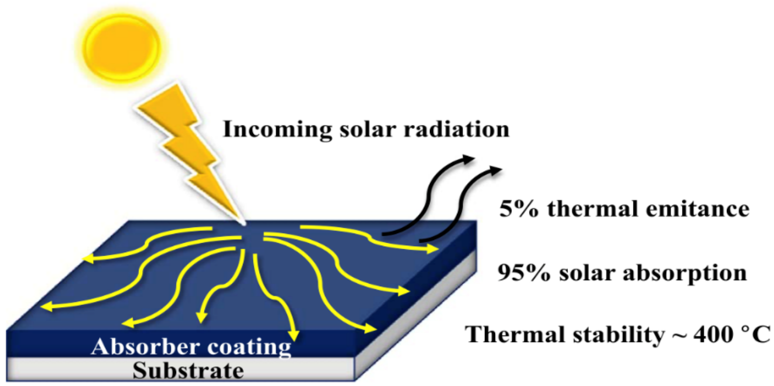

Figure 2.3 Ideal solar selective absorber [29]

Therefore, an ideal solar selective coating has reflectance = 0 in the solar spectral region to absorb the maximum amount of solar energy and reflectance = 1 in the IR region to reduce radiative energy losses. [29]

2.1.5. Active and passive solar systems

There are primarily two ways to utilize solar energy: passive or active. In passive systems, solar energy is used directly in the form of thermal energy and mechanical equipment for transferring the heat energy is not required. Natural methods of heat transfer are used in passive systems such as natural convection, thermal radiation, and thermal conduction [20][21]. In passive systems the temperature difference between different zones triggers heat flow.

For example, passive solar water heating systems are economical to build and are an effective way of using solar energy directly. These systems consider several factors to control the indoor temperature such as the building location, orientation, and thermal energy storage materials used

in the building. Trombe walls are an example of a building structure that passively uses solar energy. Trombe walls, usually have a wall made of a transparent glazing integrated with a thermal energy storage medium behind it. The wall faces the South direction to collect the maximum amount of solar energy which is then absorbed by a thermal energy storage medium. The heat energy is absorbed during the day and is released later during the nighttime or when the sun is not available. Heat is then transferred to the space using the natural methods described above.

Solar energy can be efficiently used in various applications such as space heating to reduce the heating loads, and passive systems are an economical, and yet simple technology that can contribute to space heating demands [31]. On the other hand, active systems do not use solar energy directly, but it is converted to another form of energy such as electricity, and mechanical devices are used to collect and distribute the heat energy to space.

Active solar space heating systems use a heat transfer medium such as liquid or water to gather solar energy and then distribute this thermal energy to a building using electric pumps or fans. Active systems are costlier to build, and their cost varies according to the size of the building. Active solar water heaters generate thermal energy for domestic and commercial water heating. This technology is cost-effective and commonly used. However, there should be a backup heat source in place for cloudy days or high demand.

2.2. Thermal energy storage

Thermal energy storage mediums can absorb solar energy directly or indirectly as explained in section 2.1.5 to provide heat energy to use later such as during cloudy days, or the nighttime to balance energy demand and production. The complete TES cycle involves three steps: charging, storing, and discharging. Thermal energy can be stored in the form of sensible heat, latent heat and thermochemical energy, which are discussed subsequently [34].

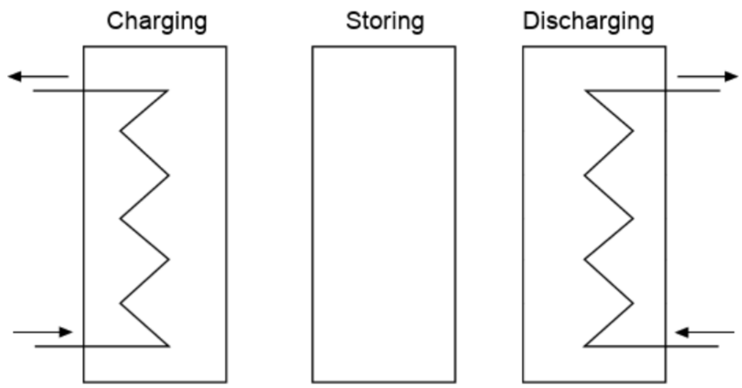

Figure 2.4. TES storage cycle [34]

2.2.1. Sensible heat storage

Sensible heat storage occurs by increasing the temperature of a storage material. The material is selected according to its heat capacity and storage space. The amount of sensible heat stored in a material is calculated as below:

$$Q = m \cdot c_p \cdot \Delta T \quad \text{(2.12)}$$

Where, Q is the amount of heat stored in the material, m is the mass of the storage material, c_p is the specific heat of the storage material, and ΔT is the temperature change. The material should have a high heat capacity and be cost effective. Suitable materials are generally selected based on properties such as their density, specific heat, thermal conductivity, and diffusivity. A material which has a high thermal conductivity or low heat capacity will have a larger thermal diffusivity. A large value of thermal diffusivity means that the heat propagates faster into the medium, and a low value means that it takes longer to propagate heat through the material [33]. The greater the heat capacity of a material, the more heat it will store for a given temperature increase [34]. The commonly used sensible thermal storage materials are shown in Table 2.1 below.

Table 2.1 Common materials used for sensible heat storage [34][37]

Material	Density (Kg/m^3)	Specific heat ($J/Kg \cdot K$)	Volumetric thermal capacity ($10^6\ J/m^3 \cdot K$)
Clay	1458	879	1.28
Brick	1800	837	1.51
Sandstone	2200	712	1.67
Wood	700	2390	1.67
Concrete	2000	880	1.76
Glass	2710	837	2.27
Aluminum	2710	896	2.43
Iron	7900	452	3.57
Steel	7840	465	3.68
Gravelly earth	2050	1840	3.77
Magnetite	5177	752	3.89
Water	988	4182	4.17
Sandstone and gravel	1950	1045	2.04
Black granite sand	2600	1000	2.6

2.2.2. Latent heat storage

Latent heat storage is achieved when a material changes phases, such as a solid-solid, solid-liquid, solid-gas, or liquid-gas phase change. Liquid-gas and solid-gas phase transformations require comparatively large amounts of heat and can be used to store more heat than solid-liquid transformations. However, it is less practical to store TES materials in the gas phase because of the large volume and pressure required for storage. Furthermore, solid-solid phase changes have a low heat of transformation and are generally slow. Therefore, solid-liquid phase changes are most used for latent heat storage applications. The materials that are used to store latent heat are known as phase change materials (PCM).

PCMs for TES applications are of three main types: Organic (e.g., paraffin and fatty acids), inorganic (e.g., hydrated salts), and eutectic which are a combination of organic and / or inorganic PCM such as organic–organic, inorganic–inorganic, and inorganic–organic. The heat transferred to or from a PCM is stored at a constant temperature when the material is melting or solidifying, which can be advantageous for maintaining comfortable temperatures in a building.

The latent heat stored in a material is calculated as:

$$Q = m \cdot \Delta h \quad \text{..... (2.13)}$$

where Q is the amount of heat stored in the material, m is the mass of the storage material, and Δh is the phase change enthalpy.

The most used PCM is water. It is used in the form of ice for cold storage. The enthalpy of water as a function of its temperature from -30 °C to 130 °C is plotted in Figure 2.5. The sensible heat increases as the temperature of the water increases from -30 °C to 0 °C. The melting process starts at 0 °C, and the vertical line from point B to point C indicates the enthalpy of melting. Once the melting process is finished, water is heated to 100 °C, and the sensible heat of liquid water increases. At 100 °C, liquid water changes state to vapor by absorbing the heat of vaporization, and the vertical line from point D to point E indicates the enthalpy change due to vaporization. After changing to vapor state, the sensible heat of the water in the vapor state increases as the temperature increases from 100 to 130 °C.

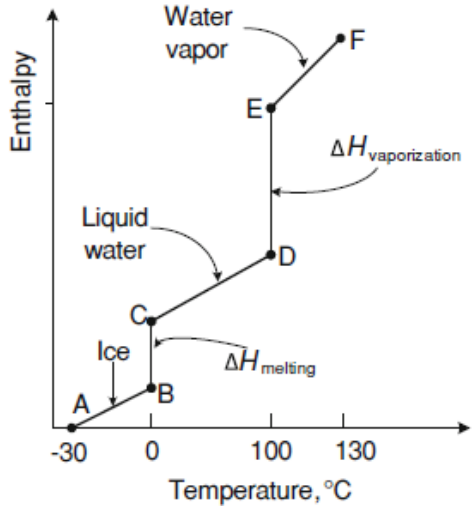

Figure 2.5. Enthalpy change of water from solid to vapor state [33]

During the phase change process, PCMs absorb energy when they undergo a state change from solid to liquid and releases energy when it is changing states from liquid to solid. A PCM should have the following properties:

- Melting point in the required operating temperature range.
- High latent heat of fusion per unit volume.

- High specific heat, energy storage density by weight and volume, and high thermal conductivity to facilitate the charging and discharging processes.
- Small changes in volume and vapor pressure when changing phases [34][35][36].

Other commonly used PCMs are shown in Table 2.2

Table 2.2. Common PCM used for latent heat storage [34][38]

Material	Melting temperature (°C)
Water	0
Paraffins	-20-100
Salt hydrates	-20-80
Chlorides	350-750

2.2.3. Thermochemical energy storage

Thermochemical energy storage is achieved when a chemical reaction is used to store energy. The products produced as a result of the reaction that occurs when heat is applied should be stored and the heat stored during the reaction should be retrievable when the reverse reaction happens [39].

2.3. Background of Trombe walls

There are various passive solar technologies available such as solar chimneys, solar roofs, and Trombe walls. Amongst these technologies, the Trombe wall is a classic passive solar technology that is grabbing attention because it is simple to build, has no operational costs, is highly efficient, and is cost-effective. A Trombe wall can reduce a building's heating demands by 30 % [41][42][43].

2.3.1. Classification of Trombe walls

Trombe walls work on the principle of using solar energy to meet the heat requirements of buildings in different climates. Trombe walls absorbs the solar thermal energy during peak sunshine hours and store that energy for later use when required by occupants. Many different configurations of Trombe walls have been studied, but they are mainly classified into the following eight categories.

- Classic Trombe wall
- Composite Trombe wall
- Phase change material (PCM) Trombe wall
- Photovoltaic (PV) Trombe wall
- Water Trombe wall
- Fluidized Trombe wall
- Electrochromic Trombe wall
- Translucent insulation material (TIM) Trombe wall [40][41]

2.3.1.1. Classic Trombe wall

A classic Trombe wall is the simplest model of a Trombe wall, which was first invented and patented by Edward Morse, an American engineer, in 1881. However, Felix Trombe and Jacque Michel were the first ones to promote the Trombe wall by building it in Odeillo, France in 1967. The classic Trombe wall, shown in Figure 2.6, consists of a glass covering or glazing, air gap, thermal storage wall, and vents. It can sometimes be built without vents. The thermal storage wall is made of high thermal capacity materials that can store as much thermal energy as possible for long durations such as bricks, concrete, and stone. The surface of the wall is usually painted black to increase absorptivity. The solar light is transmitted through the glass covering and absorbed by the thermal storage wall which creates the heating effect in the air channel.

Due to the density difference between colder air in the room and hotter air in the air channel, a space heating cycle is created. The hot air moves from the Trombe wall air channel to the room through the top vent and colder air flows from the room into the air channel through the bottom vent as shown in Figure 2.6. The vents are closed when the outside temperature is low or there is no solar energy available, to prevent air flow in the reverse direction. The thermal storage wall mass absorbs direct and diffused solar energy during the day which is then released gradually by convection or conduction. The air gap between glass and thermal storage wall is typically between 1 cm to 10 cm.

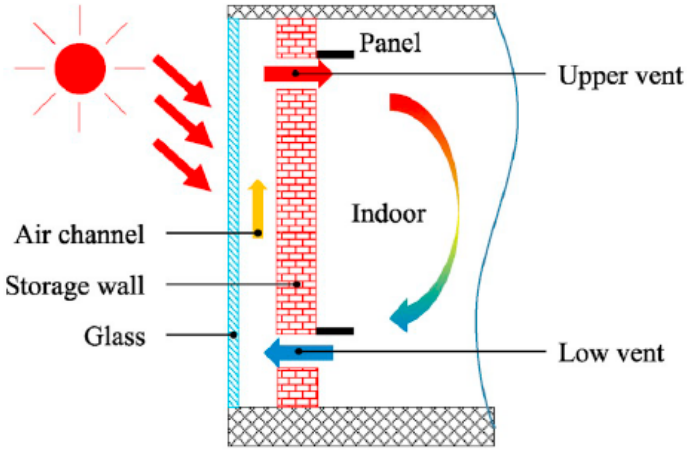

Figure 2.6. Representation of a classic Trombe wall with outer glass covering, air channel, thermal storage wall and vents [40]

Over time, several modifications to the design of the classic Trombe wall were proposed to improve the performance such as adding shades or blinds to prevent overheating during summer, adding thermal fins to the internal wall to increase heat transfer during time, building a zigzag Trombe wall to increase the heating effect during colder periods such as in the mornings or nights, and preventing overheating during the day [40][41][42]. Long et al. proposed a Trombe wall consisting of a solar collector and a reflection layer that acts as thermal insulation to the wall in the summer and stores excessive solar energy in a water tank to avoid overheating by preventing solar radiation from reaching the thermal storage wall. [43]

2.3.1.2. Composite Trombe wall

To overcome the low thermal resistance of the classic Trombe wall, a composite Trombe wall also known as the Trombe-Michel wall was proposed and built as shown in Figure 2.7.

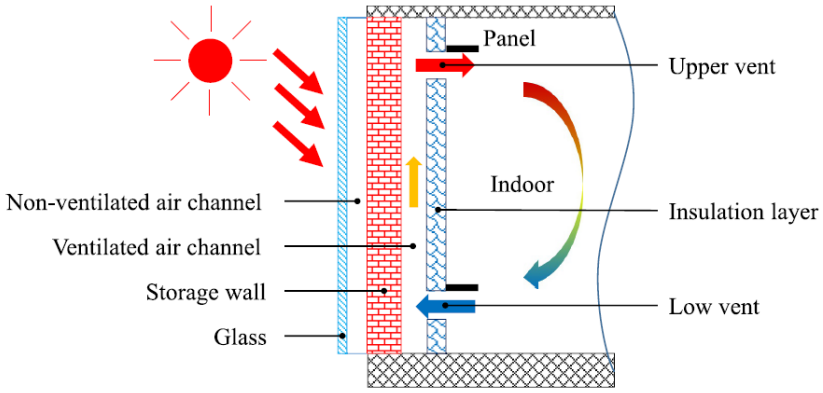

Figure 2.7. Representation of a composite Trombe wall with outer glazing, non-ventilated air channel, storage wall, ventilated air channel and vents [40]

It consists of an outer glass covering, a non-ventilated air channel between the glass covering and a thermal storage wall, and a vented air channel between the thermal storage wall and a vented insulation layer. In this model, solar energy is absorbed due to the greenhouse effect generated in the outer air channel between the thermal storage wall and glass covering, which then heats the storage wall, which in turn heats the room by air cycling in the inside air channel. The influence of the outside environment on the air flow through the Trombe wall is reduced by separating the heat collection and space heating processes. The insulation layer increases the thermal resistance of the wall and reduces the thermal loss during nighttime. Chen at al. modified the composite Trombe wall by adding a porous absorber in between the thermal storage wall and glass covering. The porous absorber is treated as a thermal insulator and heat storage buffer which absorbs the thermal energy first and then passes it to the thermal storage wall.[40] [44][45]

2.3.1.3. PCM Trombe wall

The thermal storage capacity of the classical Trombe wall is limited because it stores energy in the form of sensible heat. Therefore, PCMs were used in the Trombe wall to store latent heat to increase the thermal storage capacity of the wall. The classical Trombe wall can sometimes pose architectural problems because it increases the dead load of a building. [31] PCMs store more energy in smaller volumes and are lightweight which makes them a high-performance lightweight alternative to heavy Trombe walls. PCM Trombe wall have a PCM layer built on the outer surface of the insulation layer as shown in Figure 2.8.

A PCM Trombe wall is a south-facing wall that stores heat as the PCM material in the wall is melted during the day and releases the heat by conduction during the day and nighttime as shown in Figure 2.9. Convective heat transfer takes place between two surfaces: the glazing and PCM wall. The air in the channel flows in and out of the room through the top and bottom vents, respectively. Like the composite Trombe wall, the PCM layer can also be built into the center of the air channel.[40][41]

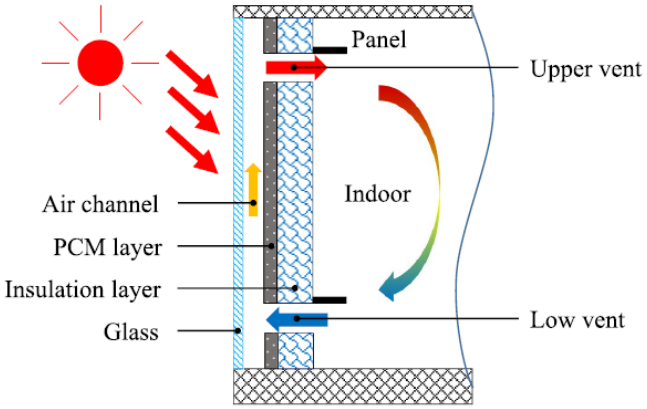

Figure 2.8. Representation of a PCM Trombe wall with outer glass covering, air channel, PCM layer integrated on the outside surface of insulation wall with vents for latent heat storage [40]

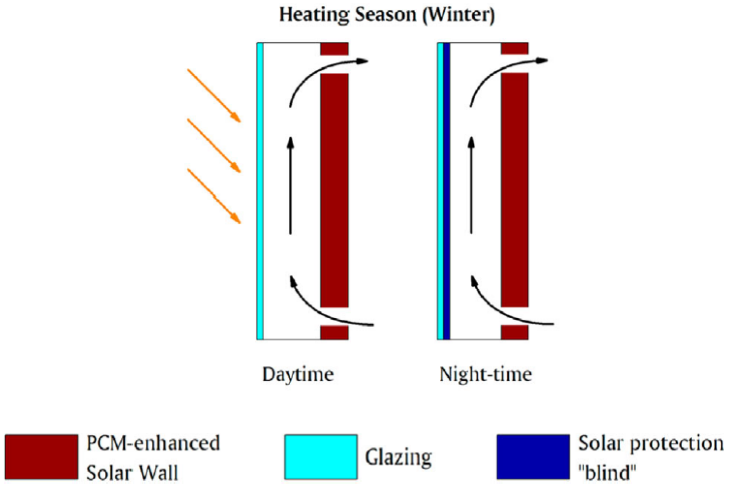

Figure 2.9. The working mechanism of a PCM Trombe wall [40]

Bourdeau conducted an experimental study to show that a 15 cm thick concrete wall can be replaced by a 3.5 cm thick PCM wall to deliver a similar performance. In another analytical study performed by Bourdeau, a Trombe wall made of a polyethylene ($CaCl_2 \cdot 6H_2O$) material, which

functioned as the PCM, attached to a wooden shelf with double glazing performed more efficiently than a concrete wall. [46]

A computational study performed by Khalifa and Abbas in Baghdad concluded that different PCMs give different results. Their studies showed that an 8 cm thick storage wall consisting of hydrated salt in copper containers with a length to diameter ratio of 0.76 performed better than a 20 cm thick concrete wall. Also, an 8 cm thick wall consisting of hydrated salt can maintain high temperatures more efficiently than a 5 cm thick wall built with paraffin wax. [47]

Some enhancements have been done to the PCM Trombe wall over time. Kara et al. developed a triple-layer glass covering. The layers consist of ordinary glass, Prisma solar glass, and low-E glass. The novel triple-layer glass allowed solar radiation with a high incident angle in summer to reflect and thus prevented over-heating. On the other hand, solar rays' incident from a lower angle during the winter were able to pass through the glazing to capture more heat. [48]

Zhou et al. utilized mini delta winglet vortex generators (DWVG) to raise turbulence to increase the heat transfer into the airflow. These generators were installed on the outer surface of the PCM wall (which was made of $CaCl_2{\cdot}6H_2O$). The results showed an increase in heat transfer rate at the PCM panel surface. Also, airflow in the air gap channel was approximately 28 % higher and the heating rate of the room was about 39 % higher when DWVGs were used. [31][40]41]

There have been several numerical and experimental studies done on the application of PCM Trombe walls. In a study conducted by Chaichan et al. in the winter season of Baghdad city, paraffin wax was used as a PCM material to improve the thermal performance of the Trombe wall. The melting point of paraffin wax is 45 $^{\circ}$C. The thermal storage wall consists of a 1m x 1m wooden box with 2 cm thickness which is separated from the outside by glass wool with a thickness of 1 cm. A black copper plate of 3 mm thickness is integrated into the interior of the wall. Nine dark black aluminum pipes with a 2.54 cm diameter and a length of 1 cm were filled with paraffin wax. The box consists of upper and lower vents for warm and cold airflows, respectively. The outer surface of the wall consists of 3 mm thick transparent glass. The results showed that PCMs can be effectively used to improve the thermal performance of Trombe walls [54].

Gracia et al. performed experiments to analyze the thermal performance of SP 22 micro-encapsulated PCMs. The experimental setup consisted of two rooms of 2.4 x 2.4 x 5.1 m

dimensions in Spain. They integrated PCMs in the ventilated air channel in one of the rooms. It was observed in the experiments that a ventilated Trombe wall with PCMs performed better than the one without PCMs. The temperature of the room that did not have a PCM Trombe wall dropped daily during the testing period according to the outer weather conditions, but the temperature of the room with the PCM Trombe wall increased from 9 °C to 18 ˚C during the same testing period, thus reducing the HVAC heating load. Further improvements can be made in the model by implementing thermal controls [55].

Sun and Wang studied the potential of integrating PCM into solar collector walls on heat transfer performance and energy savings. The model room was built in Jilin City, China. Energy balance equations were used to demonstrate the heat transfer in the Trombe wall. The Trombe wall consists of a 6 mm thick glass glazing, a 100 mm thick air ventilation channel, a 15 mm thick solar collector mortar layer, a 40 mm thick extruded board, a concrete layer of 390 mm x 190 mm x 190 mm dimensions, and a PCM layer (paraffin/expanded perlite/graphite) of 15 mm thickness. The wall has two upper and two lower vents of 200 mm x 200 mm size. The PCM has a 19.45 ˚C phase change temperature and 128.46 J/g latent heat capacity. The PCM Trombe wall showed a decrease in indoor temperature fluctuations and provided improved indoor thermal comfort as compared to an ordinary wall [56].

Fiorito performed a simulation analysis on the thermal performance of a Trombe wall in Energy Plus software under the varying winter weather conditions of five different Australian cities where the Trombe wall could be beneficial. The analysis was performed using four different PCM materials: RT21, RT27, RT31, and RT42. The results showed the reduced operative and radiative temperature fluctuation when PCMs were used. Also, the position of PCMs in the wall affected the performance of the wall according to the varying outdoor weather conditions. For example, a mild to cold climate required PCMs to be integrated on the outer surface of the partition wall to get the optimal indoor temperature, whereas mild to hot weather conditions required the PCM to be placed on the inner surface of the partitional wall. However, PCMs can be placed either on the outer or inner surface of the partition wall in hot and dry environmental conditions. In addition, an increase in the thickness of PCMs showed promising results because of the increased thermal capacity [57].

Li and Chen used eutectic inorganic hydrated salt as a PCM (27.5 °C melting point and 127 kJ/kg latent heat) in numerical analysis to study the performance of a composite wall consisting of a porous thermal storage wall. Two different models were built to study the performance of porous thermal walls with and without PCMs. The results showed that the porous wall consisting of PCM encapsulated into granular capsules showed an approximately 20 % increase in the indoor temperature at night as compared to the case when the porous wall without PCMs was used [58].

In an experimental and numerical study conducted by Bourdeau, the potential of $CaCl_2{\cdot}6H_2O$ PCMs in reducing the dead weight and improving the thermal performance of the storage wall was analyzed. The results showed that the wall with PCMs provides 10 % more energy savings than an ordinary masonry wall [31].

Leang et al. compared the performance of two composite walls: a composite Trombe wall consisting of a concrete thermal storage wall and a composite Trombe wall consisting of a commercial PCM, micronal. Both numerical and experimental studies were performed to compare the performance of the two walls. The results showed that the PCM thermal storage wall has more than 50 % additional heat storage capacity as compared to the concrete storage wall. Also, a PCM wall of 4 cm thickness was more than four-times effective in charging and distributing the warmth to the room as compared to a 15 cm thick concrete wall [59].

Zalewski et al. investigated a mixture of hydrated salts (such as water, Calcium chloride, potassium chlorides, and other additives) with a melting point temperature of 27 °C as a PCM in a composite Trombe wall. The results showed that the PCM stores more heat than a concrete material of the same volume for the same temperature range [60].

However, there are some challenges in using PCMs in Trombe wall such as:

- The optimal quantity of PCM required in a Trombe wall is challenging to determine. A low amount of PCM can decrease the performance whereas a high amount can cause overheating due to increased thermal load. Therefore, further analysis is required to find the optimal quantity or thickness of PCMs required for a particular application.
- The optimal phase change temperature of a PCM is also a challenge to determine because a high phase change temperature can cause overheating and a low phase change temperature can

reduce the inside temperature. Therefore, it is important to investigate the optimal value of the phase change temperature for materials to avoid these problems.

- Materials used to encapsulate PCMs are sometimes not compatible with medium temperature PCM systems. Therefore, new techniques should be investigated for medium temperature applications.
- PCMs can have corrosion and low mechanical strength at high temperatures. Therefore, further research is required to improve the durability of PCMs or to prohibit these conditions. [31]

2.3.1.4. Photovoltaic (PV) Trombe wall

A PV Trombe wall consists of a panel of PV cells integrated on the external glass covering as shown in figure 2.10. Similarly, to the operation of other Trombe walls, cool air leaves the room from the lower vent into the air channel which then flows into the room after being heated. The heat gain in the PV Trombe wall is lower than that of the classical Trombe wall because the PV panel obstructs the transmission of some of the solar radiation into the air channel. However, an advantage of using a PV panel is that it can also generate electricity along with generating heat. Furthermore, it prevents overheating in the summer season because some of the solar energy is consumed for power generation. [40][41]

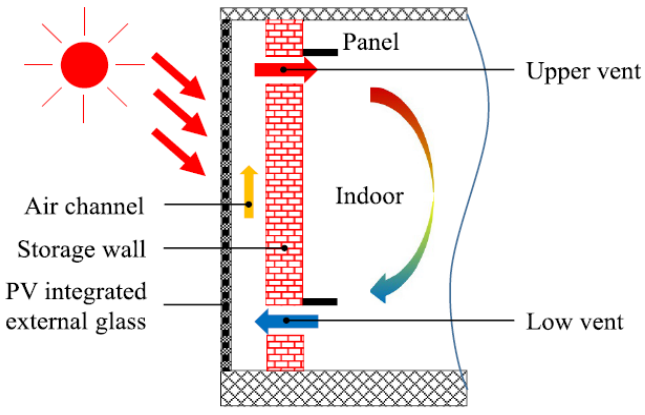

Figure 2.10. Representation of a PV Trombe wall with PV integrated outer glass covering, air channel and thermal energy storage wall with vents [40]

2.3.1.5. Water Trombe wall

Water Trombe wall makes use of a container, or a tank, filled with water as a thermal energy storage medium because of its good thermal storage capacity. The working principle of this wall is the same as that of the classical Trombe wall. The heat energy absorbed by water is distributed by convection and is transferred to the room by convection. The thermal storage capacity of water is higher than materials such as concrete, bricks, adobe, or stone due to its high specific heat. Also, heat transfer to the room is faster because of the convection phenomenon. The water Trombe wall can be used for both space heating and cooling. To increase the efficiency of the wall, the interior of the wall is sometimes insulated. The glass covering should be insulated to avoid heat loss in colder regions.

One of the main reasons for the better performance of a water Trombe wall is that the temperature of the water does not go as high as the storage wall does in the classical Trombe wall (due to the large heat capacity of water) which reduces heat losses. However, it is a bit complex to build a wall containing water as compared to a masonry wall. In a study conducted on the optimal thickness of water walls by (adam, 2010) it was found that thicker walls (6 inch – 9 inch) perform better than thin walls (~ 3 inch). A schematic diagram of a water Trombe wall is shown in Figure 2.11. [40][41] [49]

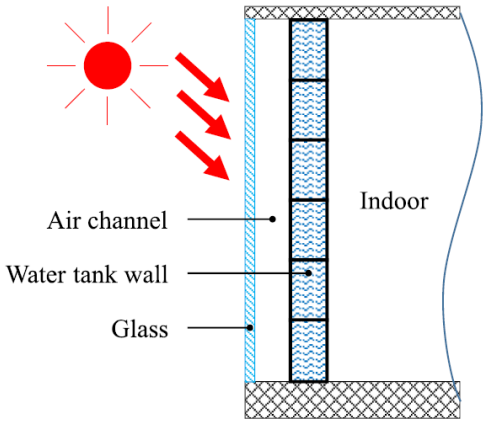

Figure 2.11. Representation of a water Trombe wall with outer glass covering, air channel, and a water tank wall as a storage medium [40]

2.3.1.6. Fluidized Trombe wall

A fluidized Trombe wall is an air channel filled with porous fluid that has low density and particles that are highly absorptive towards solar irradiation. The solar energy transmitted through the glass panel is first absorbed by fluid particles before being passed on to the air. The heating effect of the air circulating in the air channel is increased because of the larger contact surface area within the porous structure. The circulated air then moves into the room for space heating. Therefore, the performance of the fluidized Trombe wall is better than that of the classical Trombe wall. The top and bottom vents have filters to prevent small particles in the fluid from entering the room. A schematic diagram of a fluidized Trombe wall is shown in Figure 2.12. [40][41]

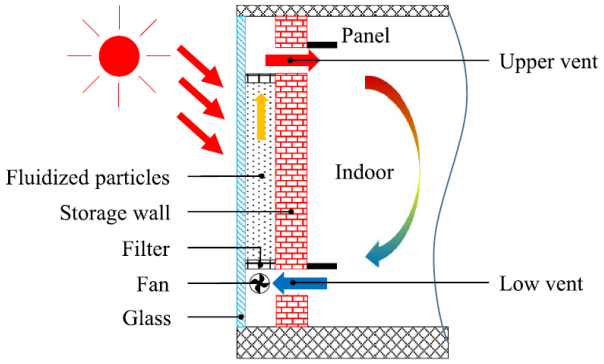

Figure 2.12. Fluidized Trombe wall [40]

2.3.1.7. Electrochromic Trombe wall

The outer glazing in this Trombe wall is made of electrochromic (EC) glass which prevents over-heating due to its electrochromic properties in the summer season and reduces the cooling load. The behaviour of the EC Trombe wall changes depending on the environmental conditions [50]. The EC glazing is inactive or clear during the cold winter season which contributes to the heating of the partition wall or air in the ventilation channel. The warm air is then circulated inside building. On the other hand, the EC glazing is activated and becomes colored in summer weather conditions to create a shield to solar radiation, which prevents overheating of the partitional wall and air in the ventilation channel. There is no additional external shield required for the system in the summer. The EC wall operates as a traditional Trombe wall in winter and works as a ventilated façade in summer. Pittaluga showed in an analytical study performed using Design Builder

Software that an EC Trombe wall can reduce the cooling load and can provide approximately 29.5 % annual energy savings [40][50][51].

2.3.1.8. Translucent insulation material (TIM) Trombe wall

The glazing is replaced with a translucent insulation material in a TIM Trombe wall. The world's largest TIM Trombe wall was built at Strathclyde University, in the UK. It was shown that the building with the TIM Trombe wall uses 40% less energy than other good buildings. The most popular TIM is aerogel insulation which has high transmittance and low thermal conductivity. It allows for 90% of the solar radiation to pass through and can have a U-value of 0.1 $W/m^2 \cdot K$. [40][53].

2.4. Background of water Trombe wall

As the focus of this thesis is on water-based Trombe walls, further background is provided in this section. Water-based Trombe walls offer a number of advantages. Firstly, water has a high heat capacity and can store more thermal energy than other Trombe walls on a per volume basis. The high heat capacity also keeps the temperature of the water Trombe wall lower than other Trombe walls, which can help reduce thermal losses to the surroundings. Also, the water can potentially be removed from the Trombe wall and used as a source of hot water for the building. The ability to remove hot water from the Trombe wall during summer months is especially attractive because many Trombe walls cause building to overheat during the summer season. Furthermore, the transparent property of water can be utilized in making aesthetically pleasing designs when architecting buildings. Indeed, translucent materials of different colors have been integrated into water Trombe walls, giving them a vibrant appearance [61]. Despite their unique combination of advantages, a limited amount of research has been done on water Trombe walls in comparison to other Trombe walls.

Weiliang et al. analyzed the thermal performance of a Trombe wall consisting of water as a thermal energy storage medium. A South facing water Trombe wall prototype with a single storey house with floor area of 700 m^2 and shape coefficient 0.374 (ratio of external surface area and inner volume) was set up in North China for experimental analysis, and a simulation model was

set up in TRNSYS. The outer layer of the Trombe wall was made of a steel plate. A total of 29 small modules of water (with dimensions of 1.1 m × 0.4 m × 2.5 m) were placed along the inner side of the wall. Numerical and experimental analysis were conducted and compared with the traditional Trombe wall. The results showed a reduction in energy consumption per year by 8.6 % and the indoor thermal comfort evaluation index was improved by approximately 13 % as compared to the classic Trombe wall [62].

Nayak did a numerical analysis of thermal performance between a south-facing drum water wall and a water Transwall. The drum wall consisted of metallic containers of water stacked upon each other. One surface of the wall is colored black and has glazing on it, but the other surface can be separated from the room by a concrete wall or insulating layer. The Transwall consists of water in containers that are made of parallel glass walls. Each wall has a semi-transparent material kept either between the water column and the room, between glazing and the water column, or in the water column itself (Transwall). Energy balance equations were used to solve the Fourier equations of heat conduction for both configurations to calculate the heat flux entering the room. The results show that the Transwall meets the daytime heating load more effectively than a drum wall whereas a drum wall performs better in terms of load levelling and day-night performance [63].

Adams et al. conducted a study to investigate the optimal thickness of a water storage wall. A controlled environment was built in the lab to analyze the effects of heat source on the water wall with 3", 6" and 9" thicknesses. The environment consisted of three parts: (i) exterior space, (ii) interior space, and (iii) the water wall. The dimensions of exterior and interior volumes were 1 ft^3 (1 ft x 1 ft x 1 ft). The exterior volume consisted of a heat source (halogen bulb), and the interior volume was a vacant space. The heat source was turned on for 5 hours and then switched off to monitor the thermal performance of exterior and interior volumes over time. It was observed that 6" and 9" thick walls performed better than 3" wall. The thinner wall allowed the indoor temperature to increase at a faster rate and maintained high temperature for longer periods of time than the thick walls. Thus, 3" wall was not able to efficiently regulate the room temperature than 6" and 9" walls. Also, the heat transfer through 3" wall was higher than that of 6" and 9" walls. It was concluded that the Trombe wall thickness should at least be greater than 3" for optimal performance [64].

Kaushik and Kaul proposed a thermal storage mixed water-mass wall and performed a heat transfer analysis. The analysis was performed on a room on the ground floor in a building without any air conditioning. The room consisted of a south facing wall made of concrete and water layers (concrete-water-concrete) for heat gain and space heating purposes into the room. The periodic heat transfer analysis included the heat transfer through walls and roof, heat conduction to the floor and furnishings, and heat loss due to infiltration and ventilation. The outer walls and roof of the room were exposed to sun and atmospheric air temperature, and inner walls were in contact with changing air temperature. Numerical analysis was performed to study the changes in indoor air temperature and heat fluxes based on hourly solar irradiance, and atmospheric temperature for a mild day of winter in New Delhi, India. The considered different configurations of storage walls consisting of concrete-water-insulation. The results showed that the concrete-water-concrete wall performed better than other mixed storage walls such water wall with insulation only for space heating and maintaining comfort temperature. The placement and thickness of concrete or insulation have considerable effect on the heat flux and inside air temperature. Varying the thickness of insulation seemed to generate desirable results than changing the thickness or placement of concrete wall [65].

Turner et al. studied the performance of a water Trombe wall consisting of a 7.6 cm diameter plastic tubes embedded into a studded wall. During winter season, the system was charged for 6 hours with hot ambient air and then passively discharged for 18 hours. The results showed that the Trombe wall temperature remained approximately 2.6 °C higher even after the discharging cycle completed which helped in reducing the heating load of the house. During summer season, water walls can be charged using cool ambient air at night to achieve thermal comfort during daytime [66].

Tiwari et al. did a comparative study of total heat gain of different south facing Trombe walls such as a glass wall, water wall, active air collector wall, and a trans wall. Several design parameters were taken into consideration such as the thickness of the water wall and trans wall, and the flow rate of the air collector wall. The design parameters were varied for a heated room under winter weather conditions to conduct different experiments. The results showed that the performance the water wall and the trans wall is better for space heating during nighttime because of their greater thermal storage capacity. On the other hand, the glass wall and the air collector

wall are efficient for space heating during sunshine hours. It was also observed that the air temperature of the room was higher during extreme winter conditions of Srinagar, India when a trans wall was used in a non-conditioned passive solar house in comparison to when a water wall is used [67].

Abdulmajeed et al. designed a novel Trombe wall to reduce the heating and cooling loads in the winter and summer seasons, respectively. The Trombe wall consists of a water tank that acts as a thermal energy storage medium and can also supply hot water if required. The proposed Trombe wall model can be used for space heating during day and night, and excess heat can be used for domestic hot water supply in the summer season. The excess heat can be extracted out of the building through vents or can be used for domestic water heating purposes to reduce the cooling load. The experimental results showed that the proposed system is more efficient in charging and discharging thermal energy as comparison to a classical Trombe wall. The thermal storage efficiency of the proposed system is more than 70%. Furthermore, a numerical analysis was performed to study the effect of the heat transfer coefficient. The study showed that the air-side heat transfer coefficient is also an important factor that needs to be depicted correctly in the model. It can be increased by adding additional extended surfaces such as (fins) or turbulent generators, but it will add weight and cost to the model. It was also observed that decreasing the water tank size, increases the temperature but the amount of energy stored does not change. [68]

In the aforementioned work done by Mohamad et al. [68], an opaque solar absorber was used at the outer surface of the water storage wall. In this thesis, the potential of using a semi-transparent absorber in a water storage wall is investigated. Specifically, a tinted acrylic sheet is integrated into the water wall, such that it retains its transparency to some degree, which is desirable for the design of aesthically pleasing Trombe walls. Furthermore, the effects of placing the acrylic sheet at different locations on the performance of the water Trombe wall (e.g., at the outer face or emerged in water at the center of the storage medium) is investigated.

2.5. Efficiency of Trombe walls

Table 2.3 shows the efficiency of different Trombe walls in the literature.

Table 2.3 Thermal efficiency of different Trombe walls in the literature

Author/Year/Location	Description	Thermal efficiency	Calculation
Kara, Y. A., & Kurnuç, A. (2012) *Location: Erzurum, Turkey*	The performance of coupled novel triple glass and phase change material wall in the summer season is studied. The novel triple glass reduced energy storage in the PCM and prevented overheating in the summer [69].	20%-36%	The daily overall efficiency of the PCM wall: $\eta_{o,d} = \frac{E_{g,d}}{E_{i,d}}$ where, $E_{i,d}$ is the daily solar energy (J/day) incident, and $E_{g,d}$ is the solar energy gain from PCM wall to the test room (J/day).
Mohamad, A., Taler, J., & Ocłoń, P. (2019). *Location: Calgary, Canada*	In this study, the utilization of a Trombe Wall consisting of a water tank as TES for space heating and domestic hot water supply purposes is numerically investigated for the winter season [68].	~ 80%	The thermal efficiency of the system is calculated as: $E\iint = \frac{E_w + E_a}{E_s}$ where, E_w is energy absorbed by the water (J/m), E_s is the solar energy received by the system over the period of 10 hours, and E_a is the energy carried by air.
Zhang, L., Dong, J., Sun, S., & Chen, Z. (2021). *Location: China*	A simulation analysis and sensitivity analysis of an improved Trombe wall consisting of an aluminum plate exterior surface coated with a Selective Absorbing Coating (SAC). The absorptivity and emissivity of the SAC is 0.9 and 0.1 respectively [70].	55.7 %	The thermal efficiency of the system is calculated as: $\eta = \frac{Q_h}{Q_t} \times 100\%$ $Q_h = m_a \, . \, c_a \, \Delta T_a$ where, c_a is the specific heat of air, m_a is the mass flow rate, ΔT_a is the temperature difference between the air passing through the inlet and outlet air vents, Q_t is the radiation heat gained by the Trombe wall per second.
Hong, X., He, W., Hu, Z., Wang, C., & Ji, J. (2015). *Location: Hefei, China*	3-D simulation analysis on the thermal performance of a novel Trombe wall with Venetian blind structure. The optimum distance between the glass and the Venetian blind is 0.09 m. Width of the air duct is 0.14 m. Area of inlet/outlet vent is 0.60 m × 0.10 m [71].	33.08 %	The thermal efficiency of the system is calculated as: $\eta = \frac{Q_{th}}{G.A}$ $Q_{th} = m \cdot C_p (T_{out} - T_{in})$ where, A is absorbing area (m^2), Q_{th} is the heat absorbed by the air in the cavity (KJ), m is the air mass (kg/s), C_p is the specific heat capacity of air (J/kg-K), T_{out} & T_{in}

			are the temperature of outlet and inlet air flow (°C)
Hu, Z., Zhang, S., Hou, J., He, W., Liu, X., Yu, C., & Zhu, J. (2020). *Location: Hefei, China*	An experimental and numerical analysis of a novel water blind-Trombe wall system [72]	Apr -Sept: 20% - 60% Dec - Mar: 30% - 50%	The thermal efficiency of the system is calculated as: $\eta_m = \frac{Q_u}{A_C . G_V}$ where, Q_u is energy gain in watts ($\frac{J}{s}$), G_V as the irradiance ($\frac{W}{m^2}$), A_C as absorbing area (m^2)

2.6. Research objectives

The research conducted in this thesis is directed towards the design and development of water Trombe walls that exhibit high performance for all seasons. During summer months Trombe walls typically do not reduce the building energy load to the same extent as they do during the winter months. Furthermore, Trombe walls can cause overheating during the summer months. The Trombe wall designs proposed in this research will utilize the incident solar energy with high thermal efficiency by storing thermal energy in water within the Trombe wall which can be used for purposes other than providing heated to the room adjacent to the Trombe wall. The thesis objectives are as follows:

- Objective 1: To design and model semi-transparent water-based Trombe walls that exhibit high performance for all seasons.
- Objective 2: To perform simulations and conduct lab-scale experiments to estimate if the amount and temperature of heated water from the water-based Trombe walls can be used to satisfy hot water demands in a typical residential household in Toronto, Canada.

Other than the previously mentioned paper by Abdulmajeed et. al., research about this design approach to water-based Trombe walls has not been reported in the literature. Thus, although the experiments conducted in this research will be on a small-scale Trombe wall prototype, these will be the some of the first experiments conducted for the design of water Trombe walls wherein the intention is to be able to remove heated water for use in other purposes throughout the building. Furthermore, some of the water Trombe wall configurations investigated in this thesis will be semi-transparent, with the appearance of a darkened window. This feature allows the Trombe wall

to be used as a tinted window in buildings, which is a unique feature that has yet to be studied in the literature. The methods that will be used to conduct the research are described below [68].

Trombe walls are designed and evaluated using Design Builder software. The Trombe walls are integrated into a simple one-floor building in the simulations and results are compared to reference cases wherein the thermal storage medium is a simple concrete structure or is absent. In the simulations weather files describing the conditions experienced in Toronto in previous summers and winters will be used. These simulations will evaluate the performance parameters for the Trombe walls including the thermal efficiency, thermal load leveling, absorption storing efficiency, and the building load reduction.

A small prototype Trombe wall is constructed in the lab to perform experiments. The objective of the experiments is to measure how much thermal energy can be stored in different water-based Trombe wall configurations. A metal-halide bulb is used to illuminate the Trombe wall with solar-simulated light. The intensity of the light incident onto the Trombe wall is measured using a power meter. In these experiments, the thermal efficiency of the Trombe wall is measured as the sum of the stored energy and energy delivered through the air vents of the Trombe wall divided by the total incident light energy.

The outcome from the thesis is an evaluation of a novel set of Trombe wall configurations that exhibit a unique combination of benefits including high thermal efficiency and high aesthetic quality. The performance metrics of these Trombe walls are evaluated using a combination of simulations performed with Design Builder software and experiments conducted on a small-scale Trombe wall prototype. The water-based Trombe walls presented in this thesis can have a positive environmental impact by reducing the energy consumed in buildings. The impact, in terms of building load reduction, is numerically evaluated and reported in the thesis. Furthermore, the water-based Trombe walls will have a unique aesthetic quality that may help promote acceptance and wide spread integration of Trombe walls in buildings.

CHAPTER 3: METHODS

3.1. Three-dimensional model

As shown in Figure 3.1, a three-dimensional (3D) model of a single-story building with a Trombe wall is created in Design Builder simulation software to numerically investigate the performance of different Trombe wall configurations.

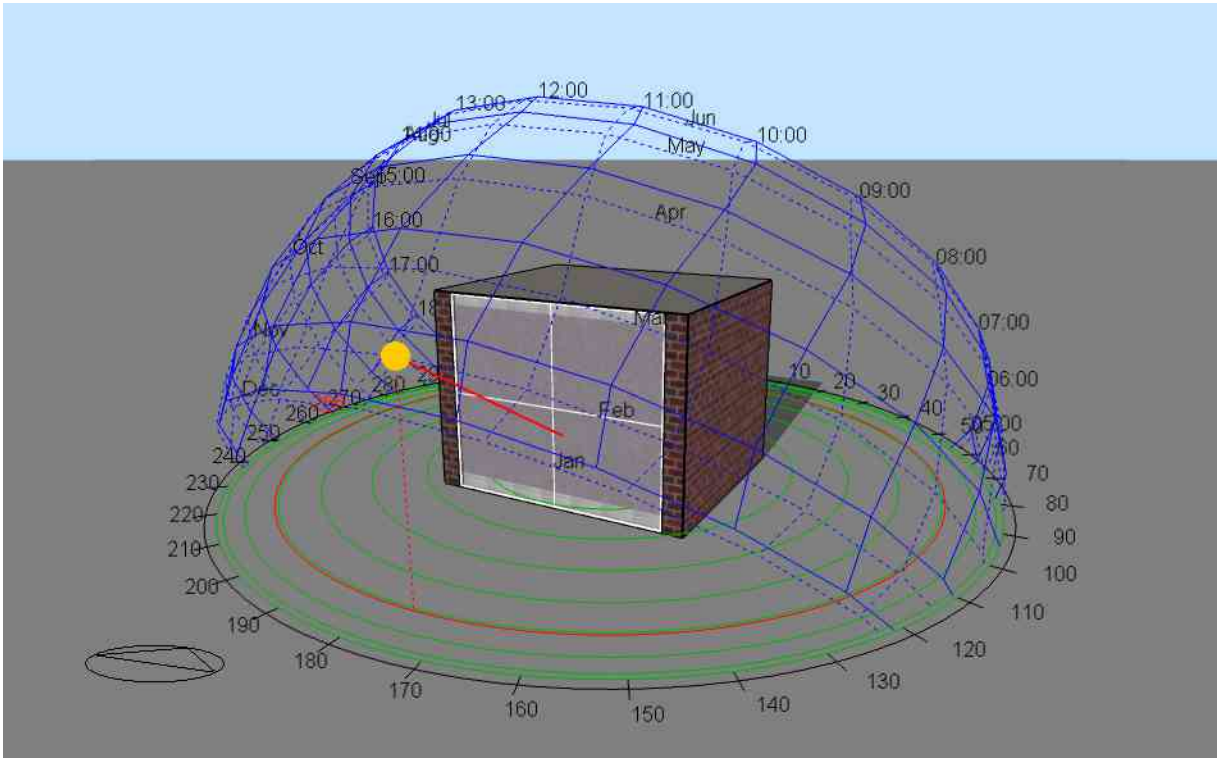

Figure 3.1. 3D model of a single-story building with a Trombe wall

As shown in Figure 3.2, the width, depth, and height of the building are 4000 mm, 3360 mm, and 3000 mm, respectively. The model consists of two zones: a room (occupied zone) and a Trombe wall with an air channel (Trombe wall zone). The occupied zone and the air channel zone are separated by a partition wall that functions as a Thermal Energy Storage (TES) medium (Figure 3.3). The Trombe wall zone consists of a sun-facing high transmissivity glazing, an air gap, and a partition wall consisting of a TES medium and two vents (upper and lower as shown in Figure 3.4) to facilitate airflow in and out of an air channel located between the partition wall and the glazed window.

Incident solar energy transmitted through the outer glazing is absorbed at the surface of the partition wall. Solar thermal energy generated in the partition wall heats the TES medium and the air within the air-channel (Figure 3.5). Warm air can be delivered to the occupied zone through the upper vent. Heat can also be transferred directly from the inside surface of the thermal storage wall to the room and thus stored thermal energy can be used at a later time when sunshine is unavailable [4]. Moreover, when water is used as the thermal energy storage medium, heated water can be used for other purposes within the building, such as in appliances, hydronic radiant heating systems at other locations in the building, and for domestic hot water supply. To date, little research has been done in this area.

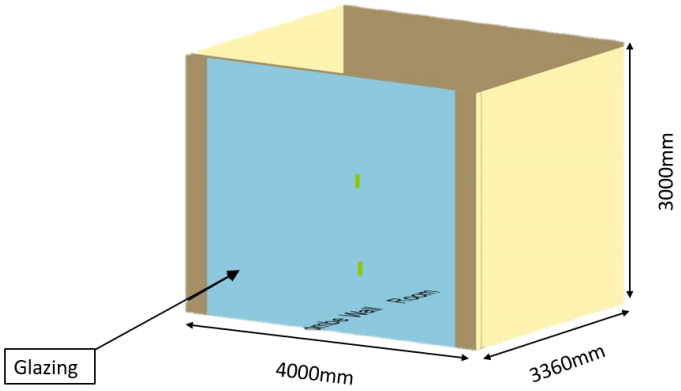

Figure 3.2. Model of the room within the single-story building showing the glazing in front of the Trombe wall.

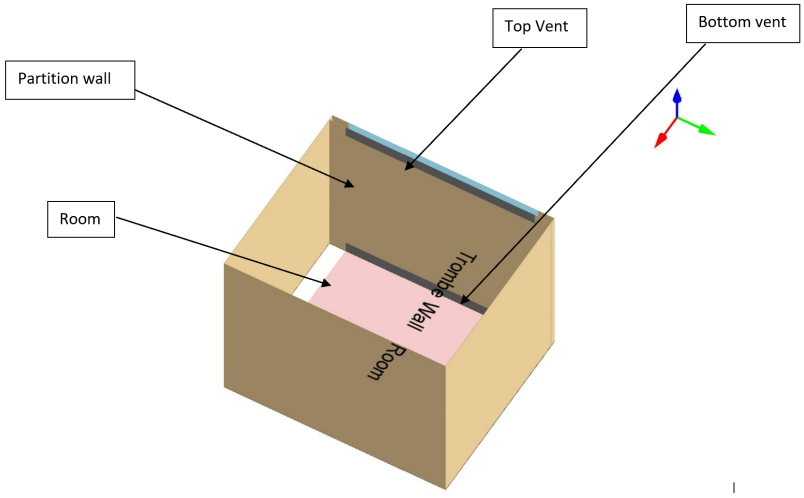

Figure 3.3. Model of the room within the single-story building showing the partition wall, Trombe wall zone between the partition wall and glazing, room zone, and the top and bottom vents.

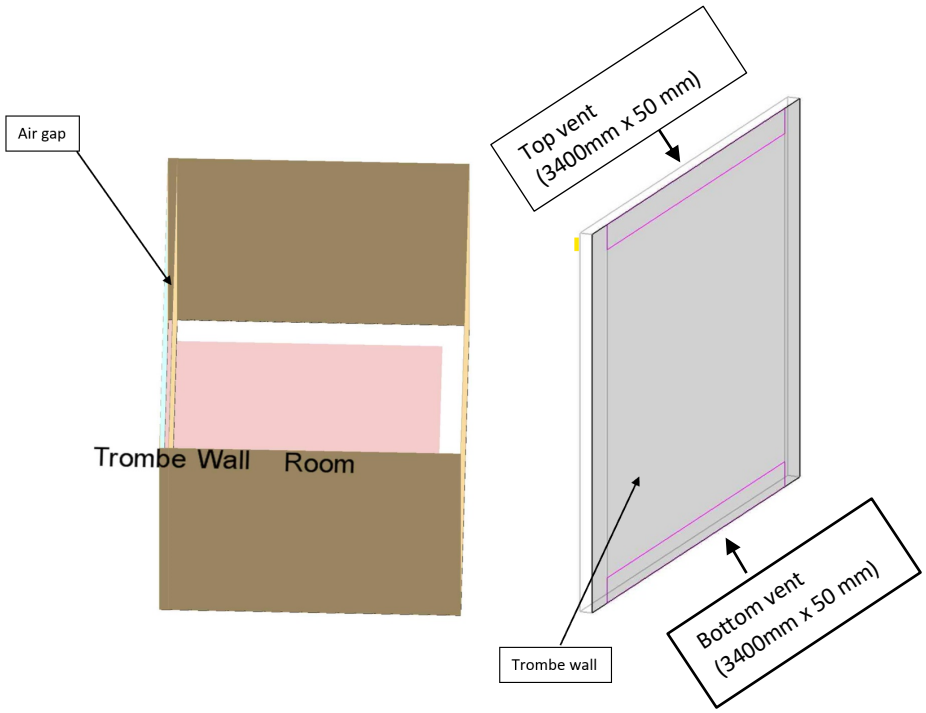

Figure 3.4. The air gap between the partition wall and the glazing for the building shown in Figure 3.2.

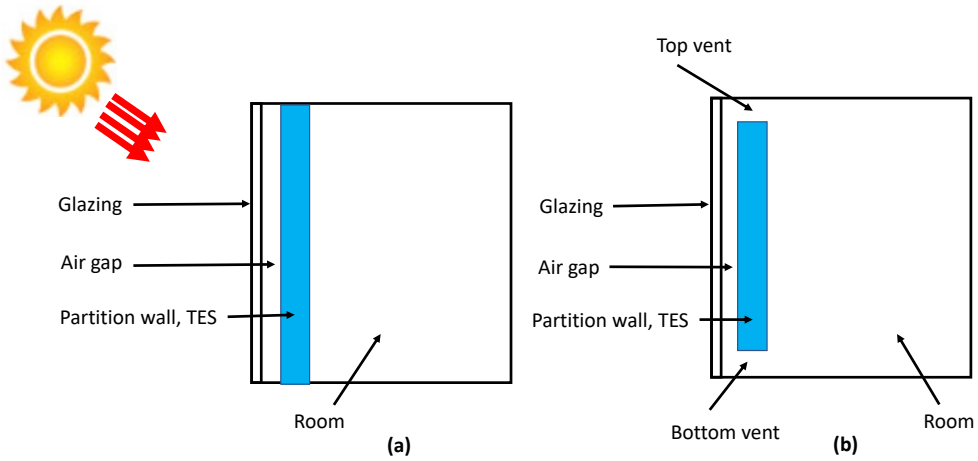

Figure 3.5. Schematic diagram of the side view of the partition wall, TES for (a) summer, and (b) winter cases

3.2. Properties of materials selected in the model

A reference model (base case) is built to perform simulations and to set the stage for a comparative analysis. The effects of altering the thicknesses and materials used for the thermal energy storage wall (the partition wall shown in Figures 3.1, 3.2, 3.3, and 3.4) on the building

cooling and heating loads, and thermal energy stored, are compared. The base case has the specifications listed as bulleted points below, and items selected in Design Builder software are underlined and bolded:

- The South-facing wall of the room has a 6 mm thick glazing. There is a 100 mm thick air gap between this glazing and a partition wall. The partition wall functions as the thermal energy storage wall. The glazing properties are defined using the Solar Heat Gain Coefficient (SHGC), direct solar transmission, visible transmission, and U-value (W/m^2). The SHGC is defined as the solar energy transmittance of the whole window or door including the glass, and frame material.
- The upper and lower vents in the partition wall have a width of 3400 mm and a height of 50 mm. The vents are opened when the room temperature is below the Trombe zone temperature during the winter season. However, the vents are always closed during summer.
- ***Double clear 6mm/13mm air*** glazing is used which consists of two glass layers. The outermost and the innermost layers are 6 mm thick generic clear glass and these are separated by a 13 mm thick air gap.
- The model is setup under ***Toronto, Ontario*** weather conditions. The data set is derived from hourly weather data recorded by a national weather service of that location such as Typical Meteorological Year – 2nd edition (TMY2) and Weather Year for Energy Calculation – Version 2 (WYEC2) in Canada.
- The simulations are performed under the summer and winter weather conditions for three consecutive days. The ***July 14, 15, and 16, 2020*** period is selected for summer simulations and the ***Feb 02, 03, and 04, 2021*** period is selected for winter simulations. The simulation periods were selected after comparing the average solar irradiance of these 3 days over the summer and winter months. The three-day average over July 14, 15 and 16 is 877 W/m^2 and is the highest over the months of July and August. The average solar irradiance over the three days of Feb 02, 03 and 04 is 843 W/m^2 and this is the highest over the months of January and February.
- A thermostat is used to control the temperature in the room zone.
- *Environment control:* Under this control, the heating and cooling setpoint thermostat settings are defined. The heating and cooling setpoint is the comfort temperature required for a zone. This setting is used by the HVAC system to automatically turn on the zone sensible heating and cooling to maintain the indoor temperature when the Trombe wall is not able to deliver heat to the room to maintain the comfort temperature.

- For summer modeling, cooling setpoint and setback temperatures are set as 20 ^{o}C and 22 ^{o}C, respectively.
- For winter modeling, the heating setpoint and setback temperatures are set as 24 ^{o}C and 20 ^{o}C, respectively.
- Both vents are set to be ON during the winter conditions. The timing and duration of vent openings is controlled based on the room and Trombe zone temperatures. The vents are opened when the room temperature is below the Trombe zone temperature.
- Both vents are always closed during summer conditions.
- The outside air definition method is selected as ***By zone***. Design Builder provides an outside air definition method to define the maximum outside delivery rate to the HVAC system. ***By zone*** means that the outside air delivery rate is defined in air changes per hour (ac/h). The airflow rate is calculated in m^3/s as shown below:

  Airflow rate (m^3/s) = (ac/h) x (Zone Volume/3600)

  Where *Zone Volume* is the volume of the space occupied by air.
- The air changes per hour is set as 5 for the room zone and as 0 for the Trombe wall zone.
- In this model, ***Grill small, light slats*** vent is used for both top and bottom. It is under the visual texture category naming as Grille small, light slats which means the grille size is small and the color of the slats is light [73].
- TARP and DOE-2 are the default algorithms used for inside and outside convections respectively in Design Builder.
- TARP is a comprehensive natural convection algorithm in which heat transfer coefficients are correlated to the orientation of the surface and the difference between surface and zone air temperature. It uses the detailed heat balance method for the energy requirements calculations of multiple rooms in the simulation. It is designed to consider the interroom complex heat transfer phenomenon for simulations. [78]
- DOE-2 algorithm is used to predict the energy usage and cost for a building based on the building layout, constructions, operating schedules, lighting, HVAC, weather data etc. [79]

3.2.1. Glazing or glass covering

The model shown in Figures 3.1 to 3.4 consists of a double layer clear glass 6mm/13mm air thick glazing with optical properties shown in Table 3.1 below. Direct solar transmission is used in this model.

Table 3.1 Properties of construction materials used for glazing or glass pane

Construction object	Construction material	Thickness	Optical properties
Glazing	Double-clear air glass	6 mm/13mm Air	Total solar transmission (SHGC): 0.703
			Direct solar transmission: 0.604
			Light transmission: 0.781
			U-value ($W/m^2 \cdot K$): 2.665

3.2.2. Walls

The walls of the single-story building are constructed with four layers. ***XPS extruded polystyrene*** insulation is used and the energy codes and insulation standards for the walls adhere to the ***Canadian energy code (homes)***. The thermal and radiative properties of each layer are shown in Table 3.2 below:

Table 3.2 Properties of construction material used for the walls in the building shown in Figure 3.1.

Construction object	Construction material	Thickness	Thermal properties	Radiative properties
Walls	**4 layers**			
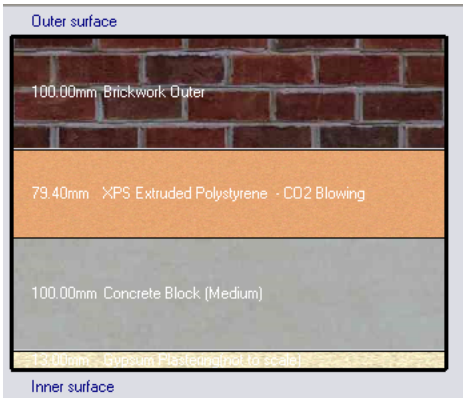	***Outermost layer:*** Bricks	100 mm	λ (W/m·K): 0.84 C (J/Kg·K): 800 ρ (Kg/m^3): 1700	A_T: 0.9 A_S: 1.0 A_V: 1.0
	Layer 2: XPS Extruded polystyrene	79.40 mm	λ (W/m·K): 2.8 C (J/KgK): 1000 ρ (Kg/m^3): 2600	A_T: 0.9 A_S: 1.0 A_V: 1.0
	Layer 3: Concrete block	100 mm	λ (W/mK): 2.8 C (J/KgK): 1000 ρ (Kg/m^3): 2600	A_T: 0.9 A_S: 1.0 A_V1.0
	Innermost layer: Gypsum plastering	13 mm	λ (W/mK): 2.8 C (J/KgK): 1000 ρ (Kg/m^3): 2600	A_T: 0.9 A_S: 1.0 A_V: 1.0

For each wall layer material in Table 3.2 the emissivity (A_T) is set to 0.9 and the solar and visible absorptance (A_S and A_V) are set to 1 in the simulations.

3.2.3. Roof

The roof of the model building shown in Figure 3.1 has four layers, and the thermal and radiative properties of each layer are shown in Table 3.3 below:

Table 3.3 Properties of construction material used for the roof of the model building shown in Figure 3.1.

Construction object	Construction material	Thickness	Thermal properties	Radiative properties
Roof	**4 layers**			
	Outermost layer: Asphalt 1	10 mm	λ (W/mK): 0.7 C (J/KgK): 1000 ρ (Kg/m^3): 2100	A_T: 0.9 A_S: 0.85 A_V: 0.9
	Layer 2: Medum weight (Mw) glass wool (rolls) polystyrene	100 mm	λ (W/mK): 0.04 C (J/KgK): 840 ρ (Kg/m^3): 12	A_T: 0.9 A_S: 0.6 A_V: 0.6
	Layer 3: Air gap	200 mm	R (m^{2}K/W): 0.1800	A_T: 0.9 A_S: 0.6 A_V: 0.6
	Innermost layer: Plasterboard	13 mm	λ (W/mK): 0.25 C (J/KgK): 896 ρ (Kg/m^3): 2800	A_T: 0.9 A_S: 0.5 A_V: 0.5

3.2.4. Floor

3.2.4.1. Ground floor

The ground floor of the building shown in Figure 3.1 complies with the Canadian energy code standard and is made of four layers with the properties shown in Table 3.4 below:

Table 3.4 Properties of construction materials used for the ground floor of the model building shown in Figure 3.1[73].

Construction object	Construction material	Thickness	Thermal properties	Surface properties
Ground floor (comprised of four layers)	***Outermost layer:*** Urea-formaldehyde foam	100 mm	λ (W/mK): 0.04 C (J/KgK): 1400 ρ (Kg/m^3): 10	A_T: 0.9 A_S: 0.6 A_V: 0.6
	Layer 2: Cast Concrete	100 mm	λ (W/mK): 1.13 C (J/KgK): 1000 ρ (Kg/m^3): 2000C	A_T: 0.9 A_S: 0.6 A_V: 0.6
	Layer 3: Floor/Roof screed	70 mm	λ (W/mK): 0.41 C (J/KgK): 840 ρ (Kg/m^3): 1200C	A_T: 0.9 A_S: 0.73 A_V: 0.73
	Innermost layer: Timber flooring	30 mm	λ (W/mK): 0.14 C (J/KgK): 1200 ρ (Kg/m^3): 650C	A_T: 0.9 A_S: 0.78 A_V: 0.78

3.2.4.2. External floor

The external floor of the model building shown in Figure 3.1 adheres to the Canadian energy code standards and has three layers with thermal and surface properties as shown in Table 3.5 below:

Table 3.5 Properties of construction material used for the external floor of the model building shown in Figure 3.1.

Construction object	Construction material	Thickness	Thermal properties	Surface properties
External floor	**3 layers**			
	Outermost layer: External rendering	25 mm	λ (W/mK): 0.5 C (J/KgK): 1000 ρ (Kg/m^3): 1300	A_T: 0.9 A_S: 0.7 A_V: 0.7
	Layer 2: Medium weight (Mw) stone wool (rolls)	144 mm	λ (W/mK): 0.04 C (J/KgK): 840 ρ (Kg/m^3): 30	A_T: 0.9 A_S: 0.6 A_V: 0.6
	Layer 3: Timber flooring	5 mm	λ (W/mK): 0.14 C (J/KgK): 1200 ρ (Kg/m^3): 650	A_T: 0.9 A_S: 0.78 A_V: 0.78

3.2.5. Thermal energy storage medium wall (partition wall)

Simulations are performed to analyse the performance of Trombe walls with different thermal energy storage mediums during summer and winter conditions. The different cases of Trombe walls simulated for winter and summer conditions are described in Table 3.6 and Table 3.7, respectively. Water is selected as a thermal energy storage medium because water has a volumetric heat capacity of 4186 kJ/(m^3·K), whereas the volumetric heat capacity of concrete is about 2000 kJ/(m^3·K) and sand is about 2600 KJ/(m^3·K). Due to the high heat capacity of water, it can store a large amount of thermal energy while maintaining comparatively low surface temperatures, which helps reduce thermal losses.

Different water Trombe wall configurations are considered for analysis. In some of these configurations, water is chosen as a TES medium and sand is used in other configurations for comparison. In some configurations, both sand and water are used as inner and outer surfaces in the same TES medium. Some configurations of the Trombe wall will be opaque whereas it will be semi-transparent in others. By using materials that absorb most of the sunlight, but transmit a small portion of it, the water-based Trombe wall can still achieve high efficiencies while being "see-through". Thus, for some designs the water-wall will have a similar appearance to a darkened or

tinted window, which can be an aesthetically pleasing aspect that is unique to the water-based Trombe walls designed in this thesis. In addition to this, different configurations of Trombe walls with transparent insulation are considered to prevent overheating.

Table 3.6 Properties of the thermal energy storage wall (partition wall) investigated for winter weather conditions

	Material	**Thermal properties** **λ (W/m·K)** **C (J/Kg·K)** **ρ (Kg/m^3)**	**Surface properties**	**Description**
Case 1: Water Trombe wall 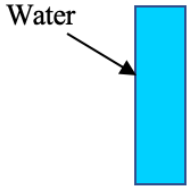	Water	λ: 0.63 C: 4190 ρ: 990	A_T: 0.9 A_S: 0 A_V: 0	Naming convention: "wat". For example, a 20 cm thick storage wall made of water is denoted as wat (20 cm). The thickness of the Trombe wall varies from 5 cm to 40 cm with increments of 5 cm.
Case 2: Water Trombe wall with tinted glass at its outer side 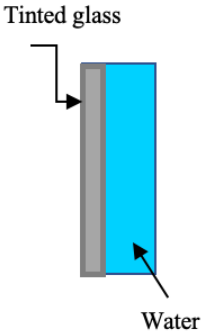	Water Tinted glass	**Water** λ: 0.63 C: 4190 ρ: 990 **Tinted glass** λ: 0.8 C: 800 ρ: 2500	**Water** A_T: 0.9 A_S: 0.8 A_V: 0.8 **Tinted glass** A_T: 0.9 A_S: 0.8 A_V: 0.8	Naming convention: "tg/wat". For example, a storage wall made of 1 cm thick tinted glass and a 10 cm thick water wall is denoted as tg(1cm)/wat(10cm). The thickness of the water wall varies from 5 cm to 40 cm with increments of 5 cm. The thickness of the tinted glass is 1 cm. The thickness of the insulation layer is 5 cm.
Case 3: Water Trombe wall with tinted glass at its center 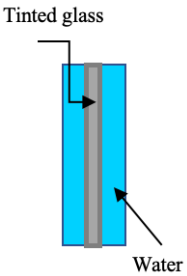	Water Tinted glass	**Water** λ: 0.63 C: 4190 ρ: 990 **Tinted glass** λ: 0.8 C: 800 ρ: 2500	**Water** A_T: 0.9 A_S: 0.8 A_V: 0.8 **Tinted glass** A_T: 0.9 A_S: 0.8 A_V: 0.8	Naming convention: "wat/tg/wat". For example, the storage wall made of 1 cm thick tinted glass and 10 cm thick water wall is denoted as wat(5cm)/tg(1cm)/wat(5cm). The thickness of the water walls varies from 5 cm to 20 cm with increments of 5 cm. The thickness of the tinted glass is 1 cm.

Case 4: Trombe wall (Sand) 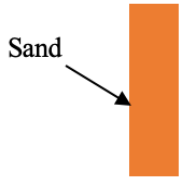	Granite sand	λ: 2.8 C: 1000 ρ: 2600	A_T: 0.9 A_S: 1 A_V: 1	Naming convention: "sand". For example, a 20 cm thick storage wall made of sand is denoted as sand (20 cm). The thickness of the Trombe wall varies from 5 cm to 40 cm with increments of 5 cm.
Case 5: Trombe wall with water at inner and sand at outer sides 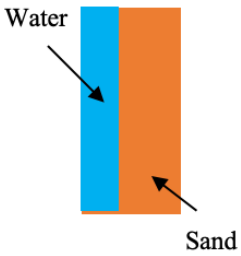	Water Sand	**Water** λ: 0.63 C: 4190 ρ: 990 **Sand** λ: 2.8 C: 1000 ρ: 2600	**Water** A_T: 0.9 A_S: 1 A_V: 1 **Sand** A_T: 0.9 A_S: 1 A_V: 1	Naming convention: "wat/sand". For example, a 5 cm thick storage wall made of water and a 17.5 cm thick sand wall is denoted as wat(5cm)/sand (17.5 cm). The total thickness of the Trombe wall varies from 20.5 cm to 32.5 cm
Case 6: Trombe wall with sand at inner and water at outer sides 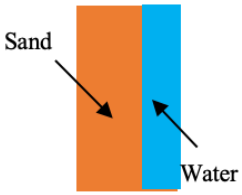	Sand Water	**Sand** λ: 2.8 C: 1000 ρ: 2600 **Water** λ: 0.63 C: 4190 ρ: 990	**Sand** A_T: 0.9 A_S: 1 A_V: 1 **Water** A_T: 0.9 A_S: 1 A_V: 1	Naming convention: "sand/wat". For example, a 17.5 cm thick storage wall made of sand and a 5 cm thick water wall is denoted as sand(17.5cm)/wat(5cm). The total thickness of the Trombe wall varies from 20.5 cm to 32.5 cm

Table 3.7. Properties of the thermal energy storage wall (partition wall) investigated for summer weather conditions

	Material	**Thermal properties** **λ (W/m·K)** **C (J/Kg·K)** **ρ (Kg/m^3)**	**Radiative properties**	**Description**
Case 1: Water wall (Reference Case) 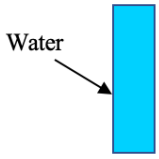	Water	λ: 0.63 C: 4190 ρ: 990	A_T: 0.9 A_S: 0 A_V: 0	Naming convention: "Wat". For example, a 20 cm thick storage wall made of water is denoted as wat(20cm). Thickness varies from 5 cm to 40 cm with increments of 5 cm.

Case 2: Water wall with transparent insulation at its inside surface 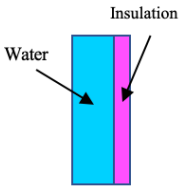	Water and Aerogel	**Water** λ: 0.63 C: 4190 ρ: 990 **Aerogels** λ: 0.014 C: 1000 ρ: 150	**Water** A_T: 0.9 A_S: 0 A_V: 0 **Aerogels** A_T: 0.9 A_S: 0 A_V: 0	Naming convention: "wat/ins". For example, a storage wall made of a 5 cm thick water wall and a 5 cm thick insulation wall is denoted as wat(5cm)/ins(5cm). The thickness of the water layer varies from 5 cm to 40 cm with increments of 5 cm. The thickness of insulation wall is 5 cm.
Case 3: Water wall with transparent insulation on both sides 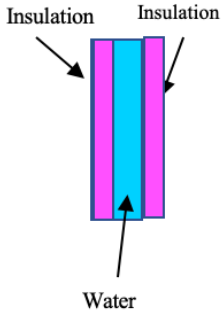	Water and Aerogels	**Water** λ: 0.63 C: 4190 ρ: 990 **Aerogels** λ: 0.014 C: 1000 ρ: 150	**Water** A_T: 0.9 A_S: 0 A_V: 0 **Aerogels** A_T: 0.9 A_S: 0 A_V: 0	Naming convention: "Ins/wat/ins". For example, a storage wall made of a 5 cm thick water wall with 5 cm thick layers on insulation on both of its sides is denoted as ins(5cm)/wat(5cm)/ins(5cm). The thickness of the water wall varies from 5 cm to 40 cm with increments of 5 cm. The thickness of the insulation layers is 5 cm for both the inner and outer sides.
Case 4: Water wall with tinted glass at Outer sides 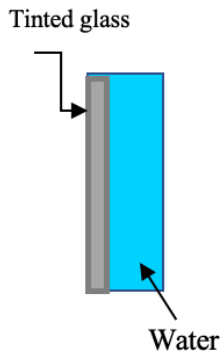	Water Tinted glass	**Water** λ: 0.63 C: 4190 ρ: 990 **Tinted glass** λ: 0.8 C: 800 ρ: 2500	**Water** A_T: 0.9 A_S: 0.8 A_V: 0.8 **Tinted glass** A_T: 0.9 A_S: 0.8 A_V: 0.8	Naming convention: "tg/wat". For example, a storage wall made of 1 cm thick tinted glass and 10 cm thick water wall is denoted as tg(1cm)/wat(10cm). The thickness of the water wall varies from 10 cm to 40 cm with increments of 10 cm. The thickness of the tinted glass is 1 cm.

Case 5: Water with tinted glass at its outer side and transparent insulation at its inner side 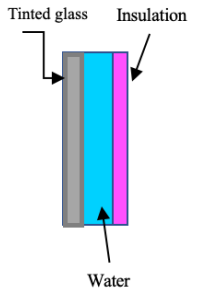	Water Tinted glass Aerogels	**Water** λ: 0.63 C: 4190 ρ: 990 **Tinted glass** λ: 0.8 C: 800 ρ: 2500 **Aerogels** λ: 0.014 C: 1000 ρ: 150	**Water** A_T: 0.9 A_S: 0.8 A_V: 0.8 **Tinted glass** A_T: 0.9 A_S: 0.8 A_V: 0.8 **Aerogels** A_T: 0.9 A_S: 0 A_V: 0	Naming convention: "tg/wat/ins". For example, a storage wall made of 1 cm thick tinted glass, a 10 cm thick water wall, and a 5 cm thick insulation layer is denoted as tg(1cm)/wat(10cm)/ins(5cm). The thickness of the water wall varies from 10 cm to 40 cm with increments of 10 cm. The thickness of the tinted glass is 1 cm, and the thickness of the insulation is 5 cm for all cases.
Case 6: Water with tinted glass at its outer side and transparent insulation on both sides 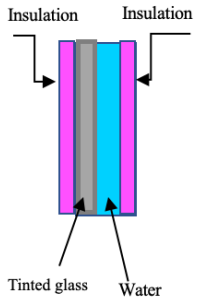	Water Tinted glass Aerogels	**Water** λ: 0.63 C: 4190 ρ: 990 **Tinted glass** λ: 0.8 C: 800 ρ: 2500 **Aerogels** λ: 0.014 C: 1000 ρ: 150	**Water** A_T: 0.9 A_S: 0.8 A_V: 0.8 **Tinted glass** A_T: 0.9 A_S: 0.8 A_V: 0.8 **Aerogels** A_T: 0.9 A_S: 0.8 A_V: 0.8	Naming convention: "ins/tg/wat/ins". For example, a storage wall made of 1 cm thick tinted glass, a 10 cm thick water wall, and 5 cm thick insulation layers on the inner and outer sides of the storage wall is denoted as ins(5cm)/tg(1cm)/wat(10cm)/ins(5cm). The thickness of the water wall varies from 10 cm to 40 cm with increments of 10 cm. The thickness of the tinted glass is 1 cm, and the thickness of the insulation layers is 5 cm on the inner and outer sides.
Case 7: Water wall with tinted glass at its center 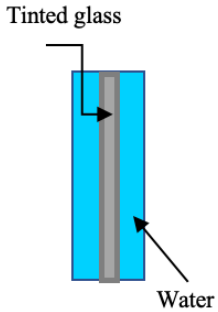	Water Tinted glass	**Water** λ: 0.63 C: 4190 ρ: 990 **Tinted glass** λ: 0.8 C: 800 ρ: 2500	**Water** A_T: 0.9 A_S: 0.8 A_S: 0.8 **Tinted glass** A_T: 0.9 A_S: 0.8 A_V: 0.8	Naming convention: "wat/tg/wat". For example, a storage wall made of 10 cm thick water walls with a 1 cm thick tinted glass layer in the middle is denoted as wat(10cm)/tg(1cm)/wat(10cm). Also, "OW" and "IW" are used specify the inner and outer parts of the storage wall. For example, "OW:wat/tg/wat" is used to refer to the thermal energy stored in the outer water wall. The total thickness of the storage wall varies from 11 cm to 41 cm with increments

				of 10 cm. For all cases considered the thickness of the tinted glass is 1 cm and the thicknesses of the outer and inner water walls are equal.
Case 8: Water wall with tinted glass at its center and insulation at its inner side 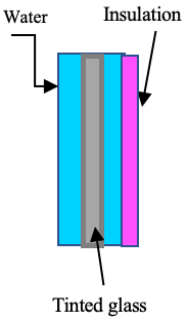 	Water Tinted glass	**<u>Water</u>** λ: 0.63 C: 4190 ρ: 990 **<u>Tinted glass</u>** λ: 0.8 C: 800 ρ: 2500 **<u>Aerogels</u>** λ: 0.014 C: 1000 ρ: 150	**<u>Water</u>** A_T: 0.9 A_S: 0.8 A_V: 0.8 **<u>Tinted glass</u>** A_T: 0.9 A_S: 0.8 A_V: 0.8 **<u>Aerogels</u>** A_T: 0.9 A_S: 0.8 A_V: 0.8	Naming convention: "wat/tg/wat/ins". For example, a storage wall made of 10 cm thick water walls with a 1 cm thick tinted glass layer in the middle and a 5 cm thick layer of insulation at its inner side is denoted as wat(10cm)/tg(1cm)/wat(10cm)/ins(5cm). Also, "OW" and "IW" are used specify the inner and outer parts of the storage wall. For example "OW:wat/tg/wat/ins" is used to refer to the thermal energy stored in the outer water wall. The thickness of the storage wall varies from 16 cm to 46 cm. with increments of 10 cm. The thicknesses of the tinted glass and insulation are always 1 cm and 5 cm, respectively. The thickness of the inner and outer water walls are kept equal.
Case 9: Water wall with tinted glass at its center and insulation at both sides	Water Tinted glass	**<u>Water</u>** λ: 0.63 C: 4190 ρ: 990 **<u>Tinted glass</u>** λ: 0.8 C: 800 ρ: 2500 **<u>Aerogels</u>** λ: 0.014 C: 1000 ρ: 150	**<u>Water</u>** A_T: 0.9 A_S: 0.8 A_V: 0.8 **<u>Tinted glass</u>** A_T: 0.9 A_S: 0.8 A_V: 0.8 **<u>Aerogels</u>** A_T: 0.9 A_S: 0.8 A_V: 0.8	Naming convention: "ins/wat/tg/wat/ins". For example, a storage wall made of 10 cm thick water walls with a 1 cm thick tinted glass layer in the middle and a 5 cm thick layers of insulation on its inner and outer sides is denoted as ins(5cm)/wat(10cm)/tg(1cm)/wat(10cm)/ins(5cm). Also, "OW" and "IW" are used specify the inner and outer parts of the storage wall. For example, "OW:ins/wat/tg/wat/ins" is used to refer to the thermal

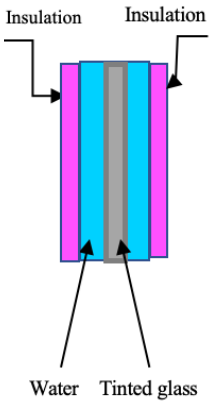				energy stored in the outer water wall. The thickness of the storage wall varies from 21 cm to 51 cm with increments of 10 cm. For all cases the thickness of the tinted glass is 1 cm and the thickness of the insulation on the inner and outer sides of the storage wall is 5 cm. The thickness of the inner and outer water walls varies but are kept equal.

3.3. Model configuration in Energy Plus Software

The simulations are carried out using Design Builder Software, which uses the building energy simulation tool Energy Plus.

3.3.1. Location

Design Builder uses the ASHRAE 2013 weather database, which provides hourly weather data and takes time zones and daylight savings into consideration**.** For the simulations performed in this thesis, the site location is set to Toronto, Ontario, and the weather data template for Toronto, Ontario is used to run simulation analysis.

3.3.2. Model options

Design Builder loads default data at the site and building level when a building is created which is known as model data. Model data settings can be overwritten and there are various options or configuration settings available to customize the model at the building level. A summary of the options selected to simulate the building structure shown in Figure 3.1 are provided in Table 3.8. A description of these model options and reasons for selecting the configurations shown in Table 3.8 are given in Appendix A.

Table 3.8 Model options configured at the building level in Design Builder [73]

Model Options	Configurations available	Configuration selected
Data tab		
HVAC	- Simple - Detailed	Simple
Natural ventilation	- Scheduled - Calculated	Calculated
Heating Design tab		
Temperature Control	- Air temperature - Operative temperature - Radiant temperature	Air temperature
Simulation tab		
Period	Simulation periods start and end the day	For Summer: July 14 – July 16 For Winter: Feb 2 – Feb. 4
Time steps per hour	- 2,4,6,10,14,30,60	4
Temperature control	- Air temperature - Operative temperature	Air temperature
Solar distribution	- Minimal shadowing - Full interior - Full interior and exterior	Full interior and exterior
Solution algorithm	- Conduction transfer function - Finite difference	Conduction transfer function
Finite difference scheme	- Fully implicit first order - Crank-Nicholson second order	Fully implicit first order
Inside convection algorithm	- Adaptive Convection - Simple - CIBSE - TARP	TARP
Outside convection algorithm	- Adaptive Convection - Simple Combined - CIBSE - TARP - DOE-2 - MoWiTT	DOE-2

3.4. Trombe wall experimental model

A small Trombe wall prototype, shown in Figure 3.6 was built to experimentally investigate and compare the ability to store solar thermal energy in water storage walls with and without tinted glass. The Trombe wall prototype is built using 3.8 x 3.8 cm wooden frames because of their low thermal conductivity. The overall dimensions of the model frame are 58.4 x 38.1 x 66.0 cm. The frame is insulated using 1.5-inch thick FOAMULAR extruded polystyrene insulation boards. Silicon sealant was used to assemble the prototype.

The front surface of the Trombe wall prototype was made from a 3 mm thick clear acrylic sheet that was tightly fitted in the insulation board frame and then sealed using silicon sealant at its edges. These seals were subsequently covered with sheathing tape. A 3 mm thick acrylic plexiglass sheet of dimensions 35 cm x 35 cm is integrated into the back side insulation of the prototype. This allows light to pass through the Trombe wall prototype, as a desired feature of the water Trombe wall is transparency or semi-transparency. The side of the Trombe wall prototype was designed as an insulated door to allow users to change the TES medium and adjust the position of the thermocouples. A 1000 W Hortilux Blue W Metal Halide bulb mounted vertically with a white reflector behind it is used to simulate solar radiation. This light source is 38 cm away from the front surface of the acrylic sheet. The Trombe wall consists of a TES medium as water and the water is stored in a clear acrylic plexiglass container. The dimensions of the water container are 30 x 20 x 20 cm.

Also, the experiments were run with a 5 mm thick tinted acrylic sheet (manufactured by Chemcast) integrated into the TES medium at the front of the water container. The plexiglass container, with and without the tinted acrylic sheet, is shown in Figure 3.7. In addition, experiments were run with two 3 mm thick clear plexiglass sheets integrated at the rear side of the Trombe wall prototype to investigate the effects of having better insulation at the "inside" of the Trombe wall (the air gap between the two clear sheets acts as an insulative layer).

A rough energy balance was conducted to compare the energy flow in and out of the Trombe wall prototype. In this energy balance the incident light was compared to the sum of the light transmitted through the prototype, and the heat loss through the windows at the front and rear sides of the prototype. The heat loss through the insulated walls of the Trombe wall was estimated to be very small and was neglected. The results showed the energy balance was satisfied to within ± 10% for all cases. A description of the energy balance and calculations made for all cases are shown in Appendix C.

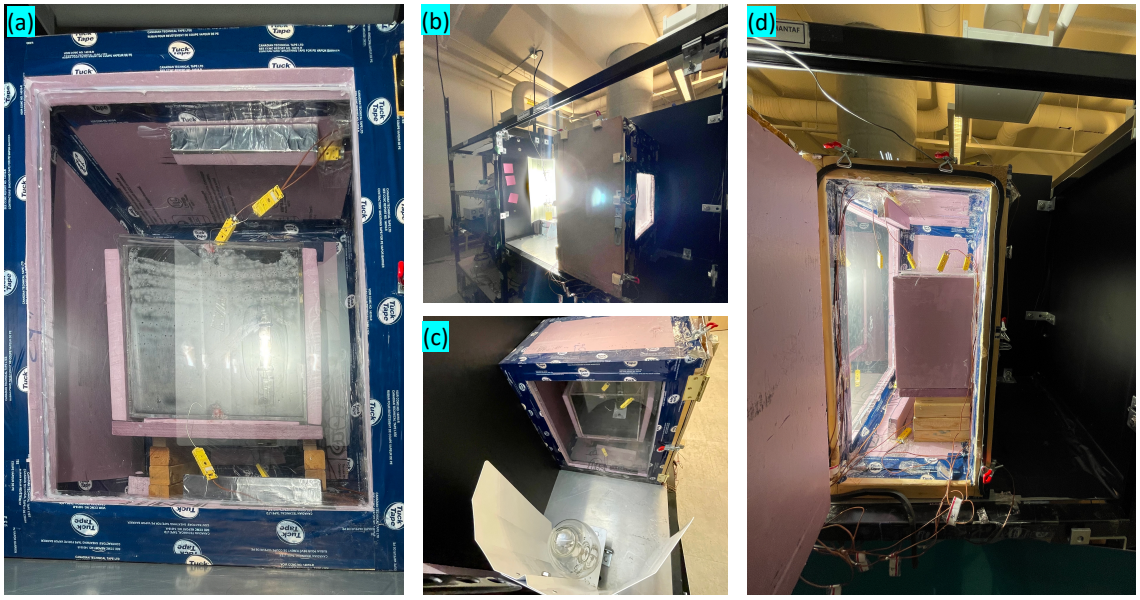

Figure 3.6 (a) Front view of the Trombe wall prototype when water with acrylic tinted plexiglass is used (b) Rear view of the transparent Trombe wall prototype showing the plexiglass at its rear side (c) Trombe wall prototype with a 1000 W metal halide light functioning as a solar simulator (d) Side view of the Trombe wall prototype with the door open.

Figure 3.7 (a) Acrylic plexiglass water container (front view) (b) Acrylic plexiglass water container (view of side and front) (c) Acrylic plexiglass water container with tinted acrylic sheet (front view) (d) Acrylic plexiglass water container with tinted acrylic sheet (view of side and front)

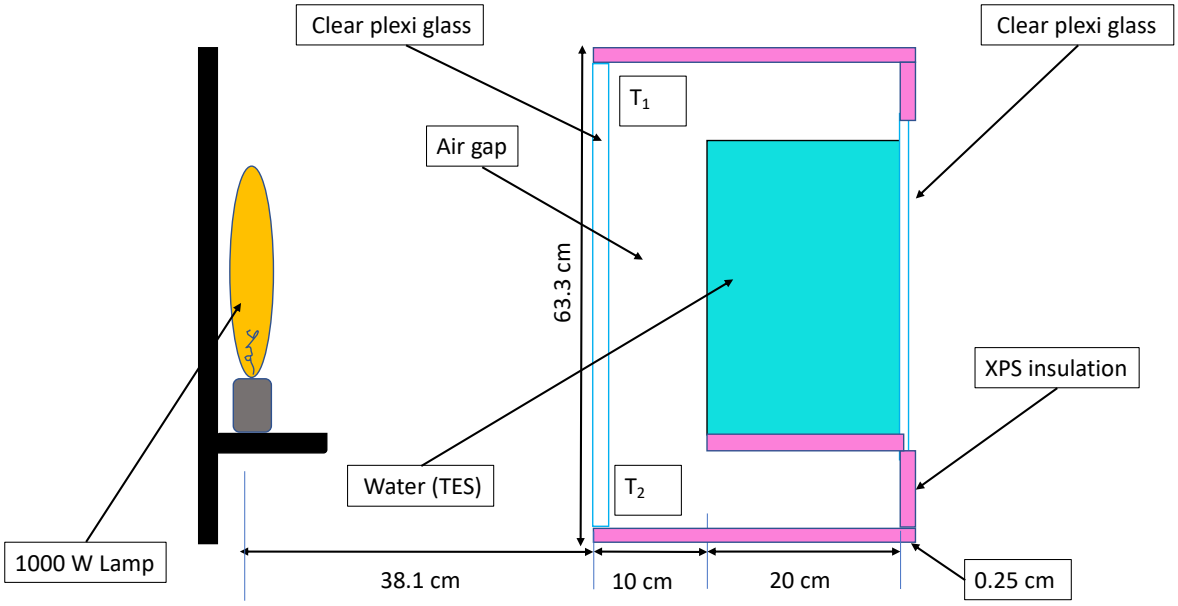

Figure 3.8 (a). Sideview of the Trombe wall prototype with water as the TES medium

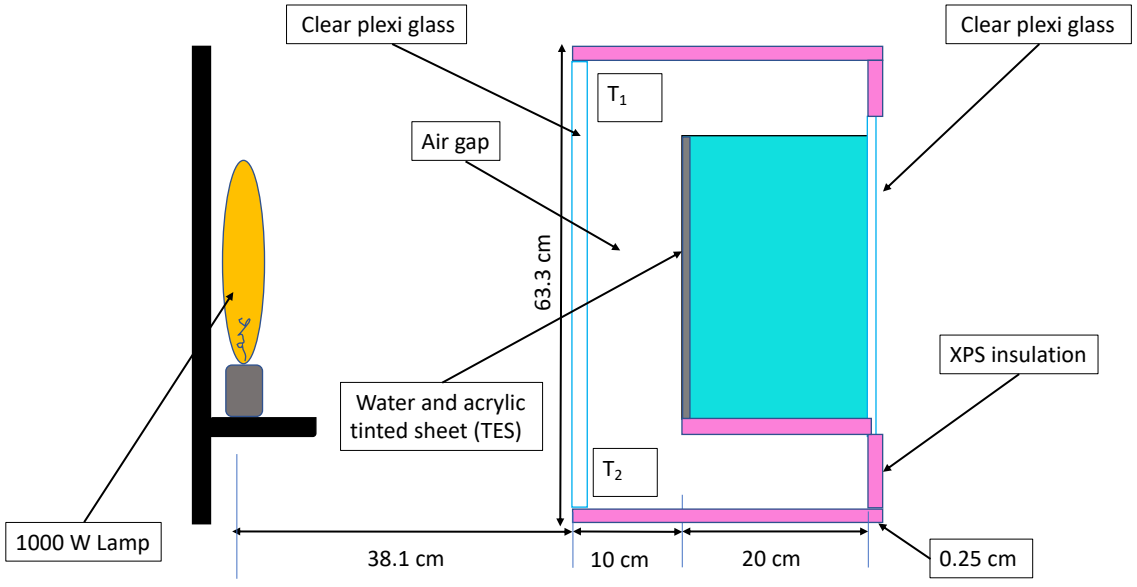

Figure 3.8 (b). Schematic showing the sideview of the Trombe wall prototype with a tinted acrylic sheet in water as the TES medium

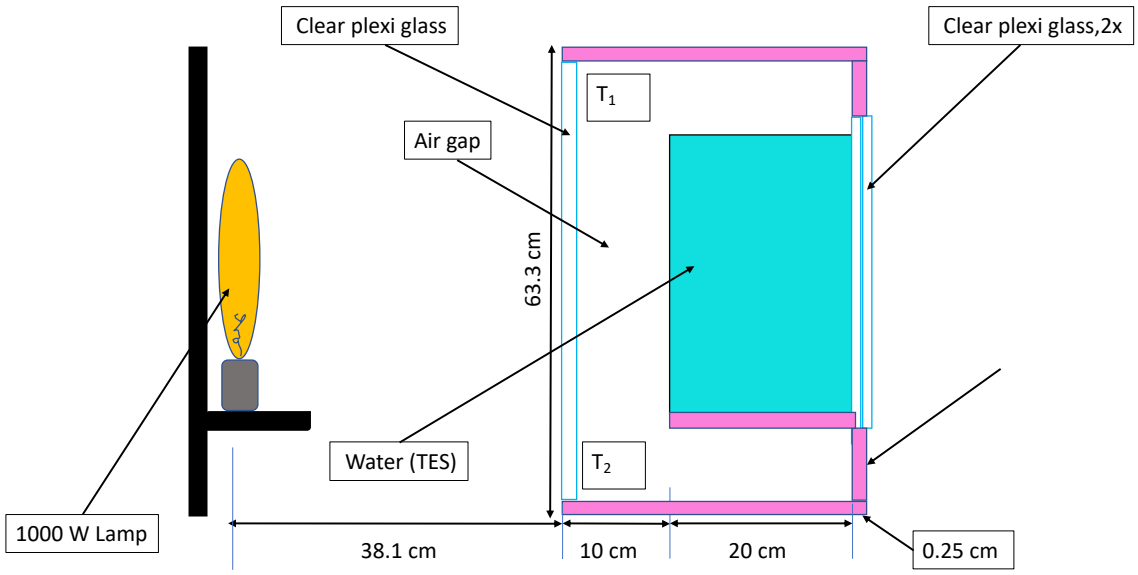

Figure 3.8 (c). Schematic showing the sideview of the Trombe wall prototype with water as the TES medium and two plexiglass sheets at the rear side

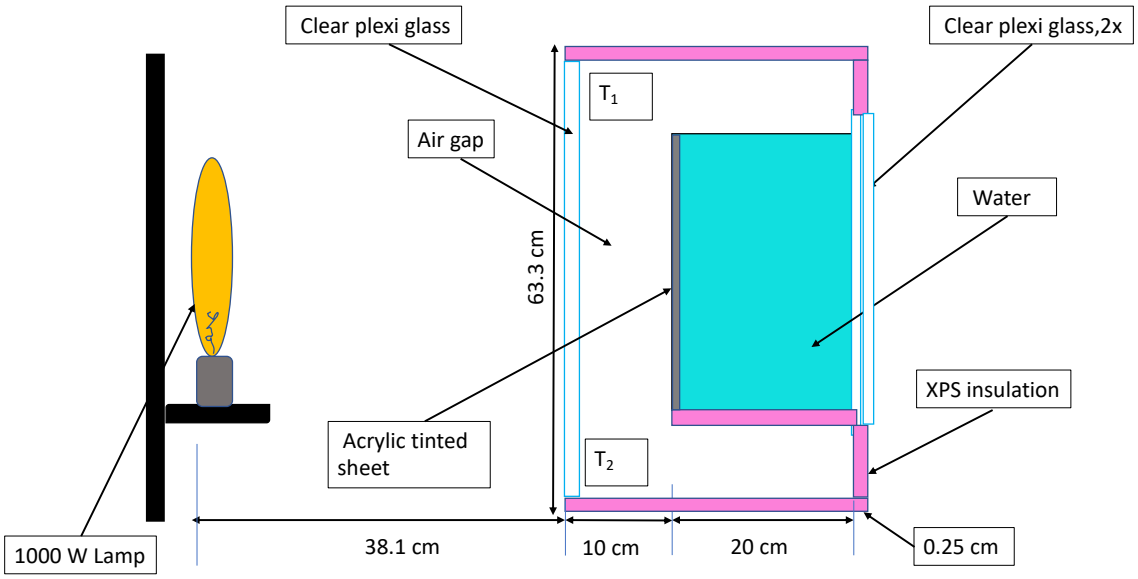

Figure 3.8 (d). Schematic showing the sideview of the Trombe wall prototype with a tinted acrylic sheet in water as the TES medium and two plexiglass sheets at the rear side

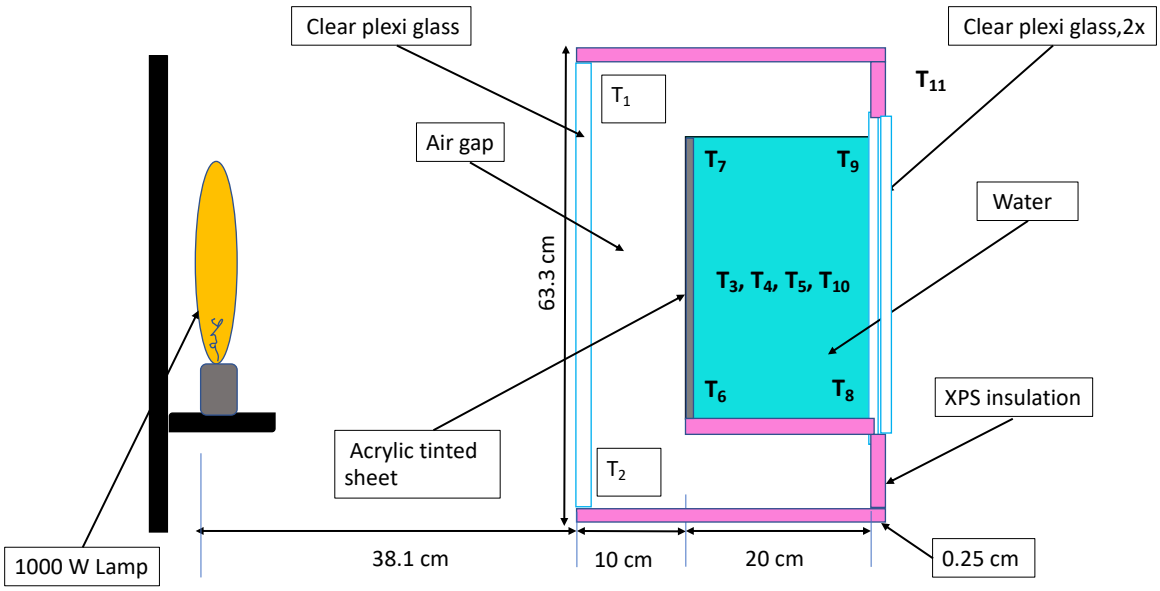

Figure 3.8 (e). Water container with K-type thermocouples mounted at different places

Type K thermocouples are mounted in different locations to analyze the thermal energy storage potential of the clear plexiglass water container within the Trombe wall prototype. There are a total of 11 thermocouples (labelled T1 through T11) used in the prototype and the positions of these thermocouples are shown in Figure 3.8 (e). The first two thermocouples T1, and T2 are installed at 20 cm from the glass and attached to the top and bottom insulation panel, which are used to measure the temperature in the air gap. There are eight other thermocouples mounted in the water container to measure the temperature at various locations. Thermocouples T6 and T7 are installed close to the front side of the water container (2.5 cm away from front side) at the bottom and top of the water container, respectively.

Similarly, thermocouples T8 and T9 are installed close to the back side of the water container (2.5 cm away from back side) at the bottom and top of the water container, respectively. Thermocouples T3, T10, and T5 are mounted in the horizontal mid-plane of the water container at 2.5 cm, 7.5 cm, and 17.5 cm from front of the container, respectively, and 15 cm from the top. Thermocouple T4 is mounted in the mid-plane of the container 2 cm from right side and 15 cm from the top. Thermocouple T11 is placed behind the Trombe wall prototype to record the room temperature. A two-point calibration was done to calibrate the thermocouples using ice water and

boiling water as two reference points. A Labjack data acquisition system (T7- Pro) is used to capture the readings from the thermocouples.

Experiments were conducted to determine the temperature profiles over time for thermocouples T1 through T11 for four cases as described below:

(i) Case 1: The TES medium is just water in a clear plexiglass container, and this serves as the reference case (see Figure 3.8 a).

(ii) Case 2: a 5 mm thick tinted acrylic sheet is integrated into the TES medium at the front of the water container (see Figure 3.8 b).

(iii) Case 3: The TES medium is just water in a clear plexiglass container, and there are two clear plexiglass sheets at the rear side of the Trombe wall prototype (see Figure 3.8 c).

(iv) Case 4: a 5 mm thick tinted acrylic sheet is integrated into the TES medium at the front of the water container, and there are two clear plexiglass sheets at the rear side of the Trombe wall prototype (see Figure 3.8 d).

Each experiment consisted of a charging period followed by a discharging period. The charging period is initiated by turning on the solar simulator lamp. The charging period lasts for 5 hours and is completed by turning the lamp off. The temperature measurements are continued as the discharging phase proceeds with the lamp off. The total duration of each experiment is 24 hours. The Trombe wall door and vents are always closed for these experiments, which is the expected operating configuration for summer conditions. Temperature profiles were measured over the entire experiment by recording the temperature from thermocouples T1 through T11 every 10 seconds.

3.4.1. Experimental methods for determining the effects of integrating a tinted acrylic sheet in water-based Trombe walls on their energy storage efficiency

The experiment is run for 24 hours, consisting of a 5-hour charging period when the lamp is turned on followed by a discharging period. Solar-simulated light from a lamp is used to illuminate the TES medium. The efficiency of a system is calculated as the ratio of output to total input. For the experimental model, the thermal efficiency is defined as follows:

$$\eta_{exp} = \frac{Q_{TES}}{Q_i} \quad (3.1)$$

Where, Q_{TES} is the energy stored in the water-based Trombe wall over the charging period, and Q_i is the total radiant energy incident onto the window of the Trombe wall prototype during the charging period. Q_{TES} is calculated as:

$$Q_{TES} = m \times c_p \times \Delta_T \ldots\ldots\ldots\ldots\ldots\ldots\ldots\ldots\ldots\ldots\ldots\ldots\ldots\ldots\ldots\ldots\ldots\ldots.. (3.2)$$

Where, m = (volume of the TES medium) x (density of the TES medium),

c_p is the specific heat of the TES medium, and

Δ_T = the average temperature of the TES medium at the end of the charging period minus its temperature at the beginning of the charging period. The average temperature at the end of the 5 hour charging period is estimated to be:

$$T_{avg,top\ water} = \frac{T_{top}+T_{middle}}{3} \ldots\ldots\ldots\ldots\ldots\ldots\ldots\ldots\ldots\ldots\ldots\ldots (3.3)$$

$$T_{avg,bottom\ water} = \frac{T_{middle}+T_{bottom}}{2} \ldots\ldots\ldots\ldots\ldots\ldots\ldots\ldots\ldots\ldots\ldots (3.4)$$

Where T_{top} is the temperature at the top, T_{middle} is the temperature at the middle, and T_{bottom} is the temperature at the bottom of the TES medium. Q_i is calculated as:

$$Q_i = average\ incident\ radiant\ energy\ flux \times time \times area$$

To calculate the average incident radiant energy form the solar simulated light provided by the lamp, the plexiglass at the front of the Trombe wall prototype is considered to be divided into equal areas in a 3 x 3 mesh. The incident light intensity is then measured at the centre of each of the nine areas in this mesh using a power meter (THORLABS, PM 100D), and the average of these measurements is taken as the average incident radiation. The results from these radiation measurements are reported in Section C.2 in the Appendix. The time used to calculate Q_i is five hours, which is the time the lamp is on during the charging phase. Furthermore, the thickness of the tinted acrylic sheet is not considered for thermal efficiency calculations because it's specific heat and volume is negligible as compared to that of the water.

CHAPTER 4: RESULTS

4.1. Simulation results

The simulation results for the cases described in Chapter 3 are discussed in the following sections. Section 4.1.1 presents the results for different Trombe walls considered under winter weather conditions. Section 4.1.2 shows the results for the simulation analysis of different Trombe walls under summer weather conditions and Section 4.1.3 shows simulation results for different Trombe walls comprising water walls with a total thickness of 20 cm under summer weather conditions.

4.1.1. Simulation analysis of different Trombe walls under winter weather conditions

Traditional Trombe walls often cause overheating in the summer season due to the storage of excess heat. However, water can be circulated, and heated water can be removed from water-based Trombe walls to prevent overheating. However, the performance of the water Trombe wall during the winter season is also of interest to see how it compares to conventional types of Trombe walls. This section presents the simulation analysis results for the building in Figure 3.1 with different Trombe walls under winter weather conditions. The different Trombe walls considered in this analysis have different thermal energy storage mediums which are shown in Figure 4.1 (the Trombe wall and building are identical for all cases considered, and only the thermal energy storage medium is varied). For all cases shown in Figure 4.1 solar energy is incident from the left side and is absorbed in the leftmost layer of the wall in the design builder simulations. There is no absorption for the case when the storage medium is just water. In this section the performance of thermal storage walls comprised of water are compared to thermal storage walls comprised of sand, which has typical properties for a TES medium in a Trombe wall.

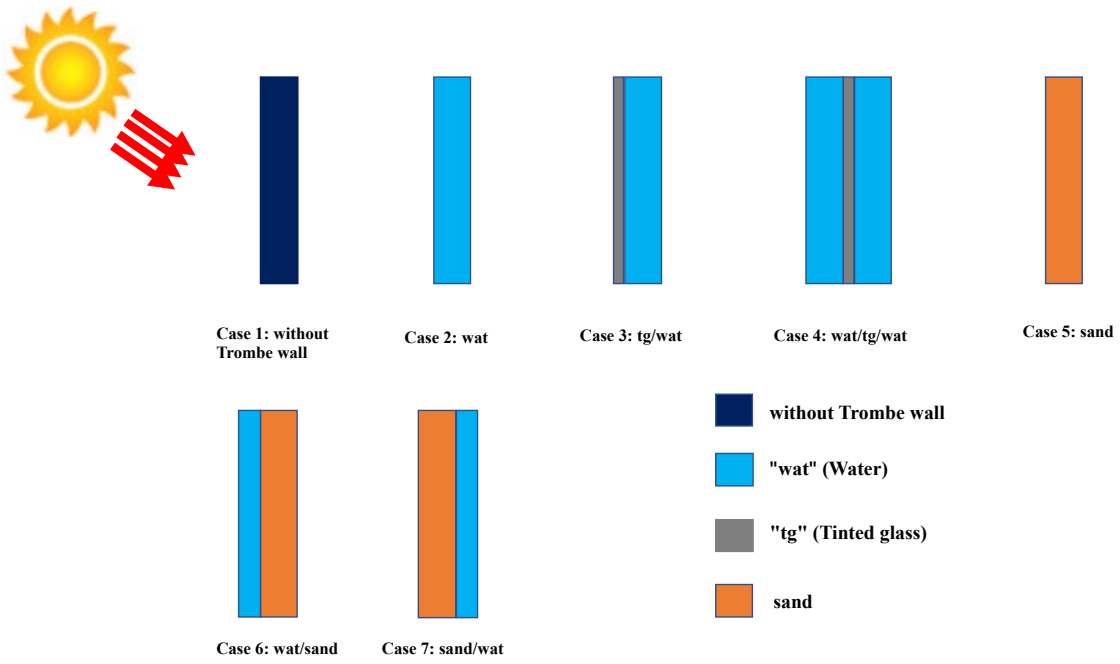

Figure 4.1. A schematic diagram of different cases of thermal energy storage mediums used in the Trombe wall facing south direction the Trombe wall facing south direction when simulating the building shown in Figure 3.1 during winter in Toronto, Ontario.

Some points to consider when comparing water with more common Trombe wall TES mediums, such as concrete or sand, are the differences in specific heat and how heat is transferred. Water has a specific heat of 4.186 kJ/(kg·K) and density of 1000 kg/m^3. Therefore, the heat capacity of water per unit volume is 4186 kJ/(m^3·K). On the other hand, concrete has a specific heat of 0.880 kJ/(kg·K) and density of 2300 Kg/m^3. Therefore, the heat capacity of concrete per unit volume is approximately 2024 kJ/(m^3·K). Moreover, the specific heat of sand is 0.83 kJ/(kg·K) and its density is 1500 kg/m^3. Therefore, the heat capacity of sand per unit volume is 1245 kJ/(m^3·K). Therefore, a water wall can store more than double the amount of heat compared to a traditional Trombe wall made of concrete, bricks or sand for a given volume.

It should be noted that in water Trombe walls, heat transfer during charging and discharging processes take place by convection, whereas the charging and discharging processes takes place by conduction in concrete or sand walls. [53] Convection is a more efficient heat transfer mechanism, however, in the Design Builder simulations presented in this work it is assumed the water within the TES medium does not move. Thus, it is assumed heat transfer in the water wall occurs by conduction and convection is not accounted for.

4.1.1.1. Comparison of total heating load for different cases of Trombe walls

One method of evaluating the performance of Trombe walls during the winter months is to monitor its ability to reduce the building heating load. To analyze the performance of the TES walls shown in Figure 4.2, the total building heating load over three days (Feb 2, Feb 3, and Feb 4, 2021) was simulated for different thicknesses of the TES medium. The results for the best cases are shown in Table 4.1.

Table 4.1 Best zone heating load results for different Trombe wall configurations

Cases	Trombe wall configuration	Best results for the heating load (W/m^2)
1	Without Trombe wall	4004.04
2	Water	4386.2
3	Tinted glass (tg) /water (wat)	1922
4	Water (wat)/ tinted glass (tg) / water (wat)	1844.57
5	Sand	2060.42
6	Water (wat)/sand	1841.36
7	Sand/water (wat)	1868.69

The heating load of the building is calculated when there is no Trombe wall and is plotted in Figure 4.2. The total heating load is approximately 4000 W/m^2 when the building doesn't have any Trombe wall. The heating loads for the thermal storage wall thicknesses that yielded the lowest heating load for each type of thermal storage walls considered (shown in the last column in Table 4.1) are also plotted in Figure 4.2. Of the cases considered, the building has the highest heating load of about 4127 W/m^2 when the thermal storage medium is a 40 cm thick water wall. This is because the water wall does not absorb incident solar radiation unless tinted glass is inserted within it, such as for Case 3 which has a much lower heating load of 1922 W/m^2. For all other cases considered the heating load is less than half that for the case when the water Trombe wall is used. A minimal heating load of about 1841 W/m^2 occurs for the case when the thermal storage medium is comprised of a 6 cm thick water wall on the outer side and a 17.5 cm thick sand wall on the inner side (e.g., wat(6cm)/sand(17.5cm)).

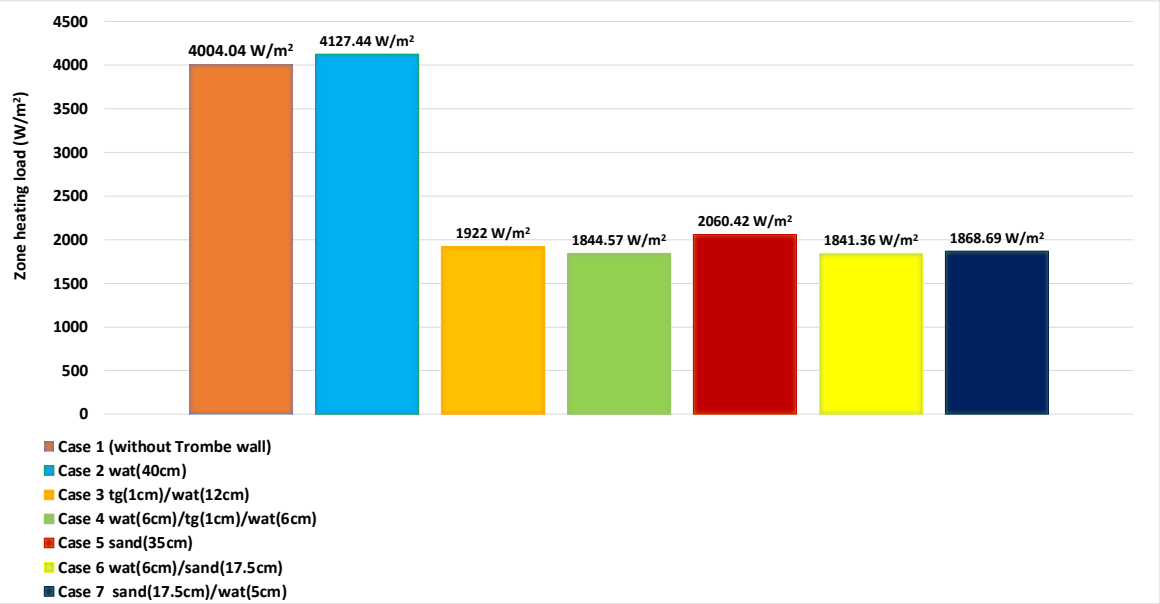

Figure 4.2. Comparison between the best cases of total heat load normalized by floor area (W/m^2) for three consecutive days (Feb 2, Feb 3 and Feb 4, 2021) in the room based on the optimal Trombe wall thickness during winter in Toronto, Ontario

4.1.1.2. Comparison of hourly heating load for different cases of Trombe walls

Figure 4.3 shows a comparison of the hourly zone heating load between the seven different cases of Trombe walls shown in Figure 4.1 for three consecutive days (Feb 2nd, Feb 3rd and Feb 4th) for the single-room building shown in Figure 3.1 The zone heating load of the building is between 50-60 W/m^2 when there is no Trombe wall. The results show that the zone heating load decreases during sunshine hours from 11 am to 2 pm for the cases when the Trombe wall is built into the building. The zone heating load increases from 2 am to 10 pm. For the cases plotted in Figure 4.3, the zone heating load is higher when a water wall with 40 cm thickness is used, and the heating load is the lowest for a 2-layer 22.5 cm thick sand and water wall. For example, on Feb 3rd the maximum zone heating load is recorded to be about 68 W/m^2 when a 40 cm thick water wall is used whereas the maximum load is around 46 W/m^2 for a 22.5 cm thick sand and water wall.

On the other hand, the minimum load for the 40 cm thick water wall is approximately 35 W/m^2 and the load is 0 W/m^2 for 22.5 cm thick sand and water wall during sunshine hours. Notably,

the heating loads shown in Figures 4.2 and 4.3 for the cases when the Trombe wall is comprised of tinted glass and water is comparable to the heating load for the case when the storage medium within the Trombe wall is water and sand (e.g., wat(6cm)/sand(17.5cm)). That is, the heating load shown in Figure 4.2 for tg(1cm)/wat(12cm) is about 1870 W/m^2, and the heating load for wat(6cm)/tg(1cm)/wat(6cm) is 1790 W/m^2. These results suggest the performance of the Trombe walls comprised of tinted glass and water are almost as good as the best performing Trombe walls considered during winter weather conditions.

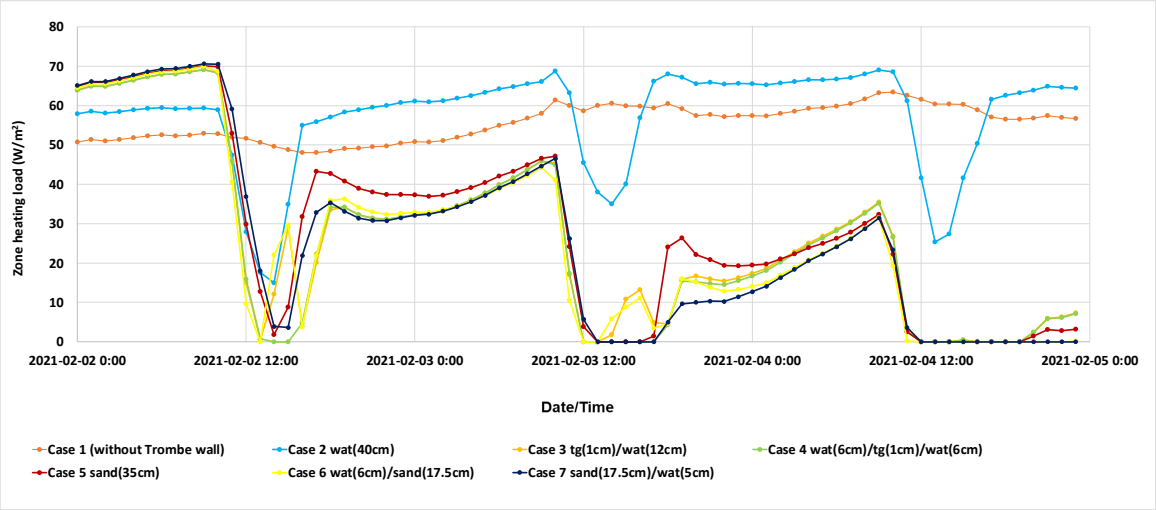

Figure 4.3. Hourly heating load normalized by floor area (W/m^2) for the single room building shown in Figure 3.1 for different Trombe wall configurations over three consecutive days (Feb 2, Feb 3, and Feb 4, 2021) in Toronto, Ontario.

4.1.1.3. Comparison of heat transferred through the different surfaces of storage wall

Figure 4.4 shows the heat transferred from the air channel into the storage wall (solid lines) for the six different cases of Trombe walls considered in this section. A maximum heat transfer of around 460 W/m^2 enters the storage wall during the peak sunshine hours between 12:00 pm to 1:00 pm on Feb 2nd for the sand storage wall of 35 cm and storage wall comprised of water (6cm) and sand (17.5cm).

The minimum heat transfer of around 121 W/m^2 enters the storage wall during the peak sunshine hours between 12:00 pm to 1:00 pm on Feb 2nd when the storage wall is comprised of

water and the wall thickness is 40 cm. It happens because solar absorptance and visible absorptance properties of water are set to 0, whereas solar absorptance and visible absorptance for sand are set to 1 in Design Builder. Therefore, sand is effectively absorbing the solar energy that passes through the glazing and air channel and is incident onto the TES medium, whereas the pure water wall is not. The heat transferred from the storage wall into the room is shown by the dashed lines in Figure 4.4. The maximum heat flow is around 35 W/m^2 when the storage wall thickness is 22.5 cm and is made of sand. The heat flux vs time curves shown in Figure 4.4 for the storage wall with tinted glass and water (tg(1cm)/wat(12cm)) are comparable to that for the storage wall comprised of sand (sand(35cm)).

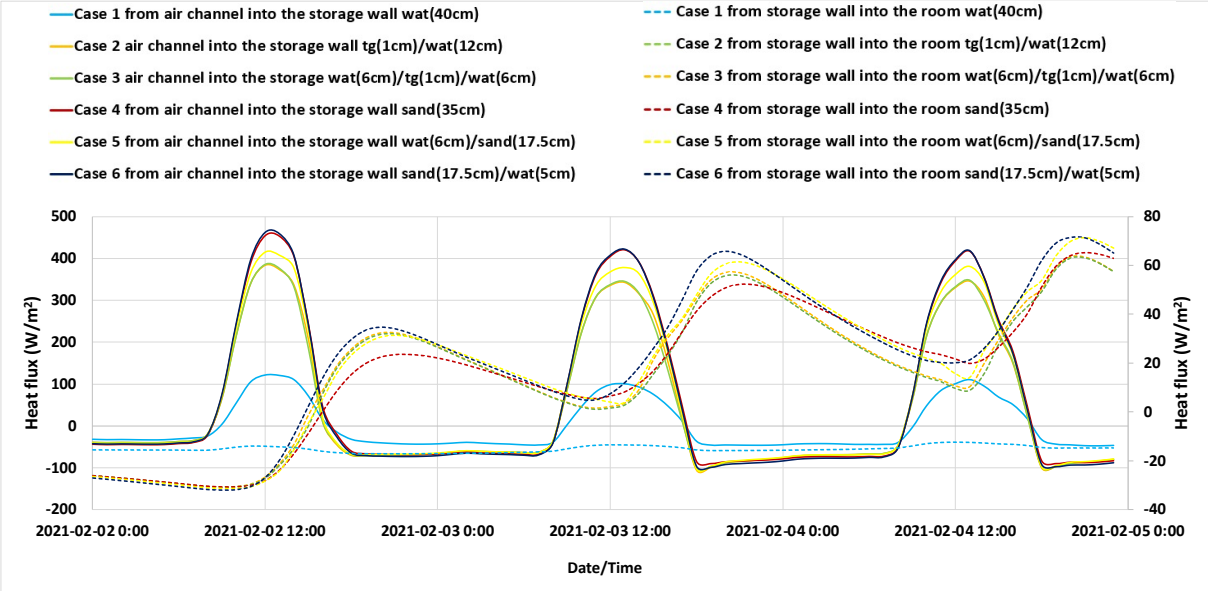

Figure 4.4. Comparison of heat transferred (W/m^2) through the different surfaces of storage wall (solid lines) to the room (dashed lines) normalized by floor area (W/m^2) for the single room building shown in Figure 3.1 for the optimal Trombe wall thickness during winter on Feb 2, Feb 3, and Feb 4, 2021, in Toronto, Ontario.

4.1.1.4. Comparison of heat transferred to the room from vent and storage wall

Figure 4.5 shows a comparison of heat transferred to the room from the vent and from the storage wall for the 6 different cases of Trombe walls (solid lines) for three consecutive days (Feb 2nd, Feb 3rd and Feb 4th) under winter weather conditions in the single-room building shown in Figure 3.1 based on the optimal Trombe wall thickness. A maximum heat transfer of around 56 W/m^2 enters the room during the peak sunshine hours between 12:00 pm to 1:00 pm on Feb 2nd for the sand storage wall of 35 cm, 13 cm, and 23.5 cm thicknesses. The minimum heat transfer

of around 24 W/m^2 enters the storage wall during the peak sunshine hours between 12:00 pm to 1:00 pm on Feb 2nd when the storage wall is made of water and wall thickness is 40 cm. The heat transferred from the storage wall into the room is shown by the dashed lines in Figure 4.5. The maximum heat flow is around 61 W/m^2 when the storage wall thickness is 23.5 cm and is made of water and sand. Notably, the heat flux vs time curves in Figure 4.5 for the case of the water wall with tinted glass (tg(1cm)/wat(12cm)) are similar to that for the storage wall made from sand (sand(35cm)).

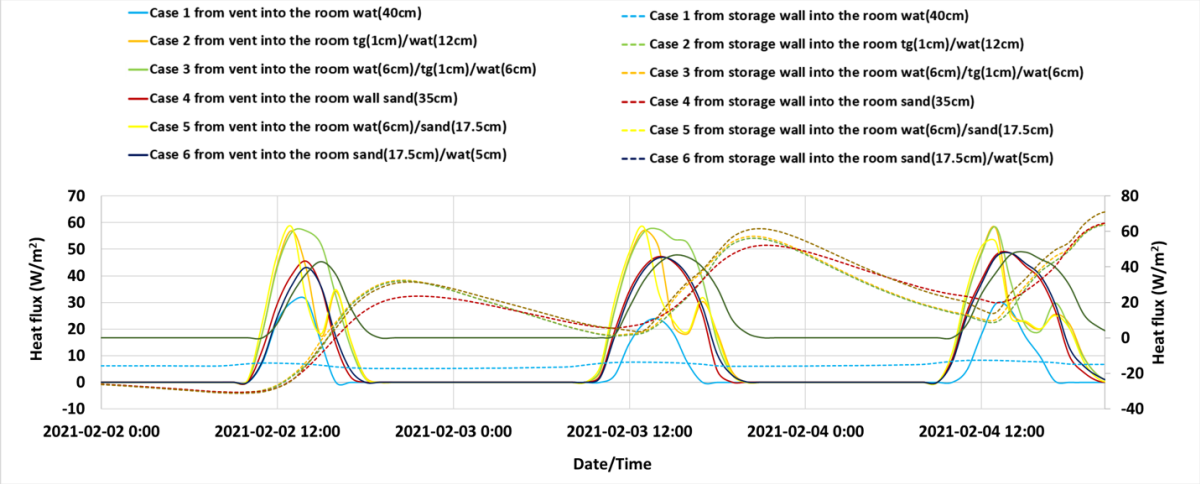

Figure 4.5. Comparison between the best cases of heat transferring to the room (W/m^2) from vent (solid lines) and storage wall (dashed lines) normalized by floor area (W/m^2) for the single room building shown in Figure 3.1 based on the optimal Trombe wall thickness during winter on Feb 2, Feb 3, and Feb 4, 2021, in Toronto, Ontario

The results shown in Figures 4.2 to 4.5 show that the performance of the Trombe wall with a water wall integrated with tinted glass is very close to the case when the Trombe wall has a storage medium made of sand. The tinted glass effectively absorbs most of the sunlight which results in heating the adjacent water, which acts as a good TES medium, especially considering its high heat capacity. This section has shown the performance of a water-based Trombe wall can be very close to that of a sand-based Trombe wall under winter conditions. Thus, there is not a big disadvantage to using a water-based Trombe wall during winter conditions. The results in the next section are used to evaluate the benefits of using a water-based Trombe wall during the summer season.

4.1.2. Simulation analysis of different Trombe walls under summer weather conditions

This section presents the simulation analysis results for different Trombe walls under summer weather conditions. The different thermal storage mediums considered in this analysis are shown in Figure 4.6. Simulations were performed to estimate the effects of the storage medium thickness on the thermal energy stored, building cooling load and heat flux entering the building from the Trombe wall for all cases shown in Figure 4.6. The effects of thickness on these parameters for when the storage medium is just water (case 1 in Figure 4.7) are presented in Section 4.1.2.1.1 while effects of the storage medium thickness for all other cases can be found in Appendix B. The Trombe wall configurations for the summer weather conditions are different than the winter cases because the objective for the summer is to prevent overheating by extracting the heated water from the top of the Trombe wall to use it for applications other than space heating such as showering, washing clothes and dishes, and providing pre-heated water for the hot water tank.

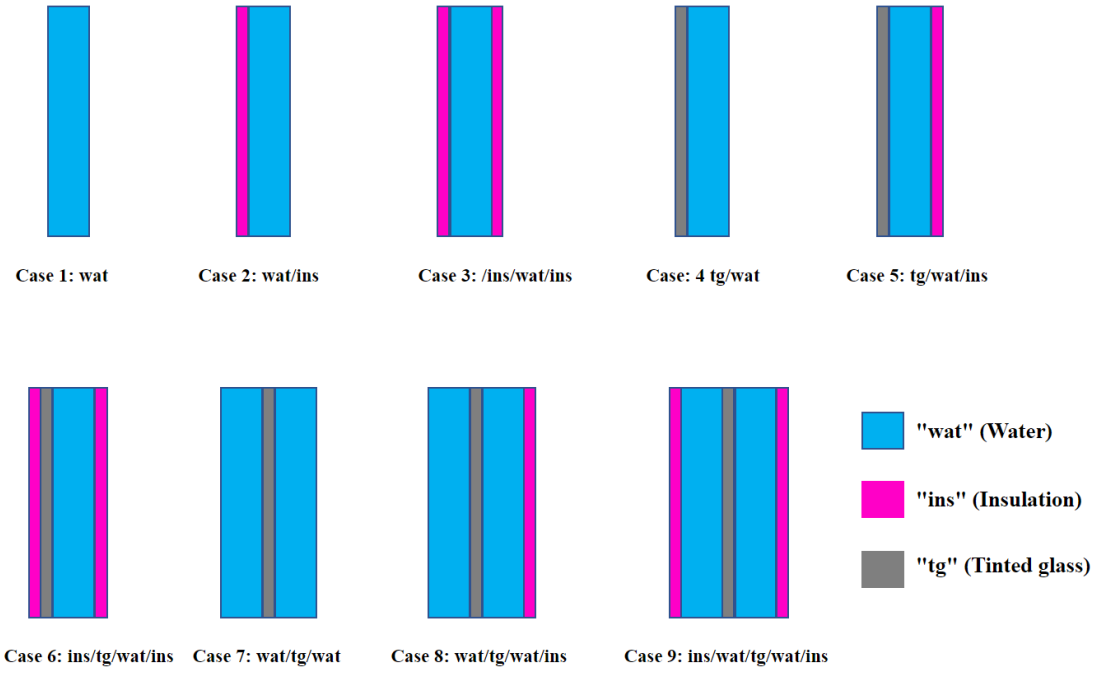

Figure 4.6. A schematic diagram of different cases of Trombe wall considered for during summer on July 15th, 2020, in Toronto, Ontario

4.1.2.1. Simulation results for a water Trombe wall under summer weather conditions

4.1.2.1.1. Effects of thickness on the thermal energy stored in a water Trombe wall under summer conditions

Figure 4.7 shows the results for the thermal energy stored in a water Trombe wall as its thickness increases from 5 cm to 40 cm in increments of 5 cm. For example, on July 15th, a maximum thermal energy of about 70 MJ is stored in a water Trombe wall that has a thickness of 40 cm. On the other hand, about 7.3 MJ is stored in the 5 cm thick water Trombe wall on July 15th.

Similarly, the maximum temperature (T_M) increases slightly with increasing thickness of the wall. For example, there is an approximately 0.6 °C increase in T_M on July 15th when the thickness changes from 5 cm to 40 cm. The maximum temperature difference between the outdoor temperature and the average temperature of the water within the storage wall on July 15th is shown as ΔT in Figure 4.7. ΔT increases with an increase in the thickness of the wall. For example, on July 15th the value of ΔT increases by approximately 0.6 °C when the water wall thickness increases from 5 cm to 40 cm.

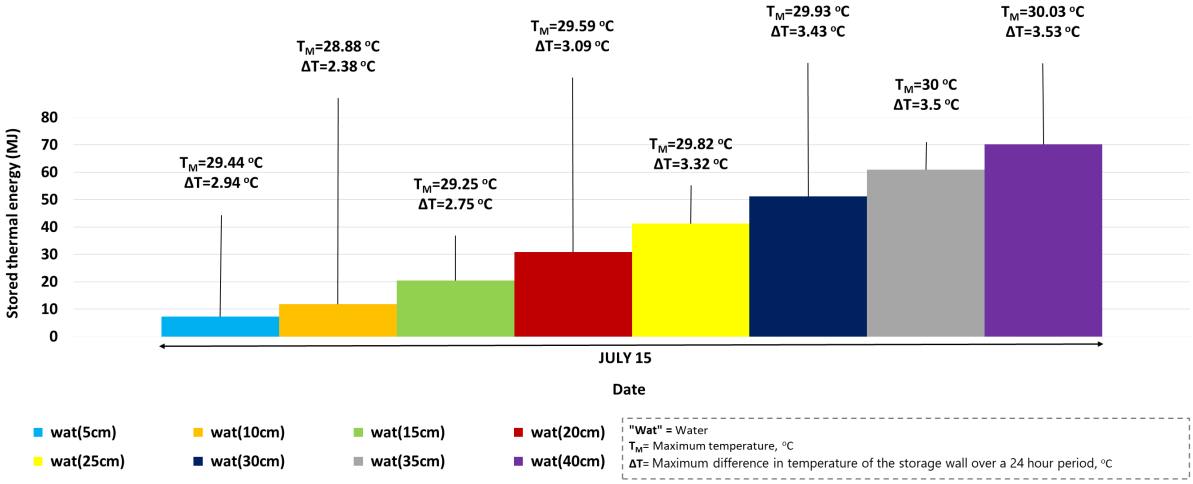

Figure 4.7. Thermal energy stored in a Trombe wall consisting of storage wall of varying thickness made of water during summer on July 14, July 15, and July 16, 2020, in Toronto, Ontario

4.1.2.1.2. Effects of thickness on heat transferred through the surfaces of the water storage wall under summer conditions

Figure 4.8 shows the heat transferred from the water Trombe wall air channel to the storage wall (solid lines) and the heat transferred from the storage wall into the building (dashed lines) for varying thicknesses of the water wall. Results show that heat enters the storage wall from the air channel during peak sunshine hours from 11:00 to 13:00 and is a maximum at 13:00. For the simulations carried out for the conditions on July 15th the maximum heat transferred from the air channel to the storage wall increases from ~ 67.6 to ~76.9 W/m^2 as the wall thickness decreases from 40 cm to 5 cm. Thus, the amount of heat entering the storage wall as a result of changing the storage wall thickness is relatively small. During the night hours the heat transferred from the storage wall to the air channel is negative, indicating that heat flows from the storage wall into the air channel. For example, at 2:00 am on July 15th the heat transferred from the storage wall into the air channel is about 20 W/m^2.

As shown by the dashed lines in Figure 4.8, when the water wall is from 10 cm to 40 cm thick, heat flow across the interior surface of the Trombe wall is always in the direction from the storage wall to the room. There is no significant effect of wall thickness on the amount of heat transferred from the storage wall to the room when the thickness is above 10 cm. The maximum amount of heat transferred into the room from 9:00 am to 5:00 pm is between 20 – 25 W/m^2 when the thickness of the wall is larger than 10 cm. When the thickness of the storage wall is 5 cm and 10 cm, the maximum heat transferred is around 48 W/m^2 and 32 W/m^2 at around 5:00 pm on July 15th, respectively. During the night hours, the heat transfer from the storage wall to the room is about 15 W/m^2, and when the sun is shining the heat transfer ranges from about 25 to 30 W/m^2. For the Trombe wall that is 5 cm thick, the amount of heat transferred from the storage wall to the

room peaks at a higher value of over 48 W/m^2. Also, during the night hours, the heat transferred from the 5 cm thick storage wall to the room is very low and reaches a value of almost 0 W/m^2.

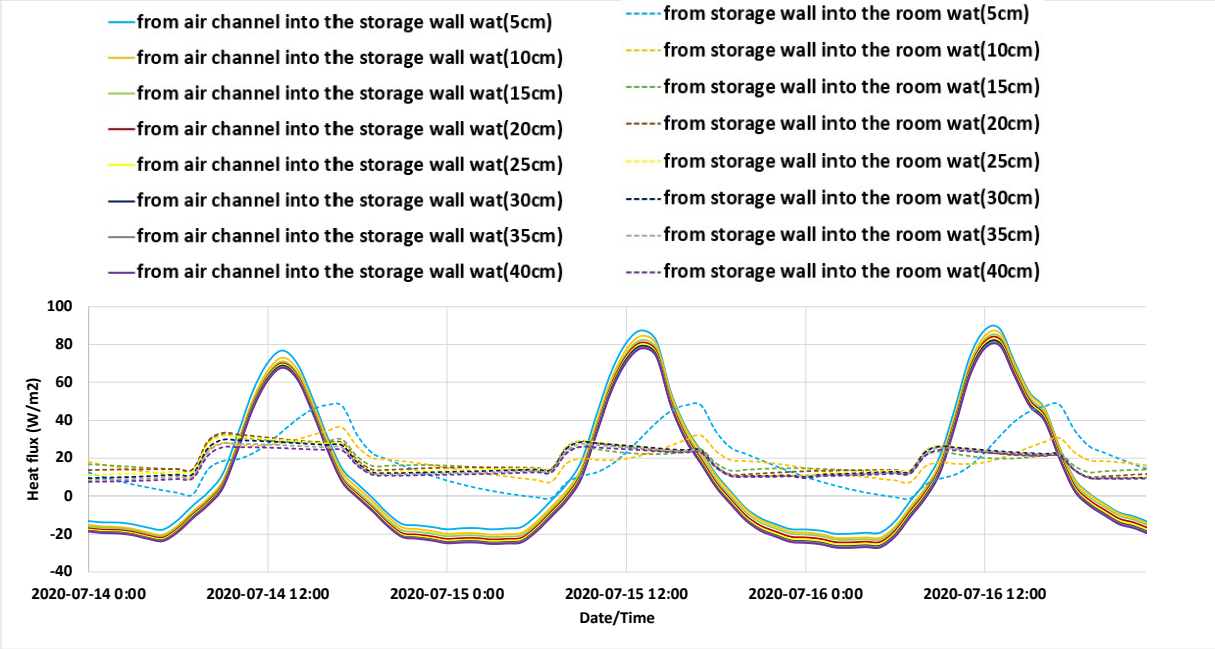

Figure 4.8. Heat transferred from the air channel into the storage wall (solid lines) and from the storage wall to the room (dashed lines) normalized by floor area (W/m^2) for the Trombe wall model shown in Figure 3.1on July 14, July 15, and July 16, 2020, in Toronto, Ontario.

4.1.2.1.3. Hourly zone cooling load for the case of the water Trombe wall under summer conditions

Figure 4.9 shows the hourly cooling load for three consecutive days (July 14, 15, and 16) for the single-room building shown in Figure 3.1 for the case when the Trombe wall has a water storage wall of varying thickness. The results show that the zone cooling load during peak hours decreases as the Trombe wall thickness increases. For example, on July 14th at around 8 am the zone cooling load is around 70 W/m^2 when the wall is 5 cm thick and is about 55 W/m^2 when the water wall is 40 cm thick. Similarly, the cooling load in the evening on July 14th around 5 pm is recorded to be 53 W/m^2 for a 5 cm thick wall. On the other hand, the cooling load on the same day/time is reduced to 43 W/m^2 with an increase in wall thickness to 40 cm.

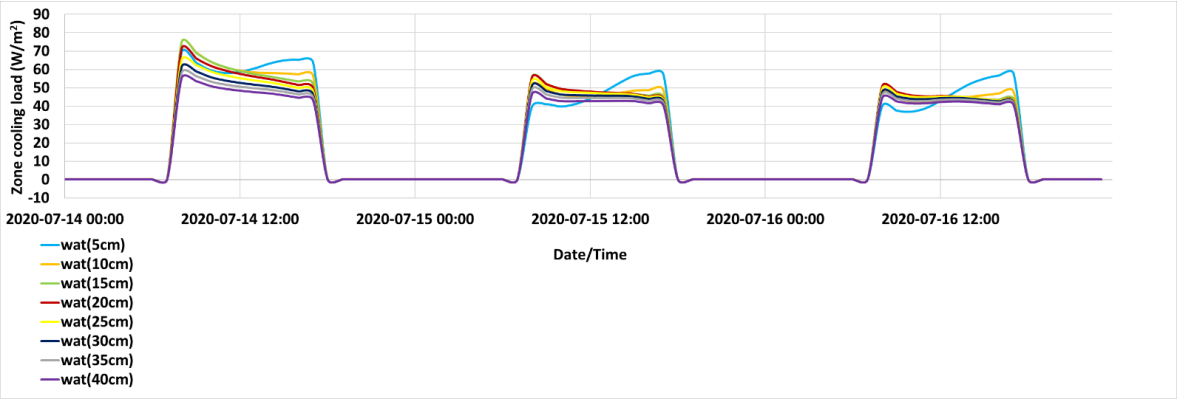

Figure 4.9. Hourly cooling load normalized by floor area (W/m^2) for three consecutive days (July 14, July 15, and July 16, 2020) in a Trombe wall model consisting of storage wall of varying thickness made of water during summer in Toronto, Ontario

4.1.2.1.4. Total cooling load for three consecutive days for the case of the water Trombe wall under summer conditions

Figure 4.10 shows the total cooling load for three consecutive days (July 14, 15, and 16) for the building shown in Figure 3.1 when the Trombe wall is comprised of a water storage wall of varying thickness. The results show that the total cooling load decreases with an increase in the Trombe wall thickness. For example, the total cooling load when the Trombe wall is 40 cm thick is 15% less than when the Trombe wall is 5 cm thick.

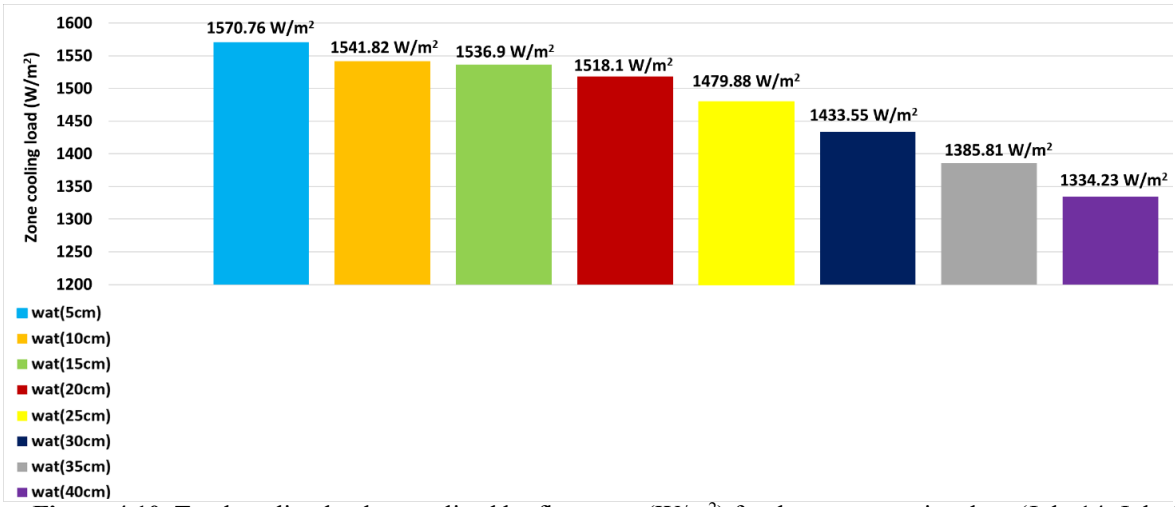

Figure 4.10. Total cooling load normalized by floor area (W/m^2) for three consecutive days (July 14, July 15, and July 16, 2020) in a Trombe wall model consisting of a storage wall of varying thickness made of water during summer in Toronto, Ontario

As shown in the previous figures, the general effect of increasing the thickness of the storage wall is to increase the amount of stored thermal energy and to decrease the total cooling load. Similar trends are observed for the other cases (cases 2 through 9 shown in Figure 4.10) and the results are presented in Appendix B. To compare the performance of the different storage wall configurations shown in Figure 4.11, the total thickness of the water layers for each case is set to 20 cm, and the results are presented next in Section 4.1.3.

4.1.3. Simulation results for different Trombe walls comprising water walls with a total thickness of 20 cm under summer weather conditions

This section presents the comparison of the thermal energy stored in Trombe walls consisting of water storage walls with a total thickness of 20 cm. A thickness of 20 cm is selected since it provides a good balance between having a large amount of thermal energy storage capacity and a reasonably sized wall (for example, the 5 cm thick water walls do not perform as well as the thicker walls whereas a 40 cm thick wall has a higher mass and volume). Furthermore, the thickness of the water walls in the experiments are 20 cm. Therefore, the simulation results for water walls with 20 cm thickness is discussed in this section. The different Trombe walls considered in this analysis are shown in Figure 4.11.

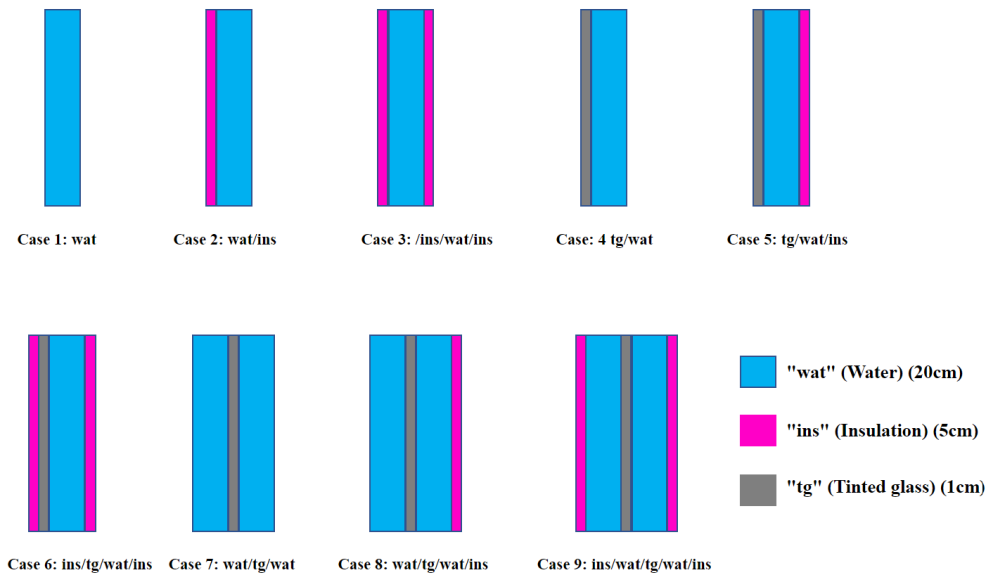

Figure 4.11. A schematic diagram of comparison of thermal energy stored in different Trombe wall models with 20 cm wall thickness during summer on July 15th, 2020, in Toronto, Ontario. The cases are similar to those shown in Figure 4.6, but with the thicknesses of the layers indicated.

4.1.3.1. Comparison of thermal energy stored in different Trombe walls with a total thickness of 20 cm under summer weather conditions

Figure 4.12 shows a comparison of the thermal energy stored in Trombe walls consisting of water storage walls with a total thickness of 20 cm. The simulations used to attain these results were performed using the weather data for July 15, 2020, in Toronto, Ontario. For the bare water storage wall, wat(20cm), 30.79 MJ of thermal energy is stored, ΔT is 3.09 °C, and T_M is 29.59 °C. When tinted glass is placed at the outer surface of the water wall, to form tg(1cm)/wat(20cm), the amount of thermal energy stored increases to 111.7 MJ, ΔT is 11.22 °C, and T_M is 37.72 °C. When the 5 cm thick insulation layer is placed at the inner surface of the water wall, to form wat(20cm)/ins(5cm), the amount of thermal energy stored increases to 111.6 MJ, ΔT is 11.22 °C, and T_M is 37.72 °C.

When tinted glass is placed at the outer surface of the water wall and insulation is placed at its inner surface, to from tg(1cm)/wat(20cm)/ins(5cm), the amount of thermal energy stored increases to 279.75 MJ, ΔT increases to 28.1 °C and T_M increases to 54.6 °C. When insulation is placed on either side of the water wall, to form ins(5cm)/wat(20cm)/ins(5cm) the amount of thermal energy stored is 137.68 MJ, ΔT is 13.83 °C, and T_M is 40.33 °C.

When the water wall has tinted glass at its outer surface and insulation on both surfaces, as in the case of the ins(5cm)/tg(1cm)/wat(20cm)/ins(5cm) sample, the amount of thermal energy stored increases to 302.08 MJ, ΔT increases to 30.3 °C, and T_M increases to 56.84 °C. If the tinted glass is placed at the midplane of the water storage medium rather than its outer surface, to form ins(5cm)/wat(10cm)/tg(1cm)/wat(10cm)/ins(5cm), T_M for the outer portion of the water wall increases slightly to 57.7 °C, although T_M for the inner portion of the water wall slightly decreases to 56.1 °C. The total thermal energy stored for ins(5cm)/wat(10cm)/tg(1cm)/wat(10cm)/ins(5cm) is 302.6 MJ.

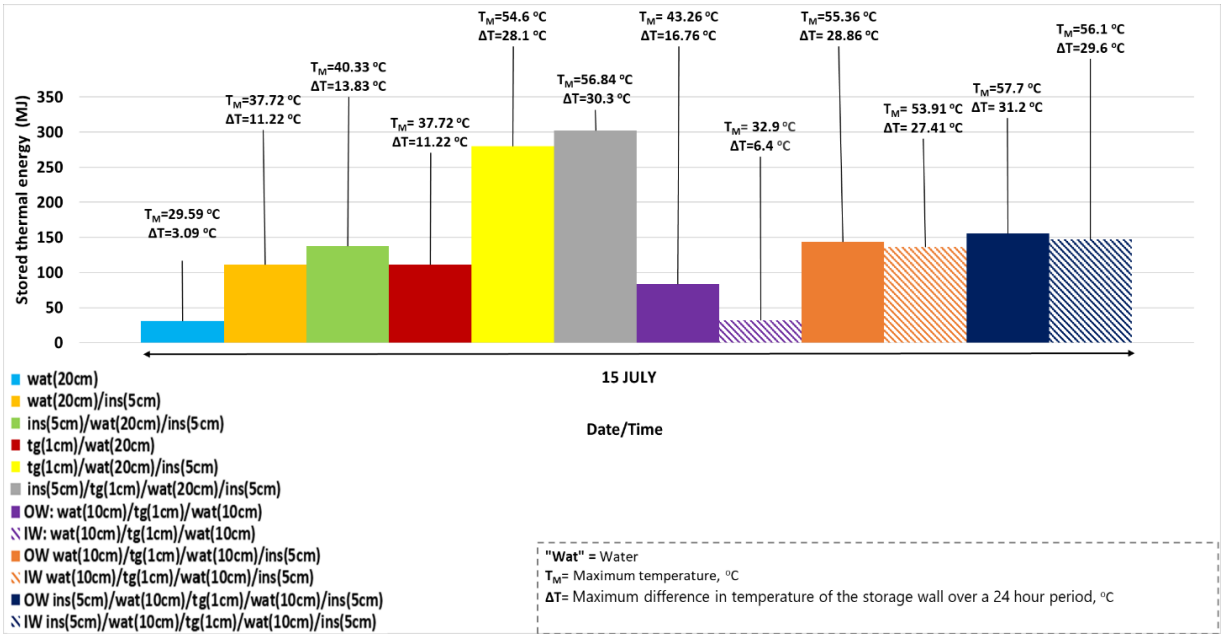

Figure 4.12. Comparison of thermal energy stored in different Trombe wall models with 20 cm wall thickness during summer on July 15th, 2020, in Toronto, Ontario (OW and IW refer to the outer and inner parts of the thermal energy storage medium, respectively)

4.1.3.2. Comparison of heat transferred through the surface of the storage walls consisting of 20 cm thick water layer during summer conditions

Figure 4.13 (a) shows a comparison of heat transferred from the air channel to the storage wall for different cases of Trombe walls (solid lines) that have water storage walls with a total thickness of 20 cm. Figure 4.13 (b) shows the hourly outside dry bulb temperature and solar irradiance for July 14, July 15, and July 16 in Toronto, Ontario. The results shown in Figure 4.40

are from simulations performed for the model building shown in Figure 3.1 using weather data for July 14, July 15, and July 16 in Toronto, Ontario.

A maximum heat transfer of around 164 W/m^2 enters the storage wall from the air channel during the peak sunshine hours between 12:00 pm to 1:00 pm on July 14 for the case when the storage wall is made of two 10 cm thick water layers with 1 cm thick tinted glass at the middle (wat(10cm)/tg(1cm)/wat(10cm)).

During the peak sunshine hours between 12:00 pm to 1:00 pm the least amount of heat (around 18 W/m^2) transferred from the air channel to the storage wall occurs for the case when the Trombe wall is comprised of a 20 cm thick water with 5cm thick insulation on both sides. The heat transferred from the storage wall into the room is shown by the dashed lines in Figure 4.13 (b). The maximum heat flow is around 60 W/m^2 when the storage wall consists of two 10 cm thick water layers with 1 cm thick tinted glass at the mid-plane.

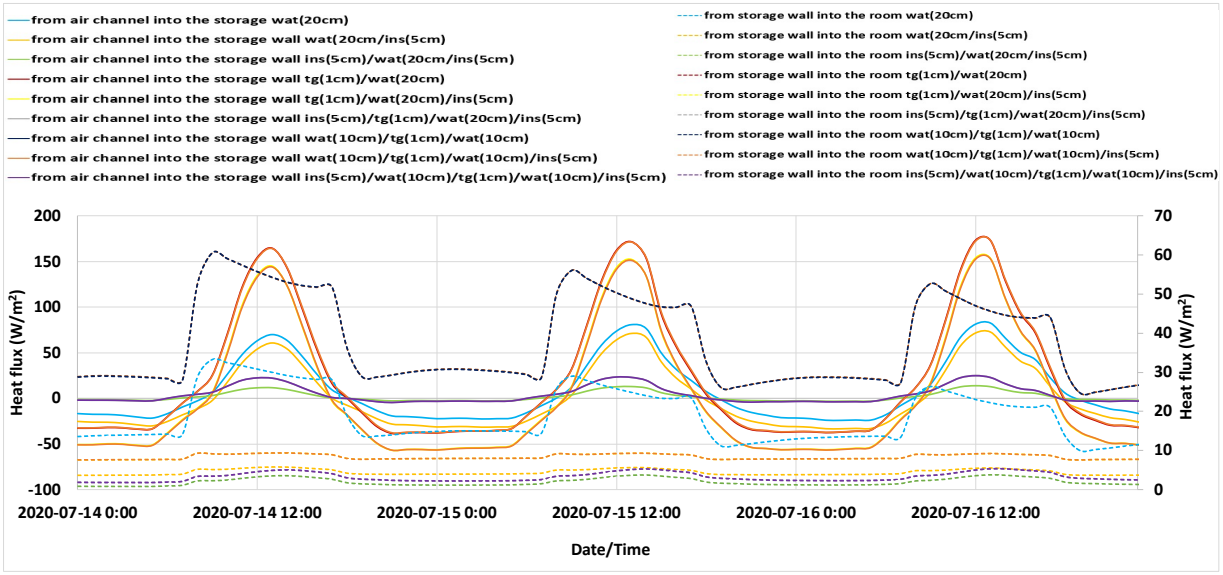

Figure 4.13 (a). Comparison of heat transferred from the air channel to the storage wall (solid lines) and from the storage wall to the room (dashed lines) normalized by floor area (W/m^2) for different Trombe walls comprised of water walls with a total thickness of 20 cm for three consecutive days (July 14, July 15, and July 16, 2020) in Toronto, Ontario

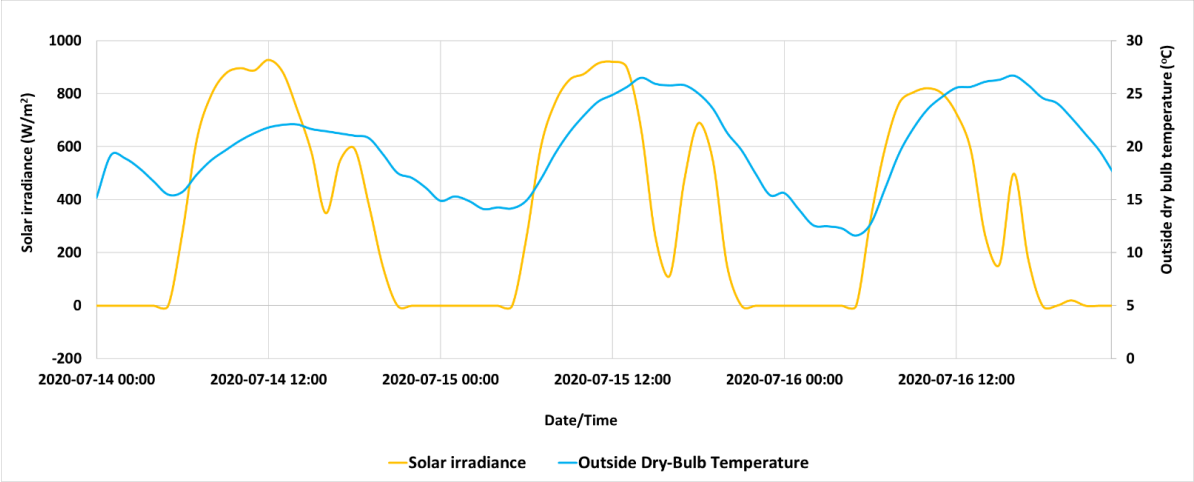

Figure 4.13 (b). Hourly outside dry bulb temperature and solar irradiance for July 14, July 15, and July 16 in Toronto, Ontario

4.1.3.3. Comparison of hourly zone cooling load in different Trombe walls consisting of 20 cm thick water layer under summer weather conditions

Figure 4.14 shows the hourly cooling load for three consecutive days (July 14, 15, and 16) for the single room building shown in Figure 3.1 for different cases when the Trombe wall consists of water walls with a total thickness of 20 cm. The results show that the zone cooling load during peak hours increases when the Trombe wall consists of a 20 cm thick water layer followed by a 5 cm thick insulation. On the other hand, the zone cooling load decreases for the Trombe wall consisting of a 20 cm thick water layer surrounded by 5 cm thick insulation layers on both sides.

For example, on July 14th at around 8 am the zone cooling load is around 120 W/m^2 for a storage wall made of 20 cm water and 5 cm insulation layer, and the cooling load decreases to 80 W/m^2 at around 5:00 pm on the same day. However, the cooling load on July 14th at around 8:00 am is around 34 W/m^2 when the wall is made of 20 cm thick water wall with 5 cm thick insulation on both sides and it is reduced to 24 W/m^2 at around 5 pm on the same day.

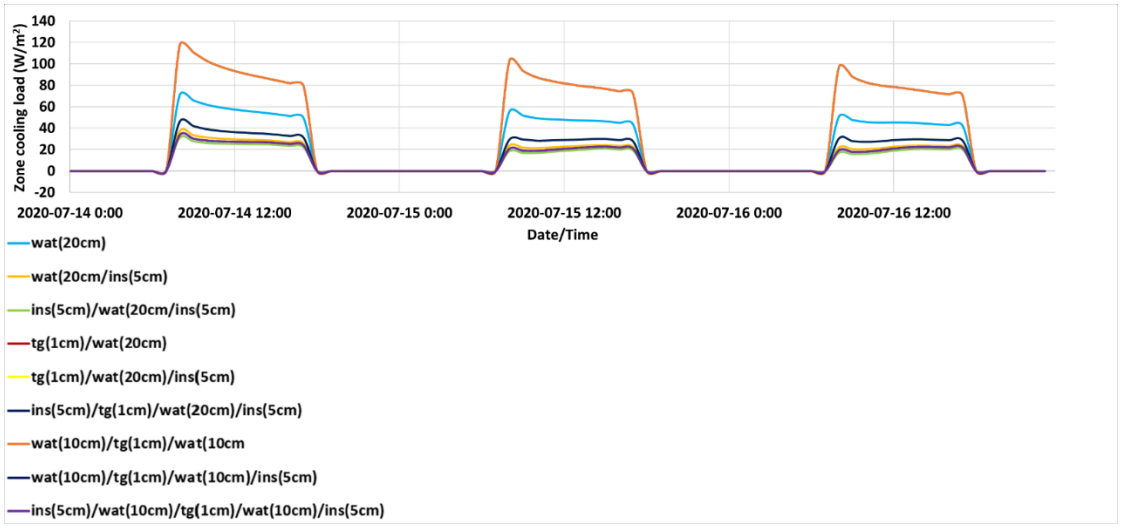

Figure 4.14. Comparison of hourly zone cooling load normalized by floor area (W/m^2) in different water Trombe wall with 20 cm thickness during summer on July 14, July 15, and July 16, 2020, in Toronto, Ontario

4.1.3.4. Comparison of total cooling in different Trombe walls consisting of 20 cm thick water layer under summer weather conditions

Figure 4.15 shows the total cooling load for the building shown in Figure 3.1 when the Trombe wall consists of a 20 cm thick water storage wall over three consecutive days (July 14, 15, and 16) in summer. The results show the total cooling load is increased to approximately 2568 W/m^2 for 20 cm water wall with 5 cm insulation on one side (represented by red color in the Figure 12(e)), and 10 cm thick water walls with 1 cm thick tinted glass at the middle (represented by orange color in the Figure 4.42. On the other hand, the cooling load is decreased to about 627 W/m^2 when the storage wall has a 20 cm thick water layer at the middle with 5 cm thick insulations on both sides.

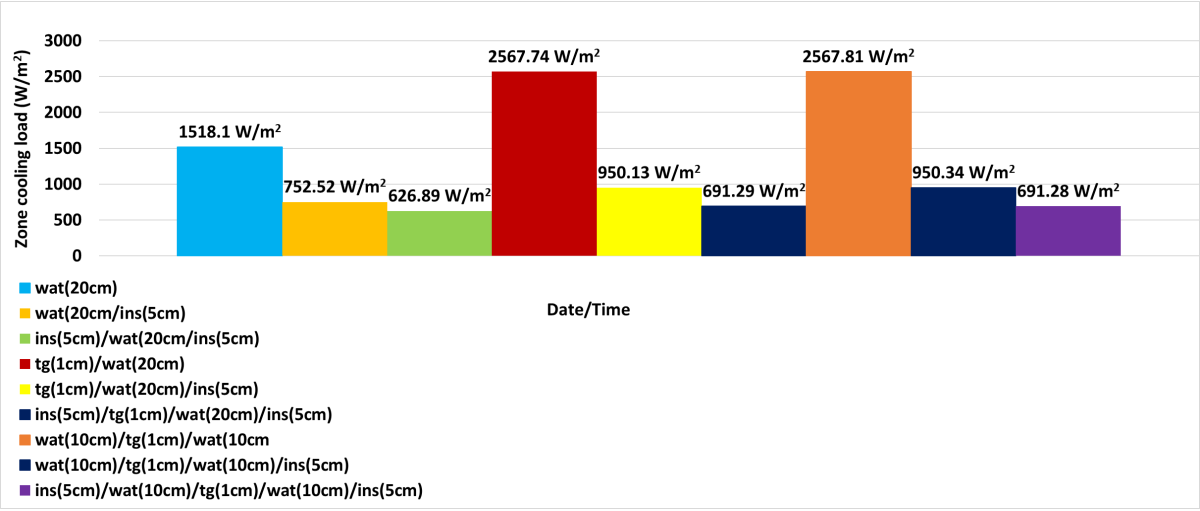

*=

Figure 4.15. Comparison of total cooling load in different water Trombe wall with 20 cm thickness during summer on July 14, July 15, and July 16, 2020, in Toronto, Ontario

4.2. Experimental Results

4.2.1. Case 1: Water as a TES medium

The resulting temperature profiles from the first experiment when the water is used as a TES medium, and the system was charged for 5 hours and then discharged afterwards is shown in Figure 4.16. The initial temperature in this case was ~22 ºC, and the temperature of the thermocouples at the top of the water container (T7 and T9) increased to ~47 ºC during the 5 hour charging period. After the lamp was turned off, the temperature of T7 and T9 gradually cooled down to ~ 26 ºC by the end of 19 hour discharging period. The temperature of T3, T4, T5, and T10 at the middle of the water container increased up to ~ 35 ºC after the light was on for 5 hours. The temperature at the end of the discharging period was approximately ~ 26 ºC for these thermocouples located at the middle of the water container. The temperature of the thermocouples near the bottom of the water container (T6 and T8) increased to ~32 ºC over the 5 hour charging period. After the lamp was turned off, the temperature dropped down to ~ 25 ºC by the end of the 19 hour discharging period.

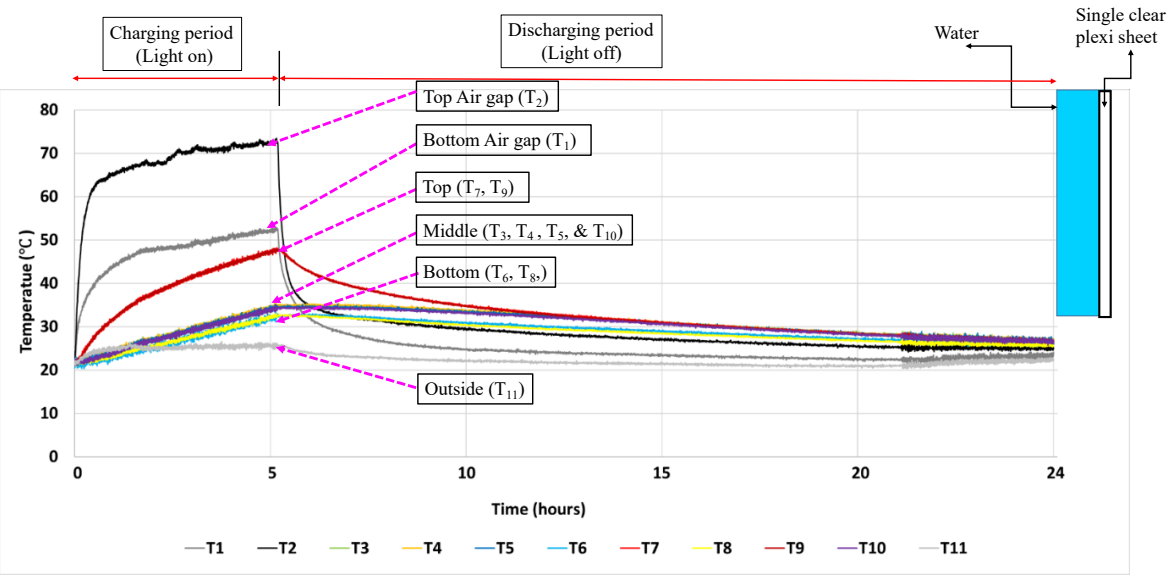

Figure 4.16. Temperature profile in the Trombe wall prototype for the case when water is used as the storage medium

The temperature at the top and bottom of the air gap within the Trombe wall prototype increased to approximately 72 °C (T2) and 52 °C (T1) during the charging period. The air within the Trombe wall prototype was elevated due to heat transferred from the inside surface of the plexiglass at the front face of the Trombe wall prototype, which was heated by absorbing light from the lamp. The air gap cooled at a faster rate than the water during the discharging period and had a lower temperature by the end of the experiment. It can also be noted that the temperature outside the Trombe wall prototype increased slightly to ~ 25 °C during the charging phase. This is because the air surrounding the Trombe wall prototype was heated by the lamp during the charging period. The experiments were repeated, and the results were within 1-2 ºC. The initial temperature in this case was ~22 ºC, and the temperature of the thermocouples at the top of the water container (T7 and T9) increased to ~49 ºC during the 5 hour charging period. However, the temperature of T3, T4, T5, and T10 at the middle of the water container increased up to ~ 35 ºC after the light was on for 5 hours. The temperature of the thermocouples near the bottom of the water container (T6 and T8) increased to ~33 ºC over the 5 hour charging period. There were some noise recorded in the experiments (for example from hour ~21 to 24 in Figure 4.1.6) which was present when other lamps, used for other experiments, were operated in the vicinity of the Trombe wall prototype.

4.2.2. Case 2: Water as a TES medium with a tinted acrylic sheet at its front side

The resulting temperature profiles when water with a tinted acrylic sheet is used as the storage medium are shown in Figure 4.17. The initial temperature in this case was ~22 ºC, and the temperature of the thermocouples at the top of the water storage medium (T7 at the front side and T9 at the back side) were elevated to ~56 ºC and ~54 ºC after the 5 hour charging period. After the lamp was turned off, the temperature of T7 and T9 dropped to ~ 32 ºC at the end of the 19 hour discharging period. The temperature of the thermocouples at the mid-plane of the water storage medium (T3, T4, T5, and T10) increased to ~ 39 ºC when the light was on for 5 hours. When the lamp was turned off, the temperature cooled and reached approximately 29 ºC by the end of the discharging phase. The temperature of the thermocouples at the bottom of the water storage medium (T6 and T8) increased up to ~32 ºC over the 5 hour charging period. After the lamp was turned off, the temperature dropped down to ~ 29 ºC by the end of the 19 hours discharging period. The airgap temperature at the top (T2) and bottom (T1) was recorded to increase to ~72 ºC and ~52 ºC, respectively. The experiments were repeated, and similar results were attained (all temperature readings were within 3 ºC for a repeated run).

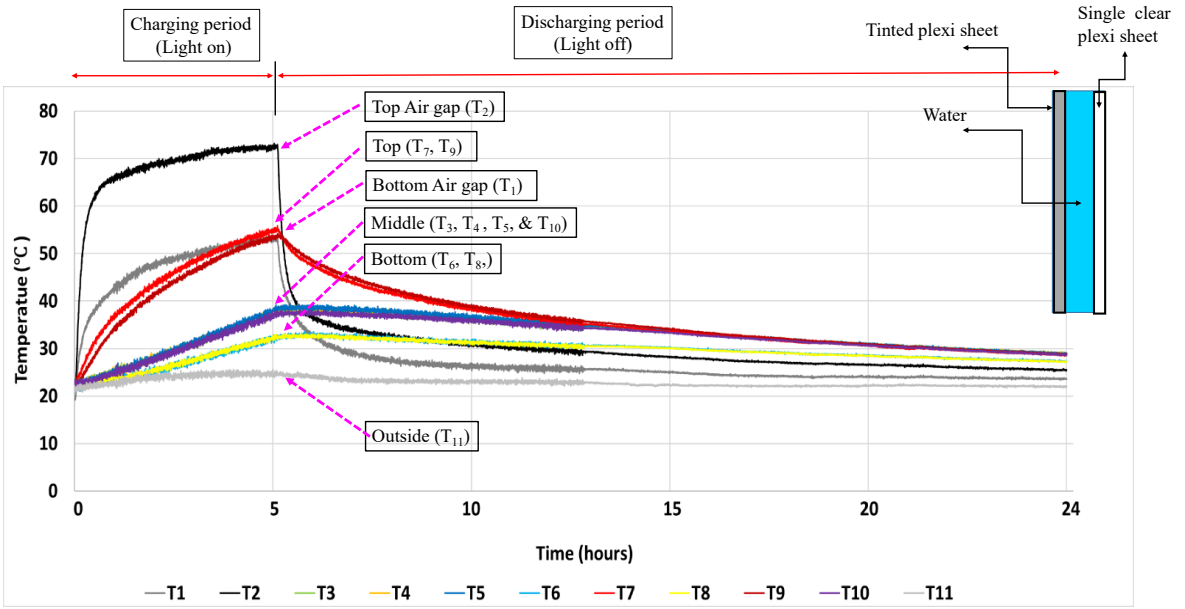

Figure 4.17. Temperature profile in the Trombe wall prototype for the case when the water is used as TES medium with tinted glass at front side.

4.2.3. Case 3: Water as a TES medium with two clear plexiglass sheets at the rear side of the Trombe wall prototype

The resulting temperature profiles from the experiment when water is used as a TES medium with two clear plexiglass sheets at the rear side of the Trombe wall prototype are shown in Figure 4.18. The initial temperature in this case was ~22 ºC, and the temperature of the thermocouples at the top of the water container (T7 and T9) increased to ~52 ºC during the 5 hour charging period. After the lamp was turned off, the temperature of T7 and T9 gradually cooled down to ~ 27 ºC by the end of 19 hour discharging period. However, the temperature of T3, T4, T5, and T10 at the middle of the water container increased up to ~35 ºC after the light was on for 5 hours. The temperature at the end of the discharging period was approximately ~ 28 ºC for these thermocouples located at the middle of the water container. The temperature of the thermocouples near the bottom of the water container (T6 and T8) increased to ~34 ºC over the 5 hour charging period. After the lamp was turned off, the temperature dropped down to ~ 27 ºC by the end of the 19 hour discharging period.

The temperature at the top and bottom of the air gap within the Trombe wall prototype increased to approximately 71 °C (T2) and 55 °C (T1) during the charging period. The air gap cooled at a faster rate than the water during the discharging period and had a lower temperature by the end of the experiment. It can also be noted that the temperature outside the Trombe wall prototype increased slightly to ~ 27 °C during the charging phase. This is because the Trombe wall prototype and lamp are surrounded by aluminum walls and the air within these surroundings is heated by the lamp during the charging period.

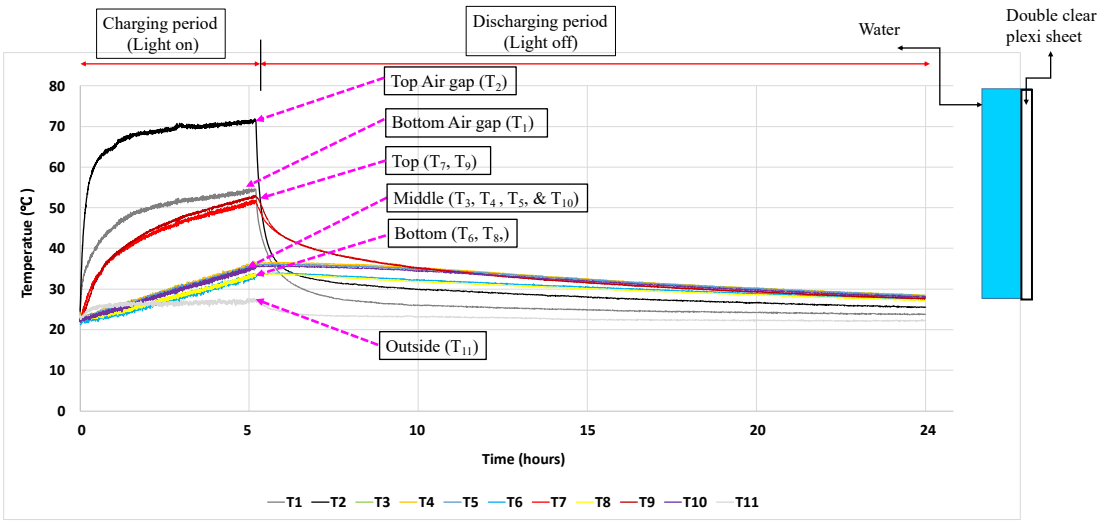

Figure 4.18. Temperature profile in the Trombe wall prototype for the case when water is used as the storage medium and two clear plexiglass sheets are used at the rear side of the Trombe wall prototype

4.2.4. Case 4: Water as a TES medium with a tinted acrylic sheet at its front side and with two clear plexiglass sheets at the rear side of the Trombe wall prototype

The resulting temperature profiles when water is used as the storage medium with a tinted acrylic sheet and double clear plexiglass sheet integrated at the back side of the Trombe wall are shown in Figure 4.19. The initial temperature in this case was ~22 ºC, and the temperature of the thermocouples at the top of the water storage medium (T7 at the front side and T9 at the back side) were elevated to ~56 ºC and ~54 ºC after the 5 hour charging period. After the lamp was turned off, the temperature of T7 and T9 dropped to ~ 29 ºC at the end of the 19 hour discharging period.

The temperature of the thermocouples at the mid-plane of the water storage medium (T3, T4, T5, and T10) increased to ~ 42 ºC when the light was on for 5 hours. When the lamp was turned off, the temperature cooled and reached approximately 29 ºC by the end of the discharging phase. The temperature of the thermocouples at the bottom of the water storage medium (T6 and T8) increased up to ~35 ºC over the 5 hour charging period. After the lamp was turned off, the temperature dropped down to ~ 27 ºC by the end of the 19 hours discharging period. The airgap temperature at the top (T2) and bottom (T1) was recorded to increase to ~70 ºC and ~51 ºC, respectively.

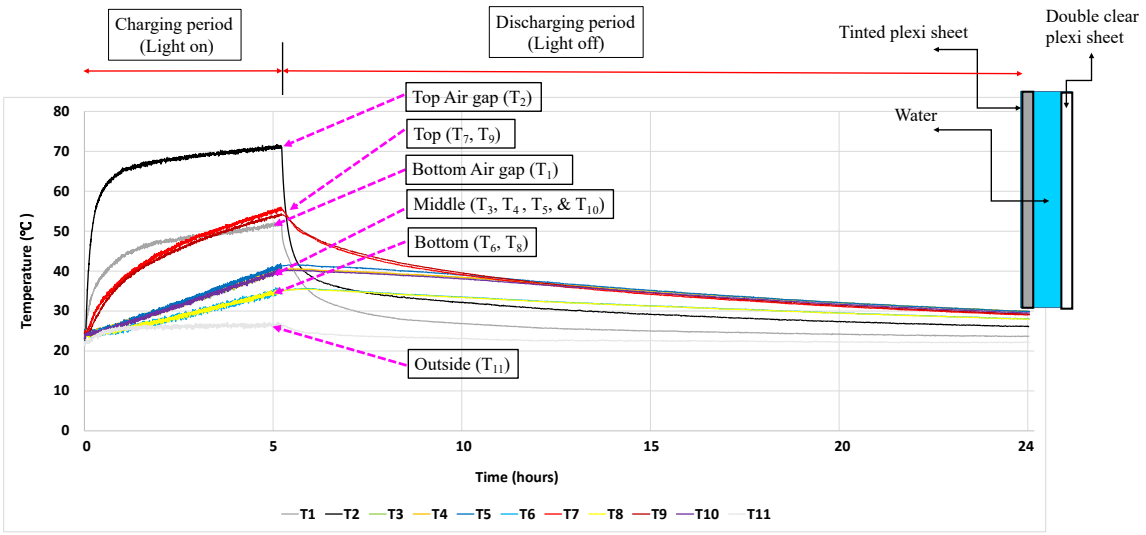

Figure 4.19. Temperature profile in the Trombe wall prototype for the case when water is used as TES medium with a tinted acrylic sheet integrated at its front side and with two clear plexiglass sheets at the rear side of the Trombe wall prototype

4.3. Thermal energy stored and thermal energy storage efficiency of Trombe wall experimental model

The thermal energy stored in the Trombe wall prototype and thermal efficiency of the Trombe wall prototype is calculated using the formulas described in Section 3.5.1 and the results are shown in Table 4.2. The detailed calculations for each case are shown in Appendix C. As shown in Figure 4.20, the thermal efficiency for the experimental model is approximately 58 % for the reference case (single plexiglass sheet wat,1x) when a single plexiglass sheet is integrated the front of the water container, however the thermal efficiency increased by approximately 2.4 % when two clear plexiglass sheets is integrated at the back of the Trombe wall (single plexiglass sheet wat,2x).

The thermal efficiency of the model increased up to about 79 % when a tinted acrylic sheet is integrated in the water based Trombe wall (single plexiglass sheet wat, tg,1x). However, the thermal efficiency of the Trombe wall with a tinted acrylic sheet further increased by approximately 4.5% when tow clear plexiglass sheets are integrated at the back of the Trombe wall (single plexiglass sheet wat, tg,2x). The thermal storage capacity and thermal efficiency of all four cases is shown in Table 4.2. The thermal energy stored by the Trombe wall in case 1 is 1.2 MJ and case 2 is 1.62 MJ. It means that Trombe wall integrated with a tinted acrylic sheet can store 0.41 MJ more thermal energy. The thermal storage efficiency and thermal energy stored in

the Trombe wall increases significantly because the tinted acrylic sheet absorbs a greater amount of incident light radiation.

On the other hand, the thermal energy storage increases by 0.05 MJ when two clear plexiglass sheets are integrated at the back of the water container, and the thermal energy storage increased by 0.09 MJ when two clear plexiglass sheets are integrated at the back of the water container for the case when a tinted acrylic sheet is used. The increase in temperature is observed when two clear plexiglass sheets are used because the space between the sheets acts as insulation.

Therefore, it can be inferred that using a tinted acrylic sheet contributes to increased thermal storage and efficiency of the Trombe wall as compared to using a two clear plexiglass sheets at the rear side of the Trombe wall prototype. The metal halide lamp used in the experiment produces a light spectrum which contains light with infrared wavelengths. Light with infrared wavelengths can be absorbed by the water and acrylic container which raises the temperature of the water for the case when water is used as a TES.

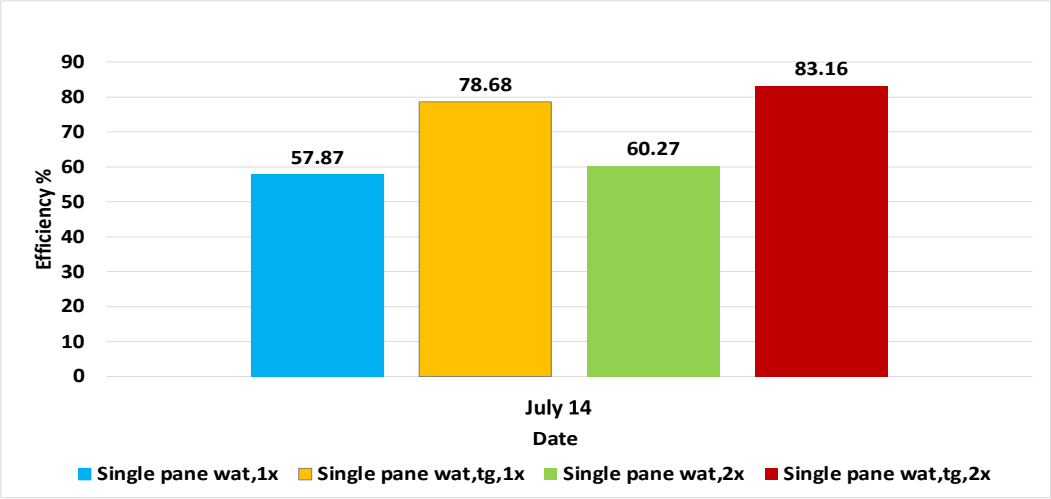

Figure 4.20. Thermal energy efficiency for Trombe walls when water is used as TES medium with or without a tinted acrylic sheet at the front and two clear plexiglass sheets at the rear side of the Trombe wall prototype during summer conditions

Table 4.2. Thermal energy stored and thermal energy efficiency for Trombe walls when water is used as a TES medium with or without a tinted acrylic sheet and two clear plexiglass sheets at the rear side of the Trombe wall prototype during summer conditions

Case	**Experiment**	
	Thermal Energy Stored (MJ)	**Thermal Efficiency η_t(%)**
Single plexiglass sheet, wat,1x	1.14	57.87
Single plexiglass sheet, wat, tg,1x	1.55	78.68
Single plexiglass sheet, wat,2x	1.19	60.27
Single plexiglass sheet, wat, tg,2x	1.64	83.16

Integrating the tinted plexiglass into the water-based Trombe wall causes a 20.81% increase in the thermal efficiency for the experimental cases. This equates to an increase in 0.41 MJ thermal energy stored for the experimental results. Integrating the double clear plexiglass sheet at the back of the Trombe wall slightly increases the thermal efficiency by approximately 2.4 % for the experimental case when tinted acrylic sheet is not used and by approximately 4.5 % when tinted glass is used, however there is a temperature increase at the top and center of the water container.

The temperature at the top of the water container increased by 5 ^{o}C when the water-based Trombe wall prototype has two clear plexiglass sheets at its back side. The temperature at the center of the water container increased by 3^{o}C when water-based Trombe wall is integrated with tinted acrylic sheet at the front and double clear plexiglass at the back. The increase in temperature is observed due to increased heat trapped in the double clear plexiglass sheets which acts as insulation.

4.4. Maximum average temperature in the TES medium for experimental and simulation models

The maximum average temperature in the TES medium is compared for the experimental and simulation models to investigate the effectiveness of Trombe wall models and is shown in Figure

4.21. The maximum average temperature is the average of inside and outside surface temperatures of the TES wall at peak sunshine hours (at 2 pm).

For the experimental reference case 1 (single plexiglass sheet wat) when only a single plexiglass sheet is integrated in the water-based Trombe wall, the maximum average temperature is noted to be 38 ºC. For the simulation reference case 1 (single glazing wat), when single glazing is used in the water-based Trombe wall, the maximum average temperature is 25.7 ºC.

The maximum average temperature of the water-based Trombe walls increases up to 42.6 ºC in the experimental model when tinted acrylic sheet is integrated at the front of water container (single plexiglass sheet wat, tg), whereas the maximum average temperature of the water-based Trombe wall increases up to 38.2 ºC when tinted glass is added at the front of water wall in the case of simulation model (single glazing wat, tg).

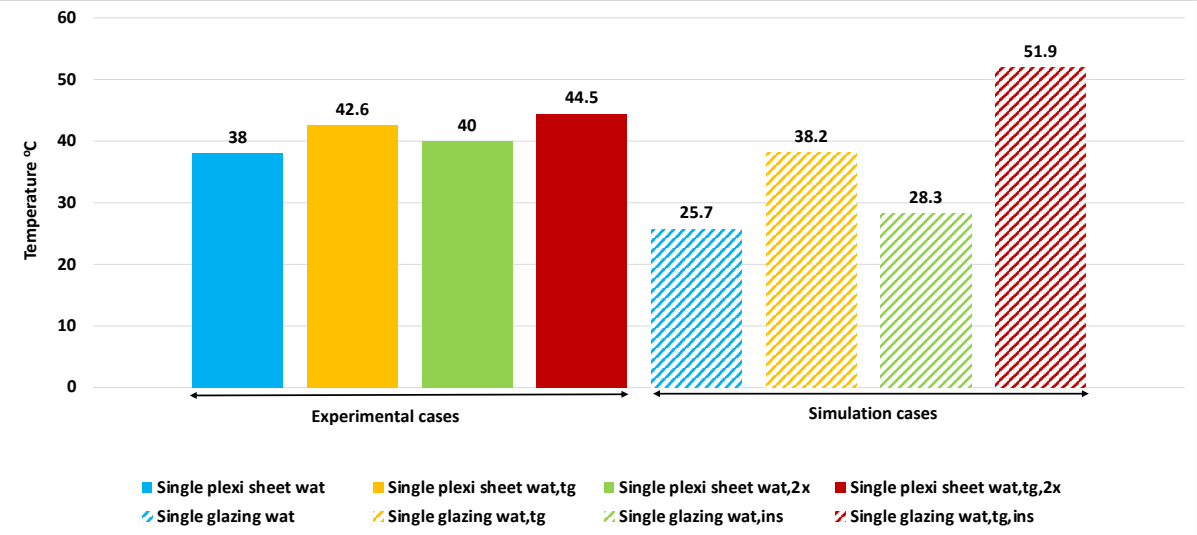

Figure 4.21. Maximum average temperature in the TES medium for the different cases of experimental and simulation models

Adding a second plexiglass sheet at the back of the water-based Trombe wall prototype increases the maximum average temperature by approximately 2 ºC (single plexiglass sheet wat, 2x, and single plexiglass sheet wat, tg, 2x). Adding the insulation at the back of the water-based Trombe wall simulation model (single glazing wat, ins) increases the temperature by 2.5ºC.

However, adding the insulation at the back of the water-based Trombe wall for the simulation case when tinted glass is integrated at the front of the water wall (single glazing wat, tg, ins) increases the average maximum temperature by 13.7^{o}C.

The trend is comparable but there is a noticeable difference between the experiment and simulation cases because of the following reasons:

- In the simulations the ambient temperature is varying similar to the real world scenarios and a cooling load is being applied to the building.
- The prototype used in the experiments is on a small scale where the room designed for simulation analysis is on the scale according to average Canadian household standards.
- The volume of the water container in the experimental prototype is very small (0.018 m^3) as compared to the simulation model (2.4 m^3) which is comparable to a realistic scale.
- The heat transfer in the simulation occurs by conduction whereas heat transfer occurs by convection in the experimental models.
- The light spectra from the lamp in the experiments is different from the solar spectrum. The light spectra from the lamp has more infrared radiation which is absorbed more strongly by water.
- In the simulations the absorptance of the water is set to zero, such that it does not absorb any sunlight unless tinted glass is inserted into it. In the experiments infrared light from the lamp is absorbed by the water in the Trombe wall.

The heated water from the Trombe wall can be used for building applications other than space heating as discussed in the next section.

4.5. Applications of thermal energy stored in water-based Trombe walls during summer conditions

The heated water at the top of water-based Trombe walls can be used for applications other than space heating during summer weather conditions. For example, it has been observed that dishwashers operate efficiently at temperatures as low as 38 ^{o}C, and comfortable temperatures for showering are between 37-40 ^{o}C. Furthermore, the recommended temperature in newer washing

machines for high efficiency is about 49 °C. The safest recommended temperature for a hot water tank is 49 °C, and the inlet water temperature in the water tank during summer is approximately 18 °C. Thus, inlet water can be preheated in a water-based Trombe wall to the desired temperature which will help reduce water heating costs and energy consumption [74][75].

In this work, the average temperature of the water in the Trombe wall when a tinted acrylic sheet is used to absorb solar radiation is approximately 38 °C at 2 pm for the results from the simulations and approximately 42.5 °C for the experimental results. However, the water temperature at the top of the water container in the Trombe wall prototype is approximately 55 °C. This hot water can be extracted from the top side of the Trombe wall by an outlet valve to use for showering, washing clothes and dishes, and providing pre-heated water for the hot water tank.

In Canada, on average 75 L/day of hot water are used per person and 255 L/day are used by households. The primary uses of hot water are in showers (~25%), faucets (~34%), baths (~17%), laundry (~15%) and dishwashers (~4%) as shown in Table 4.3.

Table 4.3. Main uses of hot water in an average household in Canada

Main uses of hot water	**Hot water usage (%)**	**Volume of hot water used (L)**
Showers	25	56.25
Faucets	34	76.5
Bath	17	38.25
Laundry	15	33.75
Dishwashers	4	9

Notably, the volume of water in the thermal energy storage medium (for the case of a 20 cm thick water wall) in the single-story building modelled in Design Builder (Figure 3.1) is 2.4 m^3 (2400 L). If water was extracted from the top third of the water wall this would amount to 800 L of heated water on a sunny day that could be used for the domestic purposes described in Table 4.3. Moreover, there would be excess heated water as 800 L is 3.5 times more than the required amount (255 L) of heated water in an average household in Canada [76][77].

CHAPTER 5: SUMMARY, CONCLUSIONS AND RECOMMENDATIONS FOR FUTURE WORK

5.1. Summary

The objective of this thesis is to design and model water Trombe walls that exhibit high performance for all seasons. The potential to store the solar thermal energy in water Trombe walls during summer months is investigated. During the summer months Trombe walls typically do not reduce the building energy load to the same extent as they do during the winter months. Furthermore, Trombe walls can cause overheating during the summer months. The Trombe wall designs proposed in this research convert incident solar energy into heat which is stored in water within a Trombe wall. Based on the amount of heat stored and water temperature it was determined that the heated water could be used for purposes other than providing heat to the room adjacent to the Trombe wall. Furthermore, water was selected as the a thermal energy storage medium because water has a volumetric heat capacity of 4186 kJ/(m^3·K), whereas the volumetric heat capacity of concrete is about 2000 kJ/(m^3·K) and sand is about 2600 KJ/(m^3·K). Due to the high heat capacity of water, it can store a large amount of thermal energy per volume basis while maintaining comparatively low surface temperatures, which helps reduce thermal losses. The performance of the water Trombe wall during the winter season is also compared to other more conventional types of Trombe walls.

The outcome from the thesis is an evaluation of a novel set of Trombe wall configurations that exhibit a unique combination of benefits including high thermal efficiency and high aesthetic quality. The performance metrics of these Trombe walls are evaluated using a combination of simulations performed with Design Builder software and experiments conducted on a small-scale Trombe wall prototype. The water-based Trombe walls presented in this thesis can have a positive environmental impact by reducing the energy consumed in buildings. The impact, in terms of building load reduction, is numerically evaluated and reported in the thesis. Furthermore, the water-based Trombe walls will have a unique aesthetic quality that may help promote acceptance and wide spread integration of Trombe walls in buildings. The heated water at the top of the water-based Trombe walls can be extracted by an outlet valve for applications other than space heating

during summer weather conditions such as for showering, washing clothes and dishes, and providing pre-heated water for the hot water tank.

To achieve the objectives, in this work a three-dimensional (3D) model of a single-story building with a Trombe wall was created in Design Builder simulation software to numerically investigate the performance of different Trombe wall configurations during summer and winter conditions in Toronto, Ontario. The July 14, 15, and 16, 2020 period was selected for summer and the Feb 02, 03, and 04, 2021 period was selected for winter simulations.

5.2. Conclusion of Trombe wall simulation and experimental model

The results have shown the performance of a water-based Trombe wall can be very close to that of a sand-based Trombe wall under winter conditions. Of the cases considered, the building has the highest heating load of about 4386 W/m^2 when the thermal storage medium is a 40 cm thick water wall (wat(40cm)). The heating load is about 2060 W/m^2 when sand is used as a TES medium (sand(35cm)). This is because the water wall does not absorb incident solar radiation unless tinted glass is inserted within it, such as for case 2 tg(1cm)/wat(12cm) which has a much lower heating load of 1922 W/m^2. Thus, there is not a big disadvantage to using a water-based Trombe wall during winter conditions.

For the summer weather conditions, simulations were performed to estimate the effects of the storage medium thickness on the thermal energy stored, building cooling load and heat flux entering the building from the Trombe wall. A thickness of 20 cm is selected for comparison since it provides a good balance between having a large amount of thermal energy storage capacity and a reasonably sized wall (for example, the 5 cm thick water walls do not perform as well as the thicker walls whereas a 40 cm thick wall has a higher mass and volume). Furthermore, the thickness of the water walls in the experiments are 20 cm. The maximum average temperature of the water-based Trombe wall increases from 25.7 ^{o}C to 38.2 ^{o}C for the simulation model when a tinted glass is integrated in the water based Trombe wall.

The maximum average temperature of the water-based Trombe wall increases from 38 ^{o}C to 42.6 ^{o}C in the experimental model when tinted acrylic sheet is integrated at the front of water

container (single plexiglass sheet wat, tg). Adding the insulation at the back of the water-based Trombe wall simulation model (single glazing wat, ins) increases the temperature by 2.5 ^{o}C. However, adding the insulation at the back of the water-based Trombe wall for the simulation case when tinted glass is integrated at the front of the water wall (single glazing wat, tg, ins) increases the average maximum temperature by 13.7 ^{o}C.

Also, integrating the tinted plexiglass into the water-based Trombe wall causes a 20.81% increase in the thermal efficiency for the experimental cases. Integrating the second clear plexiglass sheet at the back of the Trombe wall slightly increases the thermal efficiency by approximately 2.4 % for the experimental case when tinted acrylic sheet is not used and by approximately 4.5 % when tinted glass is used.

5.3. Recommendations for future work

Convection is a more efficient heat transfer mechanism, however, in the Design Builder simulations presented in this work it is assumed the water within the TES medium does not move. Thus, it is assumed heat transfer in the water wall occurs by conduction and convection is not accounted for. Therefore, further simulations should be performed that take into account the motion of heated water within the water wall.

There is an opportunity to improve the thermal efficiency of the Trombe wall prototype by using lightweight transparent silica aerogel insulation in place of the clear plexiglass sheet at the back of the Trombe wall prototype.

In addition, PCM materials can be placed in the water Trombe wall to improve its thermal storage efficiency.

The Trombe wall prototype used for experiments is built on a small scale in the lab, therefore further experiments on full-sized Trombe walls should be done to investigate the results at realistic scales. Also, future experiments should be conducted using a light source that better matches sunlight.

The potential of Trombe wall was investigated in the Toronto, Ontario region. It was good that more than 3.5 x the amount of hot water needed can be provided for the case of Toronto. Therefore, in regions with more sun even more hot water will be available, which can be useful for larger buildings. In regions with less sun it seems the Trombe wall will still provide enough hot water

on many days throughout the year. Further studies can be done to investigate the potential of the water Trombe wall concept suggested in this work at other locations.

Also, different types and colors of tinted glass could be used to achieve different appearances. To control the lighting withing the building, different shades of tinted glass could be used, but there would be a trade-off because a lighter shade could be used to achieve more lighting in the building, but this would reduce the amount of light absorbed in the water wall and the amount of heated water available.

Selective absorbers could also be used to allow more visible light to pass through into the building, while absorbing most of the infrared sunlight. It might also be possible to make the absorber removable, foldable, or retractable so that the amount of sunlight absorbed in the water wall can be optimized according to weather conditions. Further simulations and experimental work should be done to investigate these design options.

REFERENCES

[1] Salari, M., & Javid, R. J. (2016). Residential energy demand in the United States: Analysis using static and dynamic approaches. Energy Policy, 98, 637–649. https://doi.org/10.1016/j.enpol.2016.09.041

[2] IEA (2020), Energy Efficiency Indicators: Overview, IEA, Paris https://www.iea.org/reports/energy-efficiency-indicators-overview

[3] IEA (2021), International Energy Agency. *Data and statistics*. Retrieved from

https://www.iea.org/data-and-statistics/data-browser?country=WORLD&fuel=Energy%20consumption&indicator=NatGasConsBySector

[4] IEA (2021), Energy efficiency indicators. Retrieved from

https://www.iea.org/data-and-statistics/data-product/energy-efficiency-indicators#residential

[5] IEA (2020), Is cooling the future of heating? IEA, Paris https://www.iea.org/commentaries/is-cooling-the-future-of-heating

[6] Canada.ca. (2020). Natural Resources Canada. *Residential Sector-Energy Use Analysis*. Retrieved from

http://oee.nrcan.gc.ca/corporate/statistics/neud/dpa/showTable.cfm?type=AN&sector=res&juris=00&rn=11&page=0

[7] Issues in international Energy Consumption Analysis: Canadian Energy Demand

[8] Hughes, L. (2010). Meeting residential space heating demand with wind-generated electricity. *Renewable Energy*, *35*(8), 1765–1772. https://doi.org/10.1016/j.renene.2009.11.014

[9] Canada.ca (2019). Natural Resources Canada. *Residential sector -GHG Emissions.* Retrieved from
http://oee.nrcan.gc.ca/corporate/statistics/neud/dpa/showTable.cfm?type=AN&sector=aaa&juris=00&rn=2&page=0

[10] Solangi, K. H., Islam, M. R., Saidur, R., Rahim, N. A., & Fayaz, H. (2011). A review on global solar energy policy. *Renewable and Sustainable Energy Reviews*, *15*(4), 2149–2163. https://doi.org/10.1016/j.rser.2011.01.007

[11] Canada.ca (2020). Energy data and analysis. *Renewable energy facts.* Retrieved from (https://www.nrcan.gc.ca/science-and-data/data-and-analysis/energy-data-and-analysis/energy-facts/renewable-energy-facts/20069)

[12] The Canadian Encyclopedia (2021). Solar Energy. Retrieved from

https://www.thecanadianencyclopedia.ca/en/article/solar-energy

[13]. SCIENCING (2021) Pros & Cons of Solar Energy. Retrieved from

https://sciencing.com/list-6705250-pros-cons-solar-thermal-energy.html

[14] George, D., Pearre, N. S., & Swan, L. G. (2015). High resolution measured domestic hot water consumption of Canadian homes. *Energy and Buildings*, *109*(July), 304–315. https://doi.org/10.1016/j.enbuild.2015.09.067FI

[15] Szekeres, A., & Jeswiet, J. (2019). Heat pumps in Ontario: Effects of hourly temperature changes and electricity generation on greenhouse gas emissions. *International Journal of Energy and Environmental Engineering*, *10*(2), 157–179. https://doi.org/10.1007/s40095-018-0292-6

[16] Canada.ca (2017). Natural Resources Canada. *Photovoltaic and solar resource maps.* Retrieved from https://www.nrcan.gc.ca/18366

[17] Ozkan, A., Kesik, T., & O'Brien, W. (2016). *the Influence of Passive Measures on Building Energy Demands for Space Heating and Cooling in Multi-Unit Residential Buildings*. 58–69. https://wm-n.glb.shawcable.net/service/home/~/eSim 2016 Proceedings-SelPap.pdf?auth=co&loc=en&id=17884&part=2

[18] Hu, Z., He, W., Ji, J., & Zhang, S. (2017). A review on the application of the Trombe wall system in buildings. *Renewable and Sustainable Energy Reviews*, *70*(February 2016), 976–987. https://doi.org/10.1016/j.rser.2016.12.003

[19] Hordeski, Michael F. *Dictionary of Energy Efficiency Technologies*. Fairmount, 2005.

[20] The Canadian Encyclopedia (2021), Solar Energy. Retrieved from https://www.thecanadianencyclopedia.ca/en/article/solar-energy

[21] Environmental and Energy Study Institute, Solar Energy. Retrieved from https://www.eesi.org/topics/solar/description

[22] Chen, C. J. (2011). Physics of Solar Energy. *Physics of Solar Energy*. https://doi.org/10.1002/9781118172841

[23] Explaining Science. (2019). Solar energy**.** Retrieved from https://explainingscience.org/2019/03/09/solar-energy/

[24] Xu, X., Vignarooban, K., Xu, B., Hsu, K., & Kannan, A. M. (2016). Prospects and problems of concentrating solar power technologies for power generation in the desert regions. *Renewable and Sustainable Energy Reviews*, *53*, 1106–1131.

[25] Sarbu, I., & Sebarchievici, C. (2017). Chapter 2 - Solar Radiation. In I. Sarbu & C. Sebarchievici (Eds.), *Solar Heating and Cooling Systems* (pp. 13–28). Academic Press. https://doi.org/https://doi.org/10.1016/B978-0-12-811662-3.00002-5

[26] Daryl Ronald Myers. (2013). Solar Radiation, *Practical Modeling for Renewable Energy Applications.* Retrieved from

https://books.google.ca/books?id=or3MBQAAQBAJ&printsec=frontcover&source=gbs_atb#v=onepage&q&f=false

[27] Abyad, E. (2017). *Modeled Estimates of Solar Direct Normal Irradiance and Diffuse Horizontal Irradiance in Different Terrestrial Locations*.

[28] Sallaberry, F., Barriga, J., de Jalón, A. G., Goñi, F., Erice, R., & Rincón, G. (2020). Thermal emittance and solar absorptance measurement comparison on receiver tube absorber samples. *AIP Conference Proceedings*, *2303*(December). https://doi.org/10.1063/5.0029158

[29] Zhao, S. (2007). Spectrally Selective Solar Absorbing Coatings Prepared by dc Magnetron Sputtering. In Science and Technology (Vol. 273).

[30] Vartiainen, E. (2000). A new approach to estimating the diffuse irradiance on inclined surfaces. Renewable Energy, 20(1), 45–64. https://doi.org/10.1016/S0960-1481(99)00086-5

[31] Omara, A. A. M., & Abuelnuor, A. A. A. (2020). Trombe walls with phase change materials: A review. *Energy Storage*, *2*(6), 1–28. https://doi.org/10.1002/est2.123

[32] Dan, A., Barshilia, H. C., Chattopadhyay, K., & Basu, B. (2017). Solar energy absorption mediated by surface plasma polaritons in spectrally selective dielectric-metal-dielectric coatings: A critical review. Renewable and Sustainable Energy Reviews, 79(April), 1050–1077.

[33] Lucid learning. (2020). Thermal Conductivity and Diffusivity**.** Retrieved from

https://medium.com/@lucidlearning314/thermal-conductivity-and-diffusivity-e6d3b5ee7ce5

[34] Advances in Thermal Energy Storage Systems: Methods and Applications, edited by Cabeza, Luisa F., Elsevier Science & Technology, 2014. ProQuest Ebook Central, https://ebookcentral.proquest.com/lib/york/detail.action?docID=1903770

[35] Machrafi, H. (2012). Green Energy and Technology. In *Green Energy and Technology*. https://doi.org/10.2174/97816080528511120101

[36] Stutz, B., Le Pierres, N., Kuznik, F., Johannes, K., Palomo Del Barrio, E., Bédécarrats, J. P., Gibout, S., Marty, P., Zalewski, L., Soto, J., Mazet, N., Olives, R., Bezian, J. J., & Minh, D. P. (2017). Storage of thermal solar energy. *Comptes Rendus Physique*, *18*(7–8), 401–414. https://doi.org/10.1016/j.crhy.2017.09.008

[37] Team DesignBuilder. (2019). DesignBuilder v6 Simulation Documentation.

[38] Rubitherm (2021), PCM SP-Line, *PCM with high density*, Retrieved from: https://www.rubitherm.eu/en/index.php/productcategory/anorganische-pcm-sp

[39] Cabeza, L. F., Martorell, I., Miró, L., Fernández, A. I., Barreneche, C., Cabeza, L. F., Fernández, A. I., & Barreneche, C. (2021). 1 - Introduction to thermal energy storage systems. In L. F. Cabeza (Ed.), *Advances in Thermal Energy Storage Systems (Second Edition)* (Second

Edition, pp. 1–33). Woodhead Publishing. https://doi.org/https://doi.org/10.1016/B978-0-12-819885-8.00001-2

[40] Wang, D., Hu, L., Du, H., Liu, Y., Huang, J., Xu, Y., & Liu, J. (2020). Classification, experimental assessment, modeling methods and evaluation metrics of Trombe walls. *Renewable and Sustainable Energy Reviews*, *124*(January). https://doi.org/10.1016/j.rser.2020.109772

[41] Saadatian, O., Sopian, K., Lim, C. H., Asim, N., & Sulaiman, M. Y. (2012). Trombe walls: A review of opportunities and challenges in research and development. *Renewable and Sustainable Energy Reviews*, *16*(8), 6340–6351. https://doi.org/10.1016/j.rser.2012.06.032

[42] Hu, Z., He, W., Ji, J., & Zhang, S. (2017). A review on the application of the Trombe wall system in buildings. *Renewable and Sustainable Energy Reviews*, *70*(February 2016), 976–987. https://doi.org/10.1016/j.rser.2016.12.003

[43] Long, J., Yongga, A., & Sun, H. (2018). Thermal insulation performance of a Trombe wall combined with collector and reflection layer in hot summer and cold winter zone. *Energy and Buildings*, *171*, 144–154. https://doi.org/10.1016/j.enbuild.2018.04.035

[44] Chen, W., & Liu, W. (2008). Numerical analysis of heat transfer in a passive solar composite wall with the porous absorber. *Applied Thermal Engineering*, *28*(11–12), 1251–1258. https://doi.org/10.1016/j.applthermaleng.2007.10.017

[45] Chen, W., & Liu, W. (2004). Numerical analysis of heat transfer in a composite wall solar-collector system with a porous absorber. *Applied Energy*, *78*(2), 137–149. https://doi.org/10.1016/j.apenergy.2003.07.003

[46] Bourdeau LE (1980). Study of two passive solar systems containing phase change materials for thermal storage. Fifth Natl passive solar conference. Amherst, Mass: Smithsonian Astrophysical Observatory.

[47] Khalifa, A. J. N., & Abbas, E. F. (2009). A comparative performance study of some thermal storage materials used for solar space heating. *Energy and Buildings*, *41*(4), 407–415. https://doi.org/10.1016/j.enbuild.2008.11.005

[48] Kara, Yusuf & Kurnuç, Aslıhan. (2012). Performance of coupled novel triple glass and phase change material wall in the heating season: An experimental study. Solar Energy. 86. 2432–2442. 10.1016/j.solener.2012.05.012.

[49] Adams, S., Becker, M., Krauss, D., & Gilman, C. M. (2010). Not a dry subject: Optimizing water Trombe walls. *39th ASES National Solar Conference 2010, SOLAR 2010*, *2*, 1334–1340.

[50] Pittaluga, M. (2013). The electrochromic wall. *Energy and Buildings*, *66*, 49–56. https://doi.org/10.1016/j.enbuild.2013.07.028

[51] Lu, M., & Lai, J. (2020). Review on carbon emissions of commercial buildings. *Renewable and Sustainable Energy Reviews*, *119*(July 2019), 109545. https://doi.org/10.1016/j.rser.2019.109545

[52] Schultz, J. M., & Jensen, K. I. (2008). Evacuated aerogel glazings. *Vacuum*, *82*(7), 723–729. https://doi.org/10.1016/j.vacuum.2007.10.019

[53] Baetens, R., Jelle, B. P., & Gustavsen, A. (2011). Aerogel insulation for building applications: A state-of-the-art review. *Energy and Buildings*, *43*(4), 761–769. https://doi.org/10.1016/j.enbuild.2010.12.012

[54] Chaichan, M. T., & Abaas, K. I. (2015). Performance amelioration of a Trombe wall by using Phase Change Material (PCM). *International Advanced Research Journal in Science, Engineering and Technology*, *2*(4), 1–6. https://doi.org/10.17148/IARJSET.2015.2401

[55] De Gracia, A., Navarro, L., Castell, A., Ruiz-Pardo, Á., Álvarez, S., & Cabeza, L. F. (2012). Solar absorption in a ventilated facade with PCM. Experimental results. *Energy Procedia*, *30*, 986–994. https://doi.org/10.1016/j.egypro.2012.11.111

[56] Sun, D., & Wang, L. (2016). Research on heat transfer performance of passive solar collector-storage wall system with phase change materials. *Energy and Buildings*, *119*, 183–188. https://doi.org/10.1016/j.enbuild.2016.03.048

[57] Fiorito, F. (2012). Trombe walls for lightweight buildings in temperate and hot climates. Exploring the use of phase-change materials for performances improvement. *Energy Procedia*, *30*, 1110–1119. https://doi.org/10.1016/j.egypro.2012.11.124

[58] Li, W., & Chen, W. (2019). Numerical analysis on the thermal performance of a novel PCM-encapsulated porous heat storage Trombe-wall system. *Solar Energy*, *188*(January), 706–719. https://doi.org/10.1016/j.solener.2019.06.052

[59] Leang, E., Tittelein, P., Zalewski, L., & Lassue, S. (2017). Numerical study of a composite Trombe solar wall integrating microencapsulated PCM. *Energy Procedia*, *122*, 1009–1014. https://doi.org/10.1016/j.egypro.2017.07.467

[60] Bellos, E., Tzivanidis, C., Moschos, K., & Antonopoulos, K. A. (2016). Energetic and financial evaluation of solar assisted heat pump space heating systems. *Energy Conversion and Management*, *120*, 306–319. https://doi.org/10.1016/j.enconman.2016.05.004

[61] SUN-LITE (2019). THERMAL STORAGE TUBES. Retrieved from http://www.solar-components.com/TUBES.HTM

[62] Wang, W., Tian, Z., & Ding, Y. (2013). Investigation on the influencing factors of energy consumption and thermal comfort for a passive solar house with water thermal storage wall. *Energy and Buildings*, *64*, 218–223. https://doi.org/10.1016/j.enbuild.2013.05.007

[63] Nayak, J. K. (1987). Thermal performance of a water wall. Building and Environment, 22(1), 83–90. https://doi.org/10.1016/0360-1323(87)90045-X

[64] Adams, S., Becker, M., Krauss, D., & Gilman, C. M. (2010). Not a dry subject: Optimizing water trombe walls. 39th ASES National Solar Conference 2010, SOLAR 2010, 2, 1334–1340.

[65] Kaushik, S. C., & Kaul, S. (1989). Thermal comfort in buildings through a mixed water-mass thermal storage wall. *Building and Environment*, *24*(3), 199–207. https://doi.org/10.1016/0360-1323(89)90033-4

[66] Turner, R. H., Liu, G., Cengel, Y. A., & Harris, C. P. (1994). Thermal storage in the walls of a solar house. *Journal of Solar Energy Engineering, Transactions of the ASME*, *116*(4), 183–193. https://doi.org/10.1115/1.2930080

[67] Upadhya, M., Tiwari, G. N., & Rai, S. N. (1991). Optimum distribution of water-wall thickness in a transwall. *Energy and Buildings*, *17*(2), 97–102. https://doi.org/https://doi.org/10.1016/0378-7788(91)90002-K

[68] Mohamad, A., Taler, J., & Ocłoń, P. (2019). Trombe wall utilization for cold and hot climate conditions. *Energies*, *12*(2). https://doi.org/10.3390/en12020285

[69] Kara, Y. A., & Kurnuç, A. (2012). Performance of coupled novel triple glass and phase change material wall in the heating season: An experimental study. *Solar Energy*, *86*(9), 2432–2442. https://doi.org/10.1016/j.solener.2012.05.012

[70] Zhang, L., Dong, J., Sun, S., & Chen, Z. (2021). Numerical simulation and sensitivity analysis on an improved Trombe wall. *Sustainable Energy Technologies and Assessments*, *43*(November 2020), 100941. https://doi.org/10.1016/j.seta.2020.100941

[71] Hong, X., He, W., Hu, Z., Wang, C., & Ji, J. (2015). Three-dimensional simulation on the thermal performance of a novel Trombe wall with Venetian blind structure. Energy and Buildings, 89(1), 32–38. https://doi.org/10.1016/j.enbuild.2014.12.014

[72] Hu, Z., Zhang, S., Hou, J., He, W., Liu, X., Yu, C., & Zhu, J. (2020). An experimental and numerical analysis of a novel water blind-Trombe wall system. *Energy Conversion and Management*, *205*(December 2019), 112380. https://doi.org/10.1016/j.enconman.2019.112380

[73] Team DesignBuilder (2019). DesignBuilder v6 Simulation Documentation.

[74] Parachute, Hot water tap. Retrieved from

https://parachute.ca/en/injury-topic/burns-and-scalds/hot-tap-water/#:~:text=Washing%20dishes,low%20as%2038%20%C2%B0C.

[75] Government of Canada, Water temperature. Retrieved from

https://www.canada.ca/en/public-health/services/water-temperature-burns-scalds.html

[76] Natural Resources Canada. (2012). *Water Heater Guide*.

[77] Government of Canada, Water heaters. Retrieved from

https://www.nrcan.gc.ca/energy-efficiency/products/product-information/water-heaters/13735

[78] Walton, G. (1983). *Thermal Analysis Research Program.* 22–23.

[79] Doe.com. (2013). The home of DOE-2 based Building Energy Use and Cost Analysis Software. Retrieved from https://www.doe2.com/

[80] Designing Buildings Ltd. (2021), Institution of Civil Engineers. Retrieved from https://www.designingbuildings.co.uk/wiki/Dry-bulb_temperature

[81] Designing Buildings Ltd. (2021), Institution of Civil Engineers. Retrieved from https://www.designingbuildings.co.uk/wiki/Mean_radiant_temperature

[82] Designing Buildings Ltd. (2021), Institution of civil Engineers. Retrieved from https://www.designingbuildings.co.uk/wiki/Operative_temperature

APPENDIX A: DESCRIPTION OF SIMULATION MODEL OPTIONS SELECTED

A.1. Activity tab

The activity tab in Design Builder is used to describe the activity or usage of a zone. For instance, zone type, occupancy, or environmental control parameters are defined under this tab.

- *Zone type:* The room within the reference building is set to Standard zone type which is a default configuration for zone types in Design Builder. The standard configuration zone type is used for occupied zones that need to be heated or cooled. On the other hand, the Trombe wall zone is set to use the Cavity zone type, which is a configuration setting typically defined for unoccupied zones having zero activity. This setting enables the algorithms that are used to calculate the convection coefficients for cavity zone types which are based on the ISO 15099 standard, titled Thermal Performance of Windows, Doors and Shading Devices – Detailed Calculations.
- *Occupancy:* In Design Builder, the occupancy parameter states if the zone is occupied or not at different times of a day and is utilized in simulation analysis to calculate the heat gains in the zone from metabolic heat generated by people occupying the zone. In this research, no occupancy is considered for both zones.
- *Environment control:* Under this control, the heating setpoint thermostat settings are defined. The heating setpoint is the comfort temperature required for a zone. This setting is used by the HVAC system to automatically turn on the zone sensible heating to maintain the indoor temperature when the Trombe wall is not able to deliver heat to the room to maintain the comfort temperature.
- For summer modeling, cooling setpoint and setback temperatures are set as 20 ^{o}C and 22 ^{o}C, respectively.
- For winter modeling, the heating setpoint and setback temperatures are set as 24 ^{o}C and 20 ^{o}C, respectively.

A.2. HVAC tab

- The HVAC tab is used to define the heating, cooling, and mechanical ventilation systems for zones based on the type of HVAC system. This tab also consists of natural ventilation model options.
- There are two types of HVAC configurations in Design Builder: Simple HVAC, and detailed HVAC.

A.1.1. Simple HVAC

- In this research, the Simple HVAC model data option is used to carry out all simulations.
- The Simple HVAC system in Design Builder provides load calculations based on basic algorithms such as Thermal Analysis Research Program (TARP) and Design of Experiments – Version 2 (DOE-2) and meets the heating and cooling demands by supplying hot or cool air.
- TARP and DOE-2 are the default algorithms used for inside and outside surface convections respectively in Design Builder.
- TARP is a comprehensive natural convection algorithm in which heat transfer coefficients are correlated to the orientation of the surface and the difference between surface and zone air temperature. It uses the detailed heat balance method for the energy requirements calculations of multiple rooms in the simulation. It is designed to consider the interroom complex heat transfer phenomenon for simulations. [78]
- DOE-2 algorithm is used to predict the energy usage and cost for a building based on the building layout, constructions, operating schedules, lighting, HVAC, weather data etc. [79]
- EnergyPlus *ZoneHVAC:* IdealLoadsAirSystem is used to determine the heating and cooling loads.
- The source of heat is mostly a boiler or a heat pump.
- Energy consumption is calculated as a post-process.

A.1.2. Mechanical Ventilation

- In Design Builder a mechanical ventilation system can be used to supply and re-circulate the outside air to the zone using central ducted air systems.
- However, mechanical ventilation is not enabled in the simulation studies of this research.

A.1.3. Natural Ventilation

Natural ventilation is also defined under the HVAC tab. There are two control options available in Design Builder: Scheduled or Calculated. The calculated natural ventilation option is used in this research because ventilation flow rates at the top and bottom vents need to be calculated at different time steps throughout the day.

When the calculated natural ventilation option is selected, Design Builder uses an airflow network to calculate ventilation rates using factors such as the wind and buoyancy-driven pressure, size of openings and vents, and the operation schedule.

The calculated natural ventilation option provides more control and flexibility to model ventilation rates. The timing and duration of vent openings can be controlled based on air temperature. The vents are opened when the room temperature is below the Trombe zone temperature.

A.1.4. Outside air definition method

Design Builder provides an outside air definition method to define the maximum outside delivery rate. The available options are below:

- *By zone:* The outside air delivery rate is defined in air changes per hour (ac/h). The airflow rate is calculated in m^3/s as shown below:

Airflow rate (m^3/s) = ac/h x Zone Volume / 3600

Zone Volume is the air volume of the space.

- *Min fresh air (Per person):* The outside air delivery rate is defined using minimum fresh air required according to model data set on the Activity tab. The airflow rate is calculated in m^3/s as shown below:

Air flow rate (m^3/s) = MinFreshAir x Number of People / 1000

Number of People = Occupancy density (people / m^2) x Zone floor area (m^2)

MinFreshAir is the minimum fresh air flow rate per person.

In this model, the by zone option is selected.

The air change rate is used in the simulation is 5 ac/h for the room zone and the air change rate for the Trombe zone is 0.

A.1.5. HVAC template

- Various HVAC templates are available in Design Builder based on whether a simple or detailed HVAC system is selected.
- In this model, Radiator heating, boiler HW, natural ventilation templates are used.
- This template enables zone sensible heating, and natural ventilation.

A.3. Lighting control

- The Lighting tab is used to control the electric lights according to the daylight illuminance level.
- Sensors can be placed in the zone to determine the illuminance of daylight available.

A.4. Opening's tab

- The openings tab in Design Builder is used to define the data for any openings such as windows, vents, and doors in the model.
- *Glazing template:* Design Builder has predefined glazing templates available that can be used to select required glazing types for glass panels. Custom templates can also be created by defining the material properties. In this model, double clear 6mm/13mm Air glazing template is used for outside glass glazing.

Vents: The properties and scheduled operation of vents can be defined for each vent under this tab. In this model, Grille small, light slats vent is used for both top and bottom vents. The operation schedule of vents is set to ON 24/7. The Adjacent temperature heating option is selected to control the natural ventilation airflow for each vent. In this work, this feature is used to allow the vents to open only when the temperature of the Trombe wall zone is greater than the room temperature, which prevents reverse flow from occurring.

A.5. Temperature control

The setpoint temperatures defined on the activity tab in Design Builder are used by the heating and cooling systems to control the internal temperature, and there are three temperature control options that can be used by the heating and cooling systems. These are:

- **Air temperature:** defined as the average temperature of the zone air, also known as dry-bulb temperature. It is simply measured by putting a thermometer in the air and is not affected by moisture in the air. It represents the thermal comfort of the zone. [73][80]
- **Radiant temperature:** It is defined as the measure of the average temperature of surfaces around a particular point with which it will exchange thermal heat. In practice it is measured by a globe thermometer which is a black painted hollow copper sphere with high emissivity and a temperature sensor at the center.

[73][81]

- **Operative temperature:** It is defined as the mean of the air and radiant temperature of the zone and is also affected by air velocity. [79][82]

$t_o = (t_r + t_a \times \sqrt{10v}))/ (1+\sqrt{10v})$

where,

t_o is the operative temperature.

t_a is the air temperature.

t_r is the radiant temperature.

v is the air velocity.

[73][81]

For the Trombe model in this research, the air temperature control option is selected.

A.6. Simulation calculation options:

- **Simulation period:** The start and end time of simulations are defined under this option. The time periods can be defined as a specific number of days, weeks, or a year. Hourly weather data provided by a template weather data file is used as input for the simulations over the selected time period.
- **Timestep:** The timestep refers to the number of times for which the simulation results are calculated within an hour. For example, if the timestep is set to 4, the results from the

simulation will be reported for 15 minute intervals. Similarly, if the timestep value is set to 6, results will be calculated for every 10 minutes during the simulation period. This is an important factor for the overall run time and accuracy of the model. The runtime will increase with shorter timesteps, and larger timesteps may not provide accurate results depending on the model. Therefore, several tests can be run to determine the optimal timestep of setting for a given model. In this model, the timestep value is set to 4.

A.7. Solar distribution

Design Builder has a solar distribution option that defines the way solar radiation is incident and reflects from outside surfaces of a building before entering the zone. There are three options available to select from. These are:

- **Minimal shadowing:** There is only minimal shadowing available from windows or doors but there is no exterior shadow surface. Transmitted solar radiation is directly incident onto the floor and is absorbed by the floor according to its solar absorptance. The radiation reflected by the floor is spread across all interior surfaces. Solar light is absorbed by interior surfaces according to their solar absorptance if the light is not incident onto a floor. A heat balance for the zone is calculated taking into consideration the zone air and each surface of the zone, where light energy is considered to be a heat flux for the surface on which it is absorbed.
- **Full exterior:** In this option, all shadowing from exterior surfaces such as overhangs, detached shadings, wings, and doors and windows are considered in the calculations. Solar radiation is treated in the same way as in the minimal shadowing option.
- **Full interior and exterior:** In this case, instead of assuming that all solar radiation is incident only onto the floor, it is assumed that the solar beam is incident on all surfaces in the zone such as walls, windows, and the floors. It also considers shadowing from all exterior surfaces, and windows, and doors. All surfaces in the zone should be fully enclosed and convex if this option is selected. A zone is considered as a convex zone if any straight line passing through it intercepts a maximum of two surfaces. Most L-shape zones are non-convex. Examples of convex and non-convex zones are shown in Figure A1 below. If there is not any fully enclosed or convex zone, then the Full exterior option should be used.

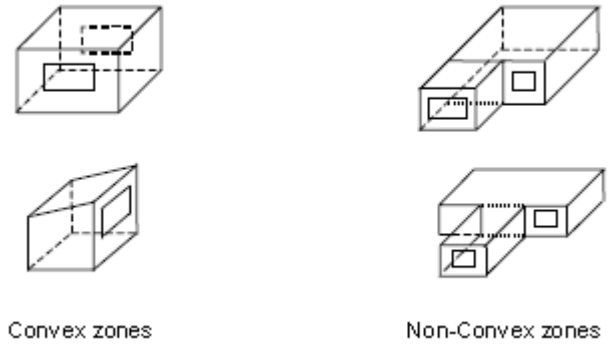

Figure A.1. Convex and non-convex zones

In the Full Interior and Exterior option, the simulation software calculates the amount of radiation absorbed by the window when the beam radiation is incident on the inside of the exterior window from other windows in the zone , the amount reflected or diffused into the zone, and the amount of beam solar radiation transmitted to the outside. It also considers all shadowing surfaces.

This option should be selected if the direct solar and light transmission through internal windows are to be considered in calculations. For the simulations performed in this thesis, the Full interior and exterior option is selected.

A.8. Solution algorithms

There are two solution algorithms available for construction elements in design builder:

- **Conduction transfer function (CTF):** The CTF solution is a solution for sensible heat, but it does not consider moisture and diffusion in the construction components. This algorithm uses the state space method for calculations.

A.9. Finite difference settings

When the finite difference algorithm is selected, the below settings are required:

- **Fully implicit first order:** This difference scheme is first order in time and is stable over time. However, it can sometimes be slower than the Crank Nicholson 2nd order.
- **Crank Nicholson 2nd order:** This scheme is 2nd order in time and is faster than the first implicit first order. However, it can become unstable over time with significant changes in boundary conditions.

In this model, a fully implicit first-order difference scheme is selected.

A.10. Surface convection

There are inside and outside surface convection algorithms available in the model data options in Design Builder. A brief description of the commonly used algorithms are below:

A.11.1. Inside convection algorithms

The inside convections algorithms are used to calculate the convection between internal zone surfaces and the zone air. The most used algorithms are:

- **Adaptive Convection Algorithm:** This algorithm allows the program to dynamically select the convection models suitable for a given surface at a given time.
- **Simple:** It uses constant heat transfer coefficients taken from Walton (1983) to aim for reduced and effective convection.
- **Chartered Institution of Building Services Engineers (CIBSE)**: It uses constant heat transfer coefficients taken from traditional CIBSE values.
- **Thermal Analysis Research Program (TARP):** It is a comprehensive natural convection algorithm. In this algorithm, heat transfer coefficients are correlated to the orientation of the surface and the difference between surface and zone air temperatures.

- In this model, the TARP algorithm is selected for inside convection. As per design builder TARP is the default algorithm that should be selected for the simulations. TARP uses the detailed heat balance method for the energy requirements calculations of multiple rooms in the simulation. It is designed to consider the inter room complex heat transfer phenomenon for simulations [78].

A.11.2. Outside heat convection algorithms: The outside convection algorithms shown below are available in Design-Builder:

- **Adaptive Convection Algorithm:** The adaptive convection algorithm for outside surfaces uses a different surface classification system that is based on wind direction and heat flow directions to calculate heat transfer coefficients.
- **Simple Combined:** It uses surface roughness and local surface wind speed to calculate exterior heat transfer coefficient.

- **CIBSE:** It uses constant heat transfer coefficients depending on the orientation and is taken from traditional CIBSE values.
- **MoWiTT:** In this algorithm, heat transfer coefficients are correlated to smooth vertical surfaces such as window glass in low-rise buildings. This algorithm is not suitable for rough surfaces, high-rise surfaces, and surfaces that have movable insulation.
- **TARP:** This algorithm correlates area and parameter values for façade or roof surfaces.

DOE-2: It is a combination of MoWiTT and TARP convection models.

As per design builder DOE-2 is the default algorithm that should be selected for the outside heat convection algorithms and is the algorithm used in this work.

APPENDIX B: SIMULATION RESULTS FOR SUMMER WEATHER CONDITIONS

B.1. Simulation results for a water Trombe wall with transparent insulation at its inside surface under summer weather conditions

B.1.1. Thermal energy stored in a water Trombe wall with transparent insulation under summer conditions

Figure B.1 shows the thermal energy stored in water Trombe walls of varying thicknesses with an insulation layer on their inner surface. The insulation layer is assumed to be a transparent 5 cm thick transparent aerogel material with a thermal conductivity of 0.014 W/m·K, specific heat of 1000 J/kg·K, and density of 150 kg/m^3. As expected, the results show that the thermal energy stored in a Trombe wall increases with an increase in the thickness of the wall. For example, on July 15th, a maximum thermal energy of 191.2 MJ is stored when the water wall is 40 cm thick, while a minimum of about 25 MJ is stored when the wall is 5 cm thick. `

On the other hand, the maximum temperature, T_M, and ΔT decreases slightly as the thickness of the wall increases. For example, there is a 0.43 °C decrease in the temperature (T_M) and ΔT on 15th July with an increase in wall thickness from 5 cm to 40 cm.

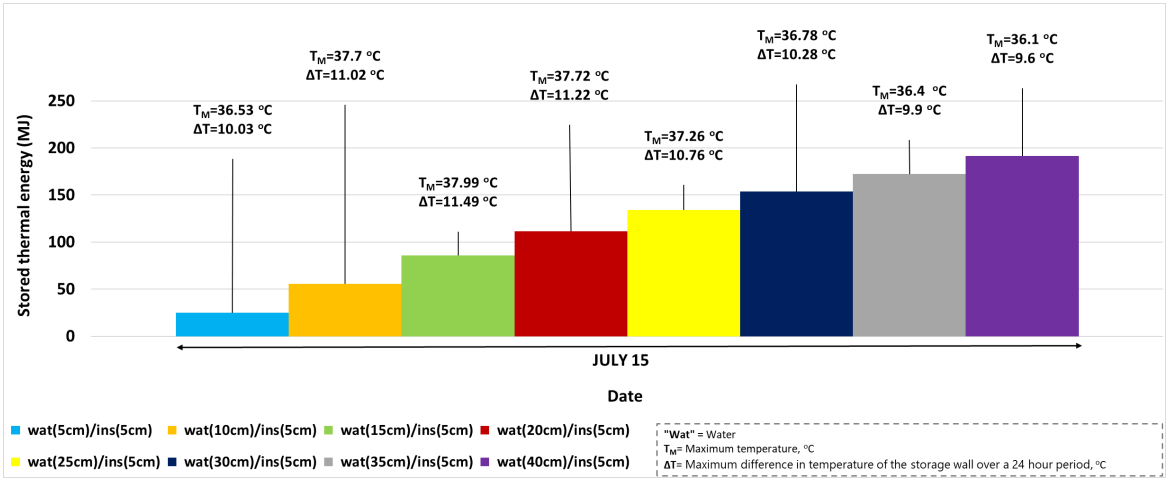

Figure B.1. Thermal energy stored in a Trombe wall consisting of a storage wall of varying thickness made of water (layer 1) and transparent insulation (layer 2) during summer on July 14, July 15, and July 16, 2020, in Toronto, Ontario

B.1.2. Heat transferred through the surfaces of the water storage wall with insulation under summer conditions

Figure B.2 shows the heat transferred from the air channel into the water storage wall with insulation on its inner surface (solid lines) for different water wall thicknesses. The amount of heat entering the storage wall from the air channel is nearly independent of its thickness. A maximum heat transfer from the air channel to the storage medium of around 64 W/m^2 occurs during the peak sunshine hours between 12:00 to 1:00 pm on July 15th. During the night hours, about 28 W/m^2 is transferred from the storage wall into the air channel. The heat transferred from the water storage wall into the room is also shown (dashed lines) in Figure B.2 Only a small amount of heat (ranging from about 2.7 W/m^2 to 5.5 W/m^2) is transferred from the storage wall to the room when there is insulation at the inner surface of the storage wall.

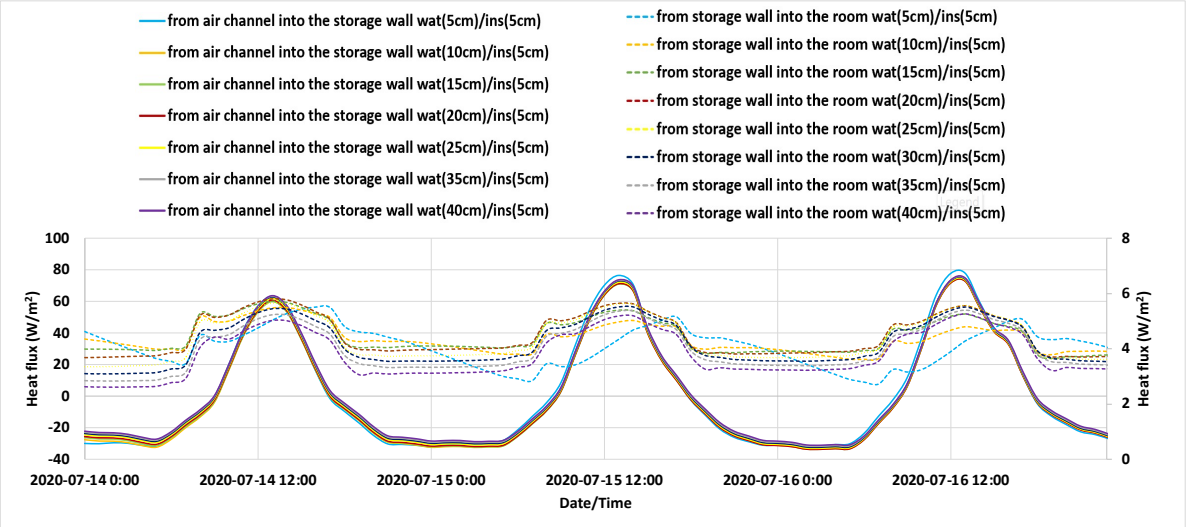

Figure B.2. Heat transferred from the air channel into the storage wall (solid lines) and from the storage wall to the room normalized by floor area (W/m^2) for the model home shown in Figure 3.1 for storage walls of varying thickness when there is an insulation layer on its inside surface during summer on July 14, July 15, and July 16, 2020, in Toronto, Ontario

B.1.3. Hourly cooling load in a water Trombe wall with transparent insulation

Figure B.3 shows the hourly cooling load for three consecutive days (July 14, 15, and 16) for the building shown in Figure 3.1 for the case when the Trombe wall has a water storage wall of varying thickness with insulation at its inner side. The results show that the zone cooling load during peak hours decreases very slightly with increasing Trombe wall thickness. For example,

on July 14th at around 8 am the zone cooling load is around 38 W/m^2 when the water wall is 5 cm thick, whereas the cooling load at the same time is about 35 W/m^2 when the water wall is 40 cm thick.

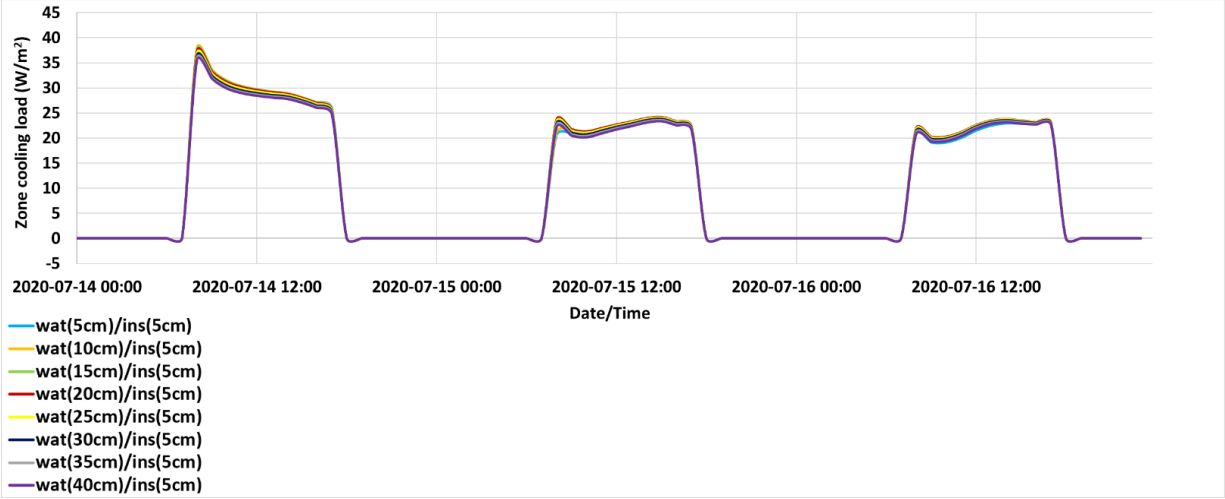

Figure B.3. Hourly cooling load normalized by floor area (W/m^2) for three days (July 14, 15, and 16) in a Trombe wall model consisting of a water storage wall of varying thickness with insulation on its inner surface during summer in Toronto, Ontario

B.14. Total cooling load for the case of the water Trombe wall with insulation at its inner surface for three consecutive days under summer conditions

Figure B.4 shows the total cooling load for the building shown in Figure 3.1 when the Trombe wall is a water storage wall of varying thickness with an insulation layer at its inner side over three consecutive days (July 14, 15, and 16). The results show the total cooling load increases with an increase in the water wall thickness up to 20 cm. On the other hand, the cooling load decreases as the water wall thickness increases from 25 cm to 40 cm. For example, when the water wall thickness is 5 cm the cooling load is about 735 W/m^2, and the cooling load is approximately 750 W/m^2 when the water wall thickness is 15 and 20 cm. When the water wall thickness is 40 cm the cooling load is around 720 W/m^2.

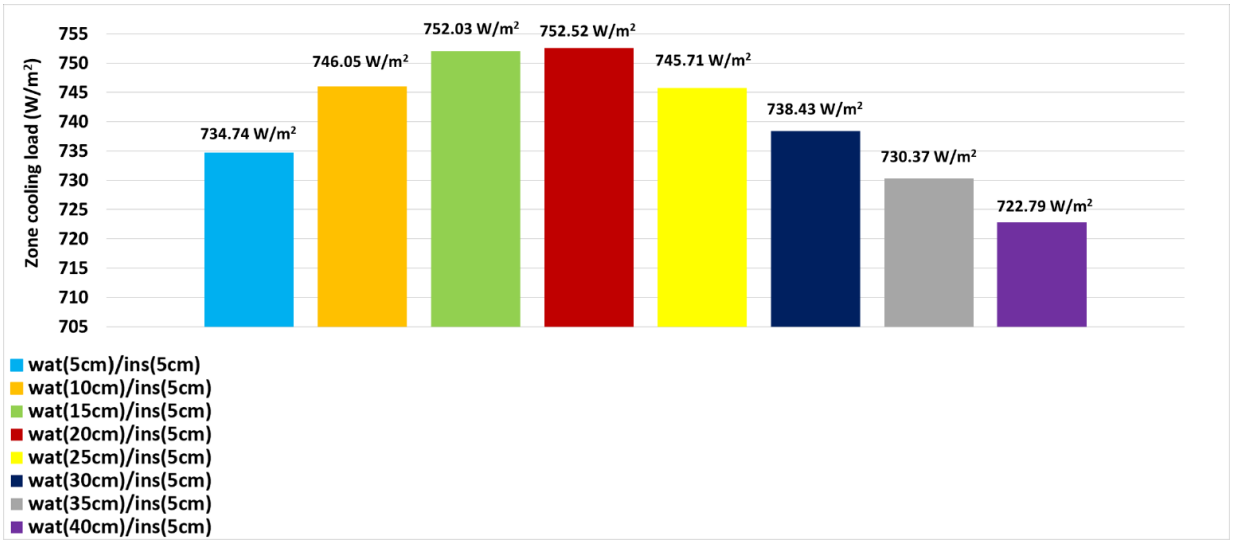

Figure B.4. Total cooling load normalized by floor area (W/m^2) for three consecutive days (July 14, 15, and 16) for the building shown in Figure 3.1 for the case when the Trombe wall consists of a storage wall of varying thickness made of water and a transparent insulation layer at its inner surface during summer in Toronto, Ontario

B.2. Simulation results for a water Trombe wall with insulation on both sides under summer weather conditions

B.2.1. Thermal energy stored in a water Trombe wall with transparent insulation on both sides under summer conditions

Figure B.5 shows the thermal energy stored in a Trombe wall consisting of a water wall with insulation on both of its surfaces. For the thicknesses considered, the maximum thermal energy stored occurs when the thickness of the wall is 40 cm whereas the minimum thermal energy stored occurs when the thickness of the wall is 5 cm. For example, on July 15th, the thermal energy stored when the wall is 40 cm thick is around 272 MJ, however, the energy stored when the wall is 5cm thick is around 35 MJ.

However, the maximum temperature (T_M) remains almost the same, at a value of around 40 ºC, irrespective of the change in the thickness of the water wall. Similarly, the ΔT values do not change significantly as the water wall thickness changes. For example, on July 15th all ΔT values are about 14 °C irrespective of the thickness of the water wall.

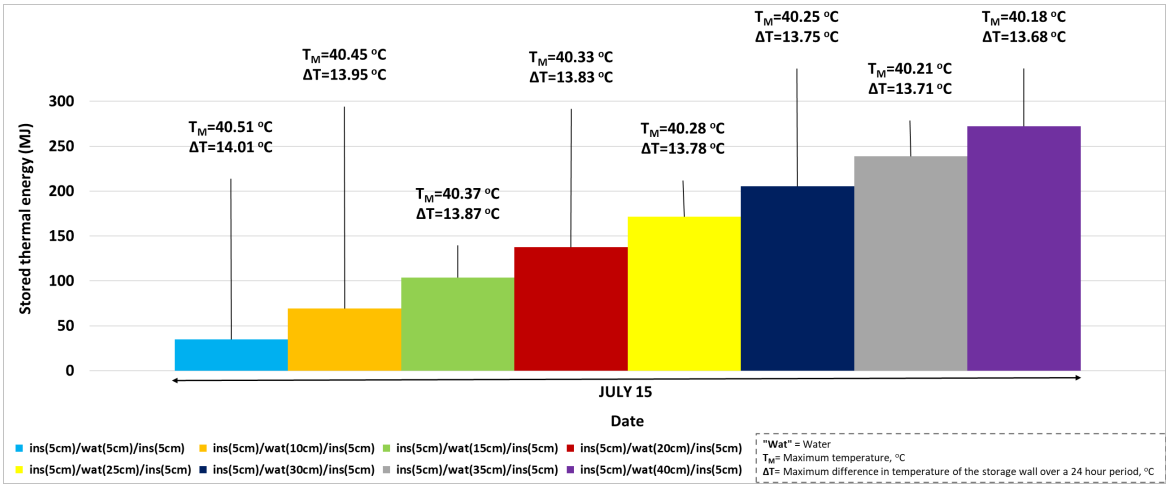

Figure B.5. Thermal energy stored in a Trombe wall consisting of a storage wall of varying thickness made of transparent insulation (layer 1), water (layer 2), and transparent insulation (layer 3) during summer on July 14, July 15, and July 16, 2020, in Toronto, Ontario

B.2.2. Heat transferred through the surfaces of the water storage wall with insulation on both sides under summer weather conditions

Figure B.6 shows the heat flux from the air channel into the storage wall (solid lines) when the storage wall is a water wall of varying thickness with insulation on both sides. There is no significant change in the amount of heat entering the storage wall due to a change in the water wall thickness. Further, on July 14th, a maximum of around 14 W/m^2 of heat enters the storage wall during peak sunshine hours between 12:00 to 1:00 pm. Figure B.6 also shows the heat transferred from the storage wall into the room (dashed lines). As there is a 5 mm thick layer of insulation on the inner surface of the water wall, the amount of heat transferred to the room is low, ranging from about 0.76 W/m^2 to about 4.2 W/m^2 for all water wall thicknesses considered.

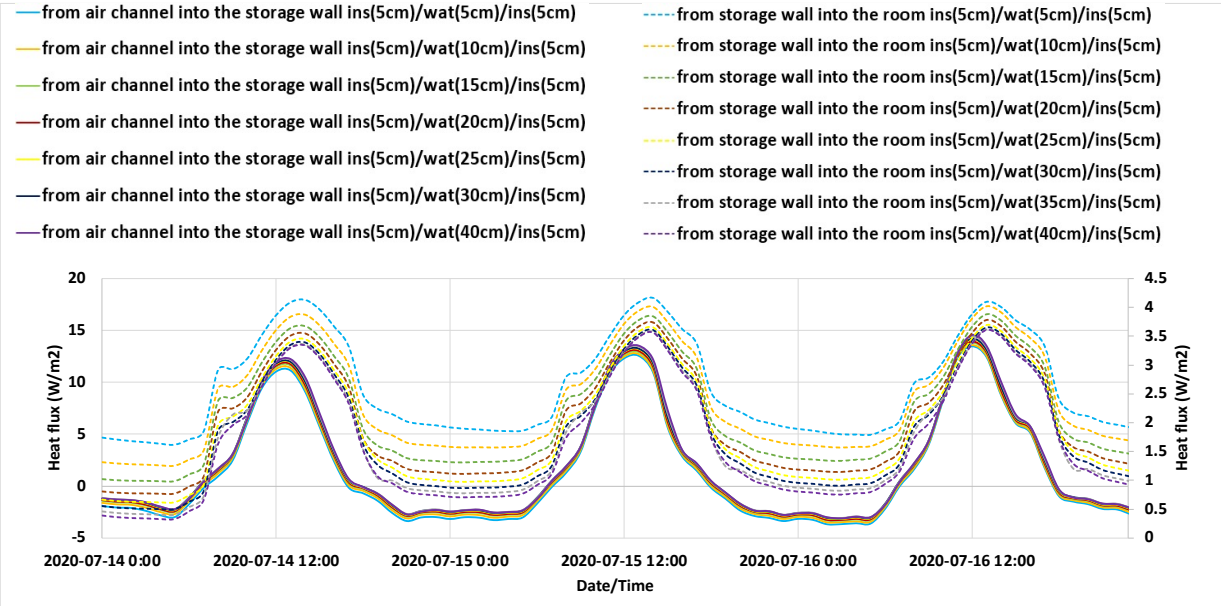

Figure B.6. Heat transferred from the air channel into the storage wall (solid lines) and from the storage wall into the room (dashed lines) normalized by floor area (W/m^2) in a Trombe wall model home shown in Figure 3.1 consisting of a water storage wall of varying thickness with insulation on both sides during summer on July 14, July 15, and July 16, 2020, in Toronto, Ontario

B.2.3. Hourly cooling load for the water Trombe wall with insulation on both sides for three consecutive days under summer conditions

Figure B.7 shows the hourly cooling load for three consecutive days (July 14, 15, and 16) for the building shown in Figure 3.1 when the Trombe wall comprises a water wall with insulation on both of its surfaces. The results show that the cooling load is nearly independent of the thickness of the water wall. For example, on July 14th at around 8 am the zone cooling load is around 32 W/m^2 when the thickness of the water wall is 5 cm, and the cooling load on the same day and time is about 30 W/m^2 when the thickness of the water wall is 40 cm. Similarly, the cooling load in the evening on July 14th around 5 pm is recorded to be 23.5 W/m^2 for a 5 cm thick wall. On the other hand, the cooling load on the same day/time is reduced to 22.05 W/m^2 with an increase in wall thickness to 40 cm.

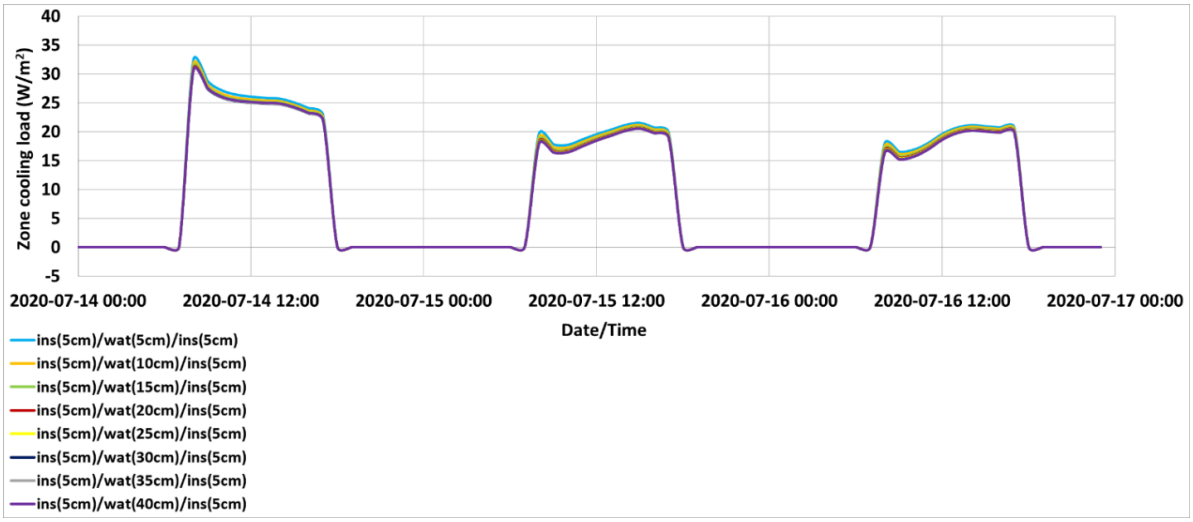

Figure B.7. Hourly cooling load normalized by floor area (W/m^2) for three consecutive days (July 14, 15, and 16) for the building shown in Figure 3.1for the case when the Trombe wall consists of a water storage wall of varying thickness with insulation on either of its surfaces during summer in Toronto, Ontario

B.2.4. Total cooling load for the case of a water Trombe wall with insulation on both sides over three consecutive days during summer conditions

Figure 34 shows the total cooling load for three consecutive days (July 14, 15, and 16) for the building shown in Figure 3.1 when the Trombe wall consists of a water storage wall of varying thickness with insulation on both sides. The results show that the total cooling load decreases as the Trombe wall thickness increases. However, the effects of the water wall thickness on the total heating load are minor. For example, the total cooling load when the thickness of the water wall is 40 cm is 5% less than for the case when the water wall thickness is 5 cm.

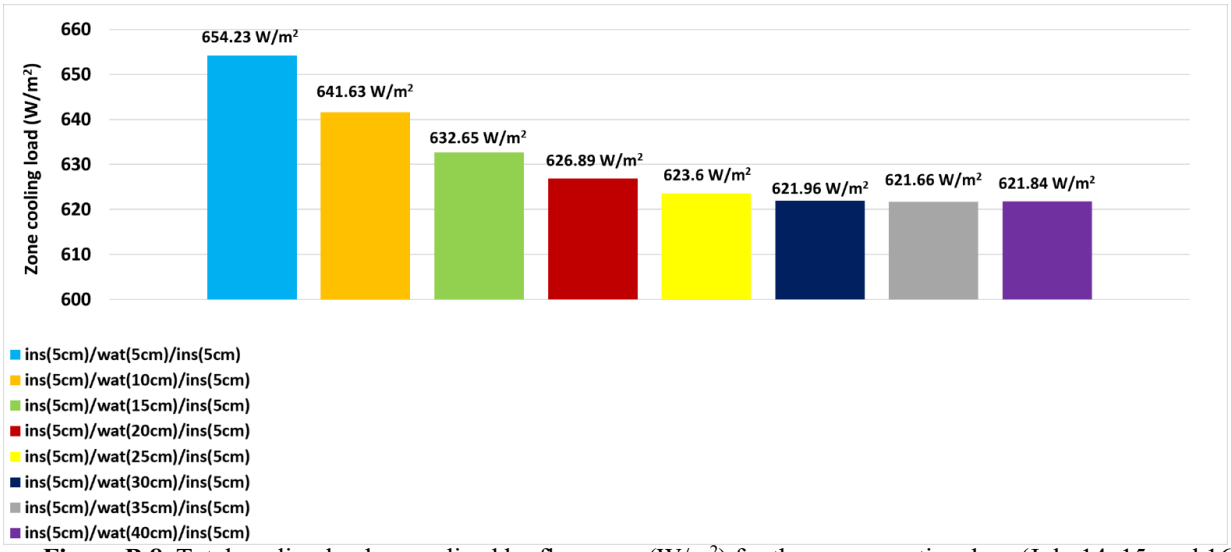

Figure B.8. Total cooling load normalized by floor area (W/m^2) for three consecutive days (July 14, 15, and 16) in a Trombe wall model consisting of a storage wall of varying thickness made of transparent insulation (layer 1), water (layer 2), and transparent insulation (layer 3) during summer in Toronto, Ontario

B.3. Simulation results for a water Trombe wall with tinted glass at its outer side during summer conditions

B.3.1. Thermal energy stored in a water Trombe wall with tinted glass at its front side during summer conditions

Figure B.9 shows the thermal energy stored in a water based Trombe wall with tinted glass at its outer side. The results show that, as expected, the thermal energy stored in the Trombe wall increases as the thickness of the wall increases. For example, on July 15th a maximum thermal energy of 238 MJ is stored when the thickness of the Trombe wall is 41cm, however, a minimum of 50 MJ of thermal energy is stored when the Trombe wall thickness is 11cm.

Similarly, the maximum temperature (T_M) and ΔT go up as the thickness of the water wall increases. For example, there is an approximately 2°C increase in the temperature (T_M) and ΔT values on 15th July with the change in thickness from 11 cm to 41 cm.

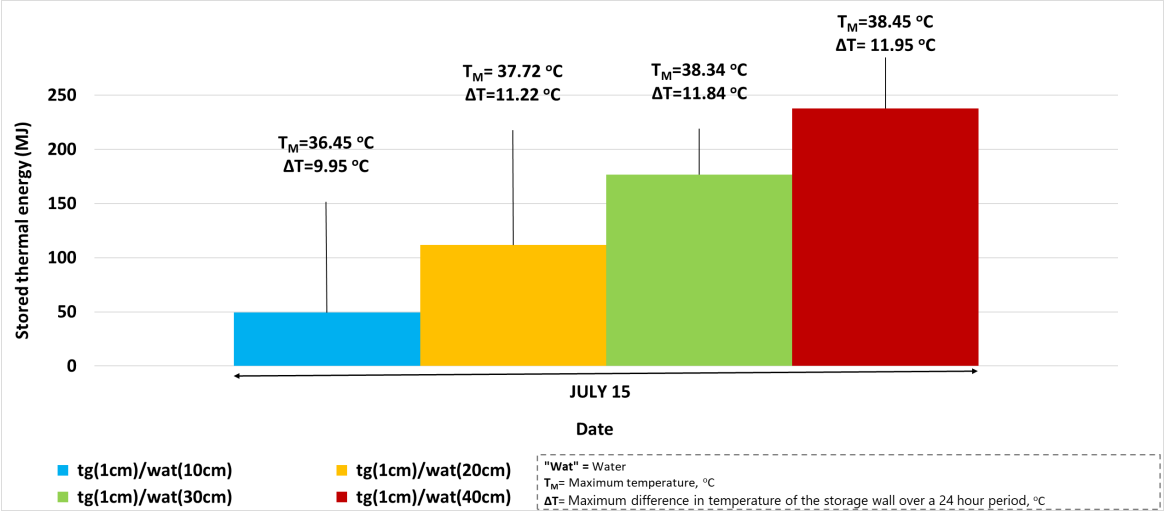

Figure B.9. Thermal energy stored in a Trombe wall consisting of storage wall of varying thickness with a tinted glass surface at its outer layer during summer on July 14, July 15, and July 16, 2020, in Toronto, Ontario

B.3.2. Heat transferred through the surfaces of the water Trombe wall with tinted glass at its outer side under summer conditions

Figure B.10 shows the heat transferred from the air channel to the storage wall (solid lines) when it is comprised of water and tinted glass at its outer surface. There is no significant change in the amount of heat transferred to the storage wall due to a change in the thickness of the water storage layer. Further, a maximum heat transfer of around 178 W/m^2 enters the storage wall during the peak sunshine hours between 12:00 to 1:00 pm on July 15th. The heat transferred from the storage wall into the room is shown by the dashed lines in Figure 4.17. The maximum heat flow from 9:00 am to 5:00 pm is between 43 – 56 W/m^2 when the thickness of the wall is 11 cm or greater. When the water wall thickness is 11 cm, the maximum amount of heat transferred is around 67 W/m^2 at around 5:00 pm on July 15th.

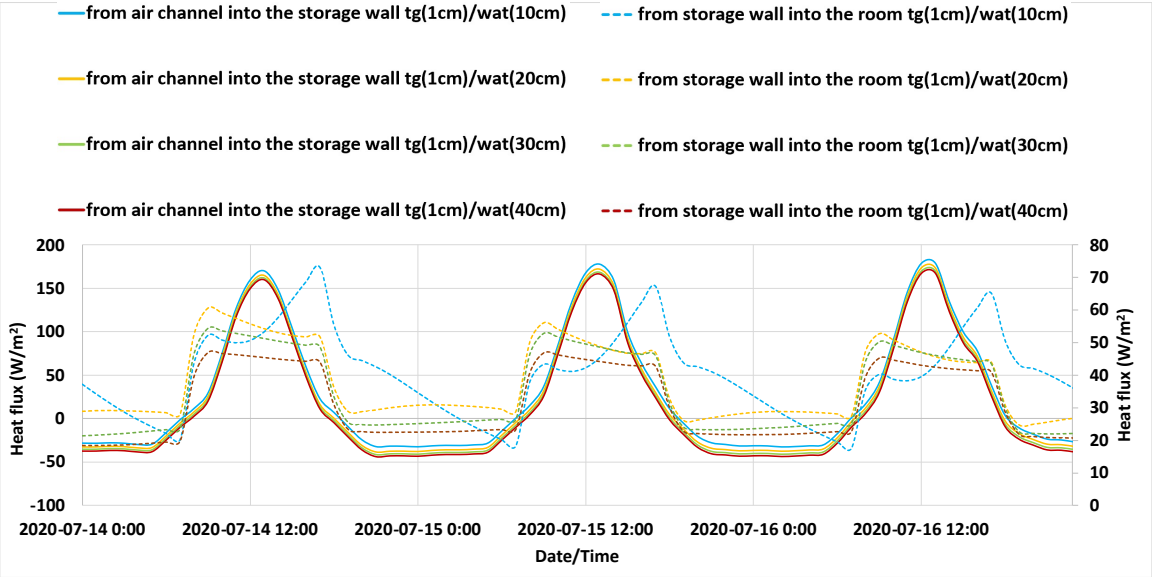

Figure B.10. Heat transferred from the air channel into the storage wall (solid lines) and from the storage wall into the room (dashed lines) normalized by floor area (W/m^2) for the model shown in Figure 3.1 for the case when the Trombe wall consists of a storage wall of varying thickness with tinted glass at its outer layer during summer on July 14, July 15, and July 16, 2020, in Toronto, Ontario

B.3.3. Hourly cooling load for the case of the Water Trombe wall with tinted glass at its outer surface under summer conditions

Figure B.11 shows the hourly cooling load for three consecutive days (July 14, 15, and 16) for the building shown in Figure 3.18 when the Trombe wall is a water wall of varying thickness with tinted glass at its outer surface. The results show that the cooling load during peak hours decreases as the thickness of the Trombe wall increases. For example, on July 14th at 8 am the zone cooling load is around 122 W/m^2 when the storage wall is 11 cm thick, whereas the cooling load at this time is about 94 W/m^2 when the thickness of the storage wall is 41 cm. Similarly, the cooling load in the evening on July 14th around 5 pm is calculated to be 97 W/m^2 for an 11 cm thick wall.

On the other hand, the cooling load on the same day/time is reduced to 66.85 W/m^2 with an increase in wall thickness to 11 cm.

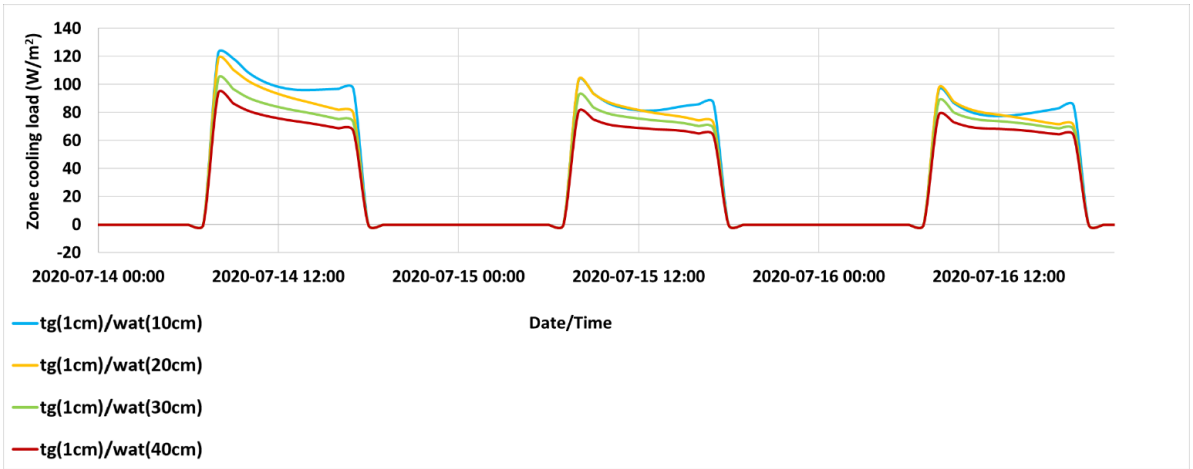

Figure B.11. Hourly cooling load normalized by floor area (W/m^2) for three consecutive days (July 14, 15, and 16) for the building show in Figure 3.1 for the case when the Trombe wall consists of a storage wall of varying thickness with tinted glass at its outer layer during summer in Toronto, Ontario

B.3.4. Cooling load for the water Trombe wall with tinted glass at its outer side over three consecutive days under summer conditions

Figure B.12 shows the total cooling load over three consecutive days (July 14, 15, and 16) for the building shown in Figure 3.1 when the Trombe wall consists of a water wall of varying thickness with tinted glass on its outer layer. The results show that the total cooling load decreases as the Trombe wall thickness increases. For example, the total cooling load when the thickness is 41 cm is 21% less than for the case when the storage wall thickness is 11 cm.

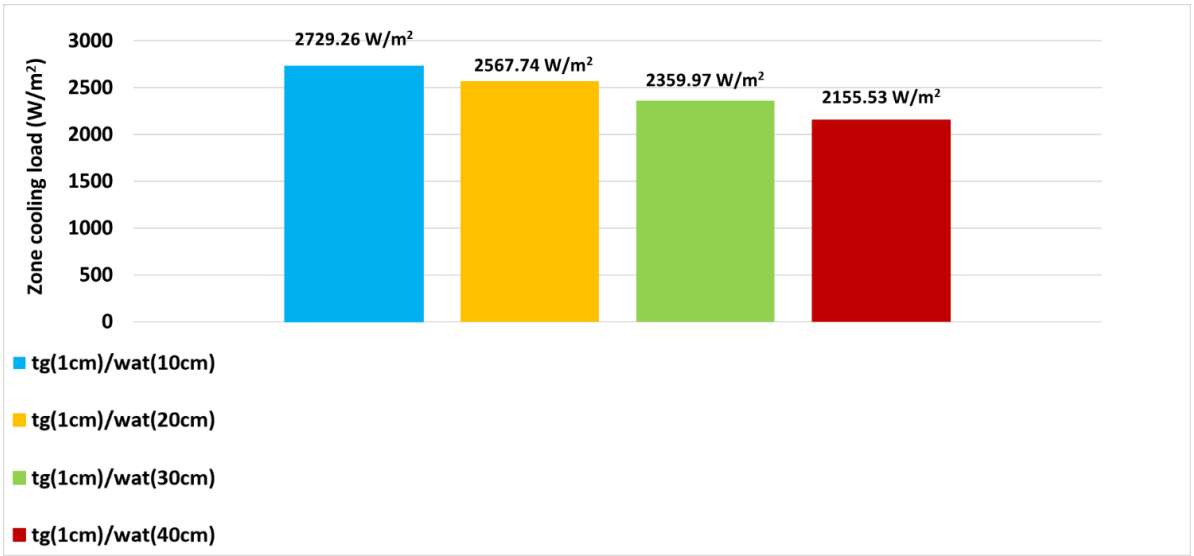

Figure B.12 Total cooling load normalized by floor area (W/m^2) for the building shown in Figure 3.1 over three consecutive days (July 14, 15, and 16) for the case when the Trombe wall comprises a storage wall of varying thickness and has tinted glass at its outer surface during summer in Toronto, Ontario

B.4. Simulation results for the water Trombe wall with tinted glass at its outer side and transparent insulation at its inner side under summer conditions

B.4.1. Thermal energy stored in a water Trombe wall with tinted glass at its outer side and transparent insulation at its inner side under summer conditions

Figure B.13 shows the thermal energy stored in a Trombe wall comprising a water storage wall with tinted glass at its outer surface and insulation at its inner surface. Expectedly, the results show that the thermal energy stored in a Trombe wall increases with an increase in the thickness of the wall. For example, on July 15th, a maximum of 500 MJ is stored when the thickness of the storage wall is 46 cm, however, a minimum energy of about 142 MJ is stored when the thickness of the storage wall is 16 cm.

On the other hand, the maximum temperature (T_M) and ΔT of the storage wall decreases as the thickness of the wall increases. For example, there is a 3.41°C decrease in the maximum temperature (T_M) and ΔT value on July 15th when the thickness of the storage wall increases from 16 cm to 46 cm.

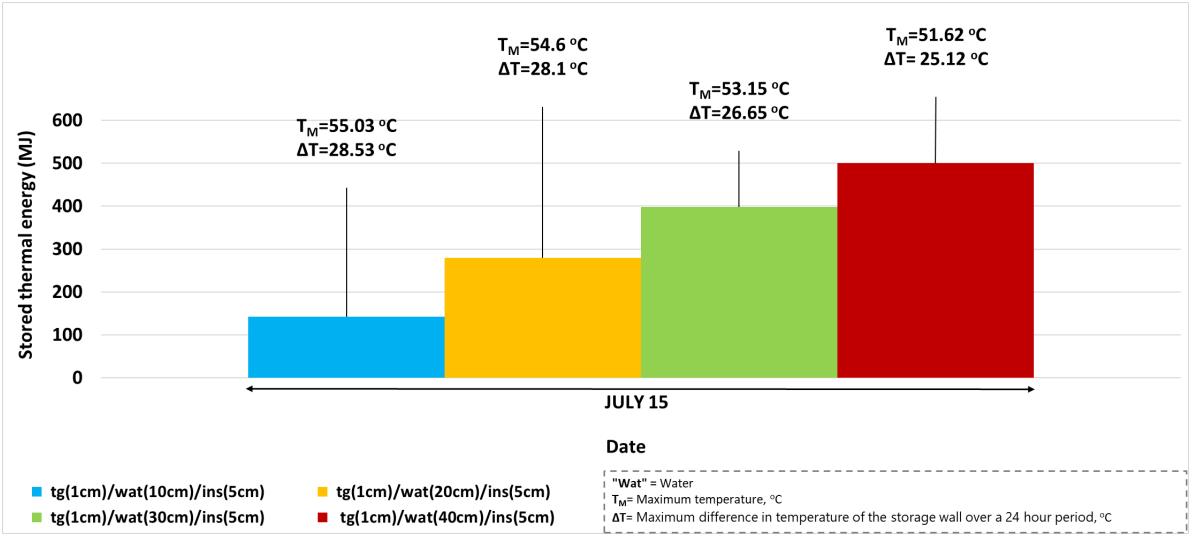

Figure B.13. Thermal energy stored in a Trombe wall consisting of a storage wall of varying thickness made of tinted glass (layer 1), water (layer 2), and transparent insulation (layer 3) during summer on July 14, July 15, and July 16, 2020, in Toronto, Ontario

B.4.2. Heat transferred through the surfaces of the water storage wall with tinted glass at its outer side and transparent insulation at its inner side under summer conditions

Figure B.14 shows heat transferred from the air channel to the storage wall when the storage wall is a water wall with tinted glass on its outer surface and insulation on its inner surface. The change in heat flux from the air channel to the storage wall is not significantly dependent on the thickness of the storage wall. Further, on July 15th a maximum heat transfer of 158 W/m^2 occurs during the peak sunshine hours between 12:00 to 1:00 pm.

The heat transferred from the storage wall into the building room is also shown in Figure B.14. There is no significant change in the heat flux entering the room due to changes in the storage wall thickness. A maximum heat transfer of about 7 – 9 W/m^2 occurs from 9:00 am to 5:00 pm. For the case when the storage wall thickness is 16 cm, the maximum heat transferred from the storage wall to the room around 8.7 W/m^2 at around 5:00 pm on July 15th.

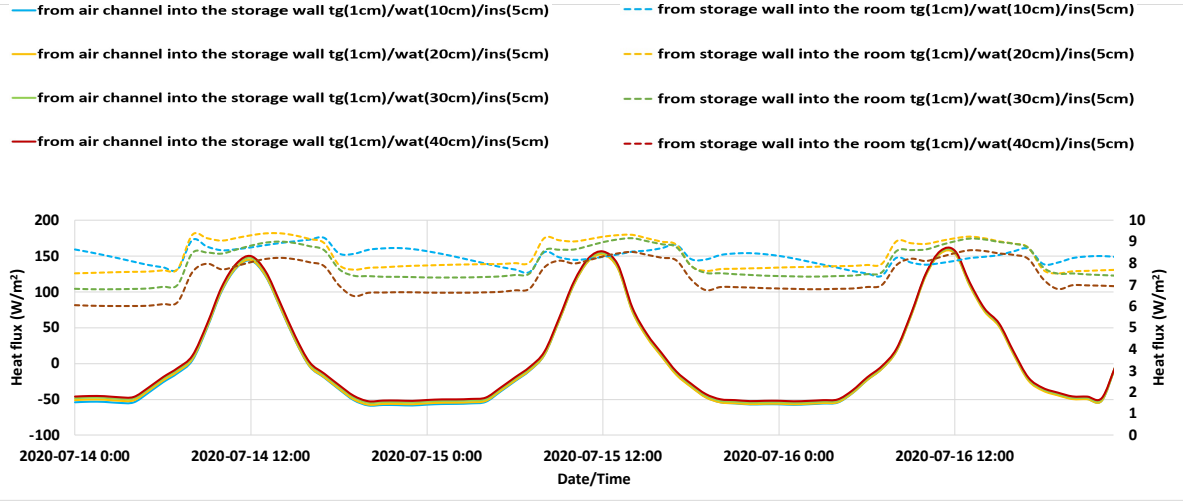

Figure B.14. Heat transferred from the air channel to the storage wall (solid lines) and from the storage wall to the room normalized by floor area (W/m^2) for the building shown in Figure 3.1 for the case when the Trombe wall is comprised of a water storage wall of varying thickness with tinted glass at its outer surface and transparent at its inner surface during summer on July 14, July 15, and July 16, 2020, in Toronto, Ontario

B.4.3. Hourly cooling load for the case of the water Trombe wall with tinted glass at its outer side and transparent insulation at its inner side

Figure B.15 shows the hourly cooling load for three consecutive days (July 14, 15, and 16) for the building shown in Figure 3.1 when the Trombe wall comprises a storage wall with a water wall that has tinted glass on its outer surface and insulation on its inner surface. The results show that the zone cooling load during peak hours decreases slightly as the Trombe wall thickness increases. For example, on July 14th at around 8 am the zone cooling load is around 47 W/m^2 when the storage wall is 11 cm thick, whereas the cooling load at this time is about 43 W/m^2 when the storage wall is 41 cm thick. Similarly, the cooling load in the evening on July 14th around 5 pm is recorded to be around 31 W/m^2 for an 11 cm thick wall. On the other hand, the cooling load at this time reduced to around 29 W/m^2 with an increase in wall thickness to 41 cm.

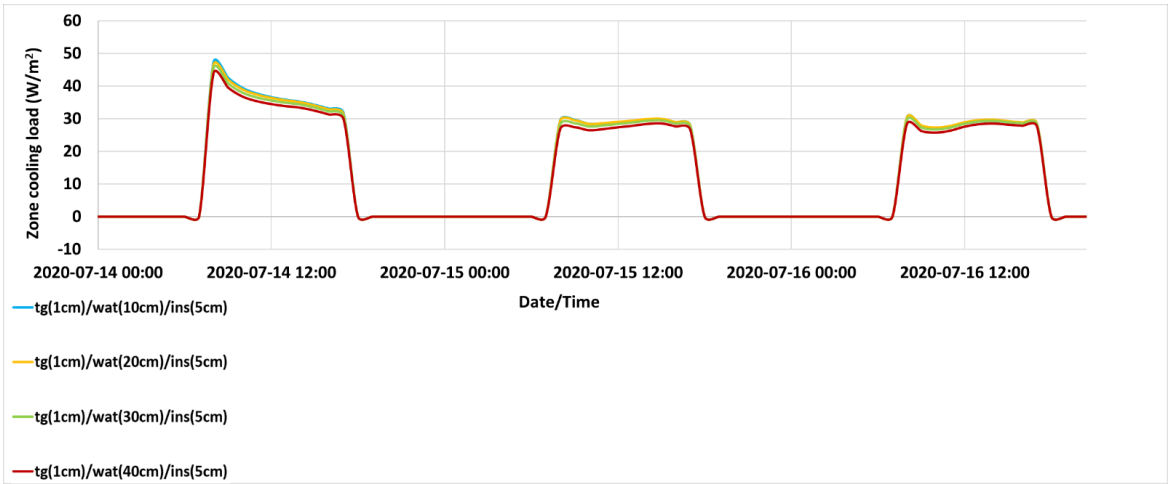

Figure B.15. Hourly cooling load normalized by floor area (W/m^2) for three consecutive days (July 14, 15, and 16) for the building shown in Figure 3.1 for the case when the Trombe wall consists of a storage wall made of tinted glass (layer 1), a water storage wall of different thicknesses (layer 2), and transparent insulation (layer 3) during summer in Toronto, Ontario

B.4.4. Total cooling load for the case of the water Trombe wall with tinted glass at its outer side and transparent insulation at its inner side over three consecutive summer days

Figure B.16 shows the total cooling load for three consecutive days (July 14, 15, and 16) for the building shown in Figure 3.1 when it has a water wall of varying thickness with tinted glass on its outer surface and insulation on its inner surface. The results show that the total cooling load decreases with an increase in the Trombe wall thickness. For example, the total cooling load when the storage wall thickness is 41 cm is 5.4 % less than the case in which the storage wall thickness is 11 cm.

Figure B.16. Total cooling load normalized by floor area (W/m^2) for three consecutive days (July 14, 15, and 16) for the building model shown in Figure 3.1 for the case when the Trombe wall consists of a storage wall made of tinted glass (layer 1), a water storage wall of varying thickness (layer 2), and transparent insulation (layer 3) during summer in Toronto, Ontario

B.5. Simulation results for a water Trombe wall with tinted glass at its outer side and transparent insulation on both sides under summer conditions

B.5.1. Thermal energy stored in a water Trombe wall with tinted glass at its outer side and transparent insulation on both sides

Figure B.17 shows the thermal energy stored in a Trombe wall model consisting of a water storage wall of varying thickness with tinted glass at its outer surface and insulation on both surfaces. The results show that the thermal energy stored in the Trombe wall increases with an increase in the thickness of the storage wall. For example, on July 15th, the maximum thermal energy stored is 599 MJ when the thickness of the wall is 51, however, the minimum energy stored is around 152 MJ which occurs when the thickness of the storage wall is 21 cm.

On the other hand, the maximum temperature achieved throughout the day in the storage wall (T_M) and ΔT decreases slightly as the thickness of the wall increases. For example, there is a 0.42 °C decrease in the maximum temperature (T_M) and ΔT on 15th July when the thickness of the water wall is increased from 21 cm to 51 cm.

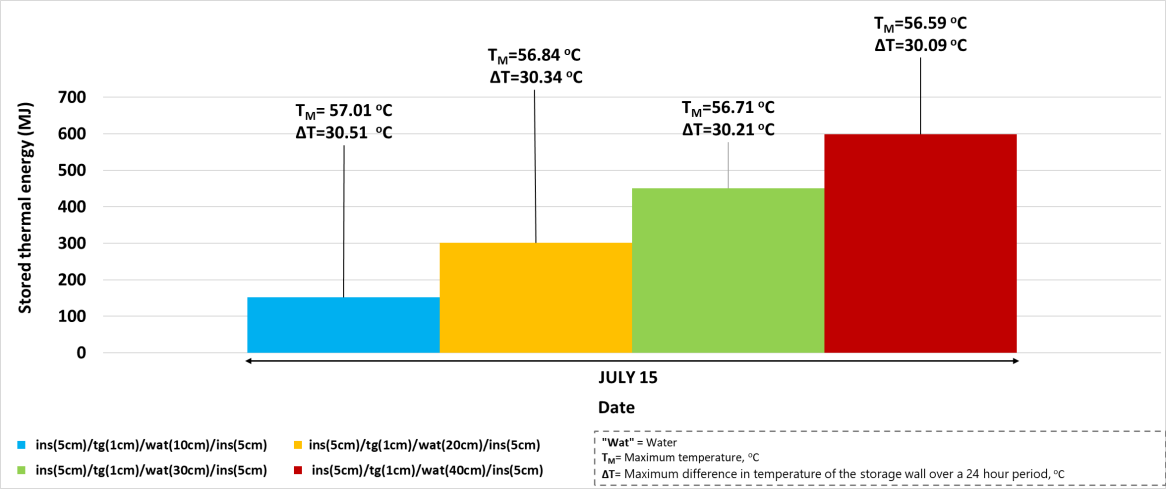

Figure B.17. Thermal energy stored in a Trombe wall consisting of a storage wall of varying thickness made of transparent insulation (layer 1), tinted glass (layer 2), water (layer 3), and transparent insulation (layer 4) during summer on July 14, July 15, and July 16, 2020, in Toronto, Ontario

B.5.2. Heat transferred through the surfaces of the water storage wall with tinted glass at its outer side and insulation on both sides under summer conditions

Figure B.18 shows the heat transferred from the air channel into the storage wall (solid lines) for the case of a water wall with tinted glass at the outer side, and insulation at both sides. The amount of heat entering the storage wall barely changes as the thickness of the storage wall changes. Further, a maximum heat transfer of around 26 W/m^2 entering the storage wall occurs during the peak sunshine hours between 12:00 to 1:00 pm on July 16th. A small amount of heat, up to a maximum of about 6 W/m^2 for the 5 cm thick Trombe wall, is transferred from the storage wall into the room, as shown by the dashed lines in Figure B.17.

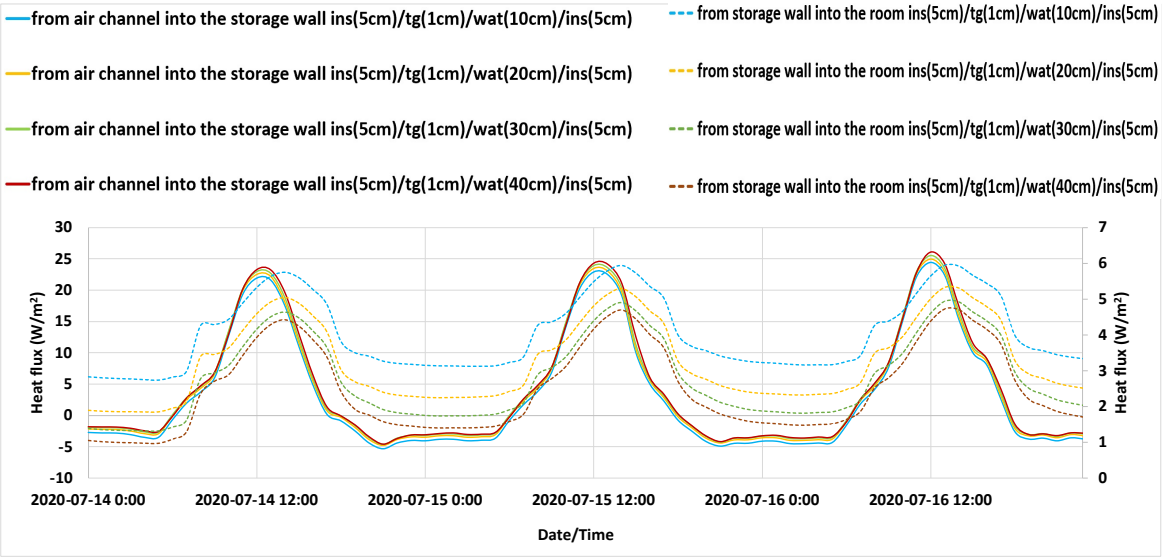

Figure B.18. Heat transferred form the air channel into the storage wall (solid lines) and from the storage wall into the room (dashed lines) normalized by floor area (W/m^2) for the case when the Trombe wall consists of a storage wall made of transparent insulation (layer 1), tinted glass (layer 2), water of varying thickness (layer 3), and transparent insulation (layer 4) during summer on July 14, July 15, and July 16, 2020, in Toronto, Ontario

B.5.3. Hourly cooling load for the case of the water Trombe wall with tinted glass at its outer side and insulation on both sides over three consecutive summer days

Figure B.19. shows the hourly cooling load for three consecutive days (July 14, 15, and 16) for the building shown in Figure 3.1 when it is equipped with a Trombe wall comprised of a water storage wall of varying thickness with tinted glass at its outer surface and insulation on both of its surfaces. The results show that the zone cooling load during peak hours decreases as the thickness of the Trombe wall increases. For example, on July 14th at 8 am the zone cooling load is around 36 W/m^2 when the thickness of the storage wall is 11 cm, whereas the cooling load at this time is about 32 W/m^2 when the wall thickness is 41 cm thick. Similarly, the cooling load in the evening on July 14th around 5 pm is calculated to be around 25 W/m^2 for an 11 cm thick storage wall. On the other hand, the cooling load on the same day/time is reduced to around 23 W/m^2 with an increase in wall thickness to 41 cm.

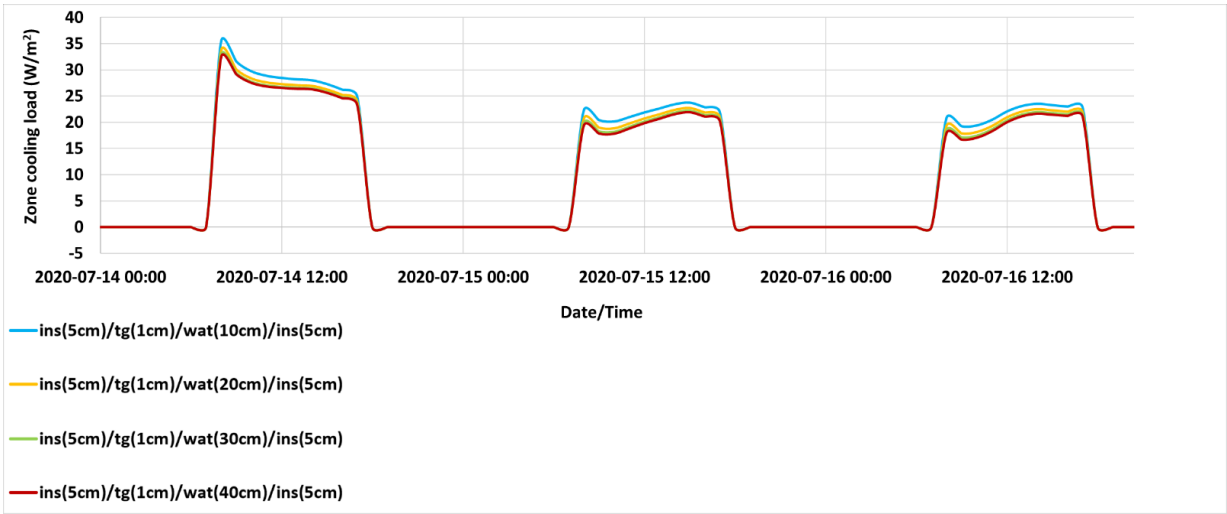

Figure B.19. Hourly cooling load normalized by floor area (W/m^2) for three consecutive days (July 14, 15, and 16) for the building model shown in Figure 3.1 for the case when the Trombe wall is comprised of a storage wall made of transparent insulation (layer 1), tinted glass (layer 2), water of varying thickness (layer 3), and transparent insulation (layer 4) during summer in Toronto, Ontario

B.5.4. Total cooling load for the case of the water Trombe wall with tinted glass on its outer side and insulation on both sides over three consecutive summer days

Figure B.20 shows the total cooling load for three consecutive days (July 14, 15, and 16) for the building shown in Figure 3.1 when it has a Trombe wall made of a water storage wall with tinted glass at the outer side and insulation at both surfaces. The results show that the total cooling load decreases as the thickness of the storage wall increases. For example, the total cooling load when the thickness of the storage wall is 41 cm is 8.6 % less than the cooling load for the case when the thickness is 11 cm.

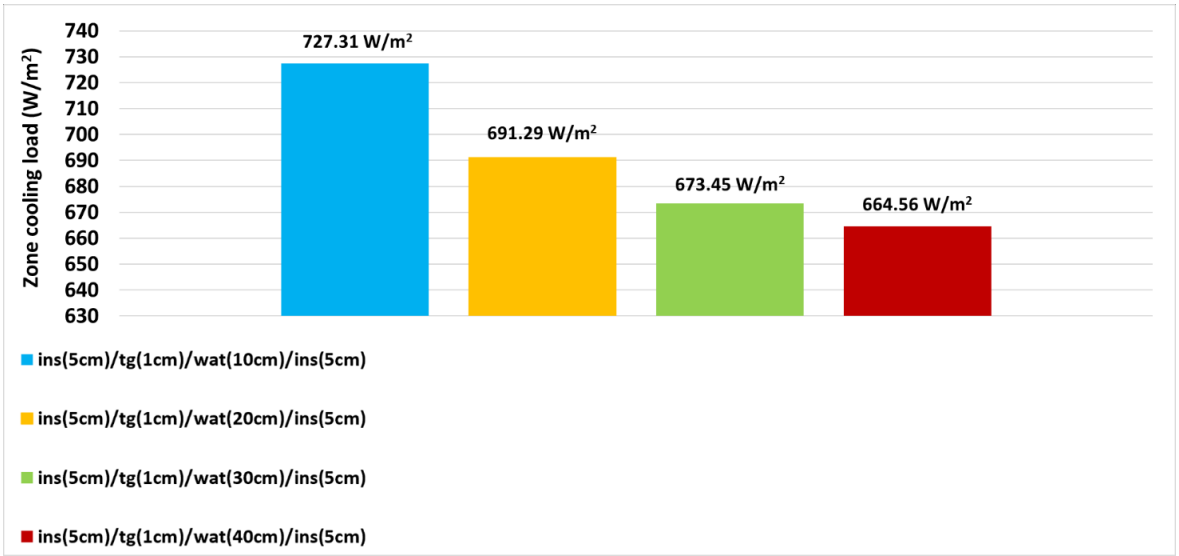

Figure B.20. Total cooling load normalized by floor area (W/m^2) for the building shown in Figure 3.1 over three consecutive days (July 14, 15, and 16) for the case when the Trombe wall consists of a storage wall made of transparent insulation (layer 1), tinted glass (layer 2), water of varying thickness (layer 3), and transparent insulation (layer 4) during summer in Toronto, Ontario

B.6. Simulation results for a water Trombe wall with tinted glass at its center under summer weather conditions

B.6.1. Thermal energy stored in a water Trombe wall with tinted glass at its center under summer conditions

Figure B.21 shows the thermal energy stored in the Trombe wall comprised of a water wall with tinted glass at its center for varying thicknesses of water. The solid bars show the stored thermal energy, the maximum temperature, T_M, and the change in temperature ΔT, for the outer half of the water storage wall (between the tinted glass and the air channel). The bars with the diagonal lines indicate the amount of thermal energy stored, T_M and ΔT for the inner half of the water storage wall (between the tinted glass and the room).

The maximum thermal energy storage in the inner and outer wall is achieved when the thickness of the wall is 41 cm whereas the minimum thermal energy storage is stored when the storage wall is 11 cm thick. For example, on July 15th the maximum thermal energy stored in the 41 cm thick storage wall is around 62.4 MJ, and the maximum stored in the outer wall is around 181.1 MJ. However, the energy stored for the case when the storage wall is 11 cm thick is around

16.5 and 37 MJ for the inner and outer portion of the water storage wall, respectively. For all cases the amount of thermal energy stored, T_M, and ΔT are substantially larger for the outer half of the wall as compared to that for the inner half of the storage wall.

Furthermore, the maximum temperature (T_M) and ΔT values of the outer portions of the storage wall both increase as the thickness of the wall increases. On the other hand, the maximum temperature (T_M) and ΔT values of the inner portions of the wall decrease as the thickness of the wall increases. For example, there is a 3.43 °C increase in the temperature (T_M) and ΔT values on 15th July with an increase in thickness from 11 cm to 41 cm for the outer portions of the water wall. However, there is a 0.34 °C decrease in the temperature (T_M) and ΔT values on 15th July with an increase in thickness from 11 cm to 41 cm for the inner portions of the water wall.

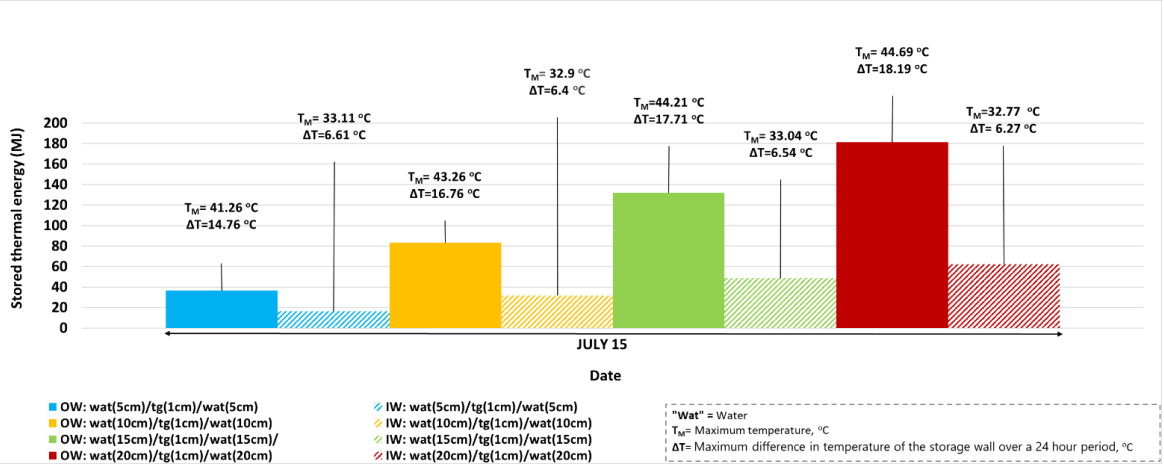

Figure B.21. Thermal energy stored in a Trombe wall consisting of a storage wall made of water with different thicknesses and a tinted glass layer at its center during summer on July 14, July 15, and July 16, 2020, in Toronto, Ontario

B.6.2. Heat transferred through the surfaces of the water storage wall with tinted glass at its center in summer conditions

Figure B.22 shows the heat transferred from the air channel to a water storage wall with a pane of tinted glass at its center (solid lines). There is no significant change in the heat entering the storage wall due to a change in the thickness of the storage wall. Moreover, on July 15th a maximum heat flux of around 179 W/m^2 occurs during the peak sunshine hours between 12:00 to

1:00 pm. The heat flux from the storage wall to the room is also shown by the dashed lines in Figure 48. When the thickness of the wall is 21 cm or greater, the maximum airflow from 9:00 am to 5:00 pm is between 40– 56 W/m^2. When the water storage wall is 11 cm thick the maximum heat transfer rate from the storage wall into the room is about 67 W/m^2 at 5:00 pm on July 15th.

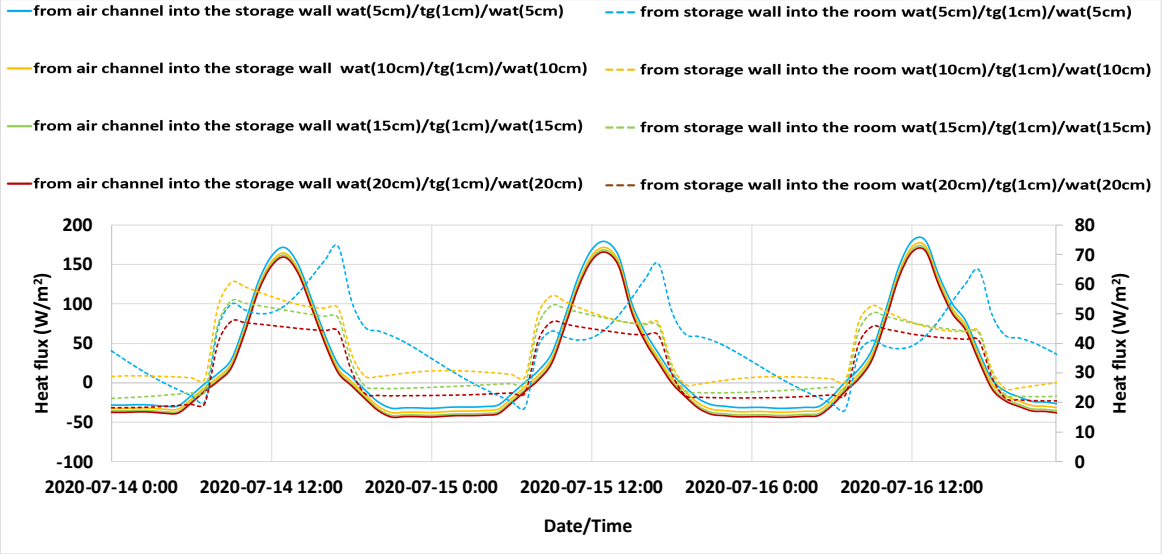

Figure B.22. Heat transfer from the air channel into the storage wall (solid lines) and from the storage wall into the room (dashed lines) normalized by floor area (W/m^2) for the case in which the Trombe wall model shown in Figure 3.1 consists of a water wall of varying thickness with tinted glass at its center during summer on July 14, July 15, and July 16, 2020, in Toronto, Ontario

B.6.3. Hourly cooling load for the case of a Trombe wall with tinted glass at its center over three consecutive summer days

Figure B.23 shows the hourly cooling load for three consecutive days (July 14, 15, and 16) for the model building shown in Figure 3.1 for the case when the Trombe wall consists of a water storage wall with a tinted pane of glass at its midplane. The results show the zone cooling load during peak hours decreases as the thickness of the Trombe wall increases. For example, on July 14th at around 8 am the zone cooling load is around 122 W/m^2 when the storage wall thickness is 11 cm, whereas the cooling load on the same day and time is about 94 W/m^2 when the thickness of the storage wall is 41 cm. Similarly, the cooling load in the evening on July 14th around 5 pm is calculated to be around 97 W/m^2 for an 11 cm thick wall. On the other hand, the cooling load on the same day/time is reduced to around 66 W/m^2 with an increase in wall thickness to 41 cm.

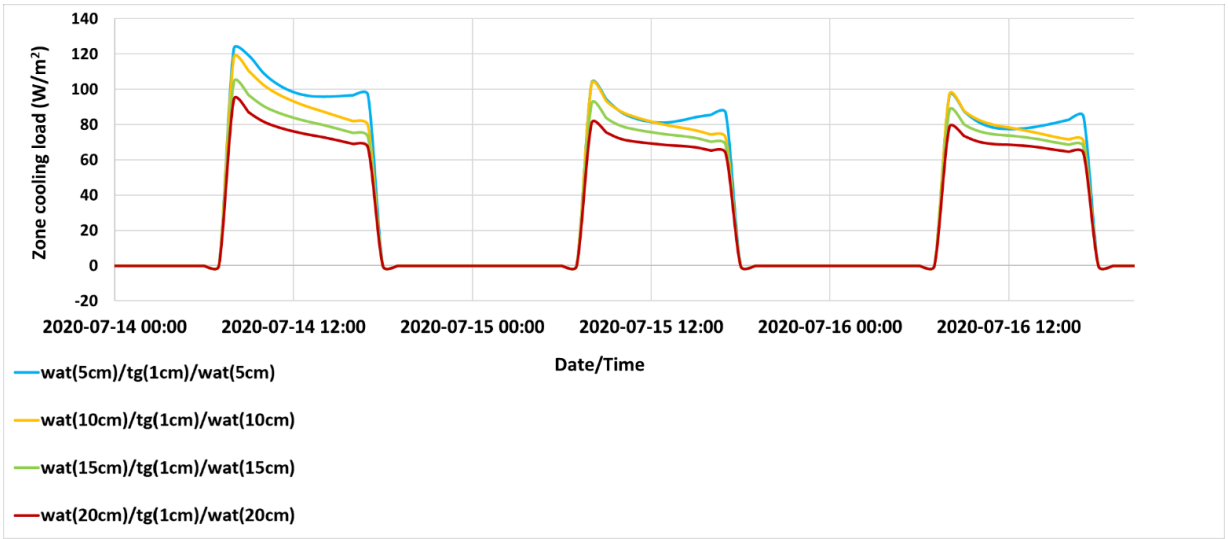

Figure B.23. Hourly cooling load normalized by floor area (W/m^2) for the building shown in Figure 3.1 for three consecutive days (July 14, 15, and 16) for the case when the Trombe wall is comprised of a water wall with varying thickness and tinted glass at its midplane during summer in Toronto, Ontario

B.6.4. Total cooling load for the case of the water Trombe wall with tinted glass at its center over three summer days

Figure B.24 shows the total cooling load for three consecutive days (July 14, 15, and 16) for the building shown in Figure 3.1 for a Trombe wall comprising a water storage wall with tinted glass at its midplane. The results show the total cooling load decreases as the Trombe wall thickness increases. For example, the total cooling load when the wall thickness is 41 cm is 20.9 % less than for the case when the storage wall thickness is 11 cm.

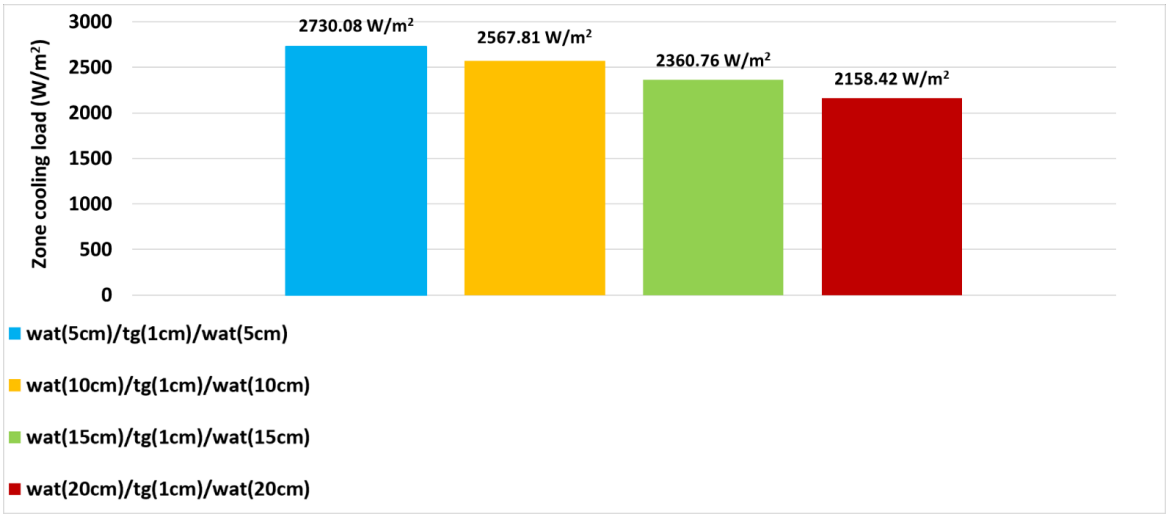

Figure B.24. Total cooling load normalized by floor area (W/m^2) for three days (July 14, 15, and 16) for the model building shown in Figure 3.1 for the case when the Trombe wall consists of a water wall of varying thickness with tinted glass at its midplane during summer in Toronto, Ontario

B.7. Simulation results for a water Trombe wall with tinted glass at its center and insulation at its inner side under summer weather conditions

B.7.1. Thermal energy stored in a water Trombe wall with tinted glass at its center and insulation at its inner side under summer conditions

Figure B.25 shows the thermal energy stored in a Trombe wall model consisting of a water storage wall of varying thickness with tinted glass at its midplane and insulation at its inside surface. As expected, the results show that the total thermal energy stored in the inner and other portions of the Trombe wall increases with an increase in the thickness of the wall.

The maximum thermal energy storage in the inner and outer portions of the storage wall is achieved when the thickness of the wall is 46 cm whereas the minimum amount of thermal energy stored occurs when the wall thickness is 16cm. For example, for the case when the thickness of the storage wall is 46 cm, on July 15th the maximum thermal energy stored in the inner portion of the wall is around 239 MJ, and the maximum energy stored in the outer part of the wall is around 263 MJ. However, the minimum energy stored for the case when the thickness is 16 cm is around 69 MJ and 71 MJ for the inner and outer portions of the wall, respectively.

On the other hand, the maximum temperature (T_M) and ΔT of both the inner and outer portions of the wall decreases as the thickness of the wall increases. For example, there is a 2.21°C and 3.88 °C decrease in T_M and ΔT values on 15th July as the thickness increases from 16 cm to 46 cm for the outer and inner wall, respectively.

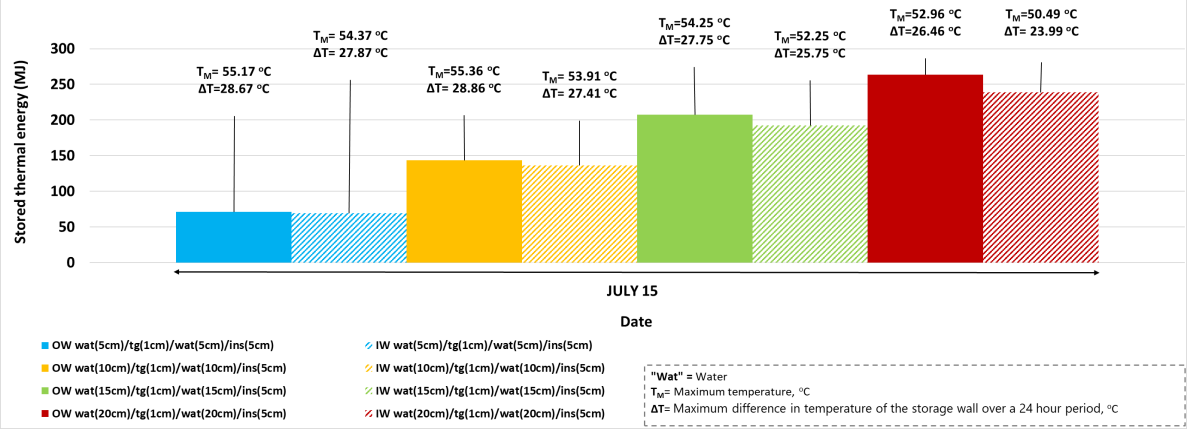

Figure B.25. Thermal energy stored in a Trombe wall consisting of a water wall of varying thickness with tinted glass at its midplane and transparent insulation at its inner surface during summer on July 14, July 15, and July 16, 2020, in Toronto, Ontario

B.7.2. Heat transferred through the surfaces of the water storage wall with tinted glass at its center and insulation at its inner side under summer conditions

Figure B.26 shows heat transferred from the air channel to the storage wall (solid lines) for the case of the water storage wall with tinted glass at its midplane and insulation at its inside surface. There is no significant change the heat transferred from the air channel to the storage wall due to a change in the storage wall thickness. Furthermore, a maximum heat transfer of around 150 W/m^2 enters the storage wall during the peak sunshine hours from 12:00 to 1:00 pm on July 14th. The heat flux from the storage wall into the room is also plotted in Figure 4.29 as the dashed lines. There is no significant change in the heat flux from the storage wall into the room when the thickness of the storage wall changes. The maximum heat transferred, occurring from 9:00 am to 5:00 pm, is between 6.4– 9 W/m^2.

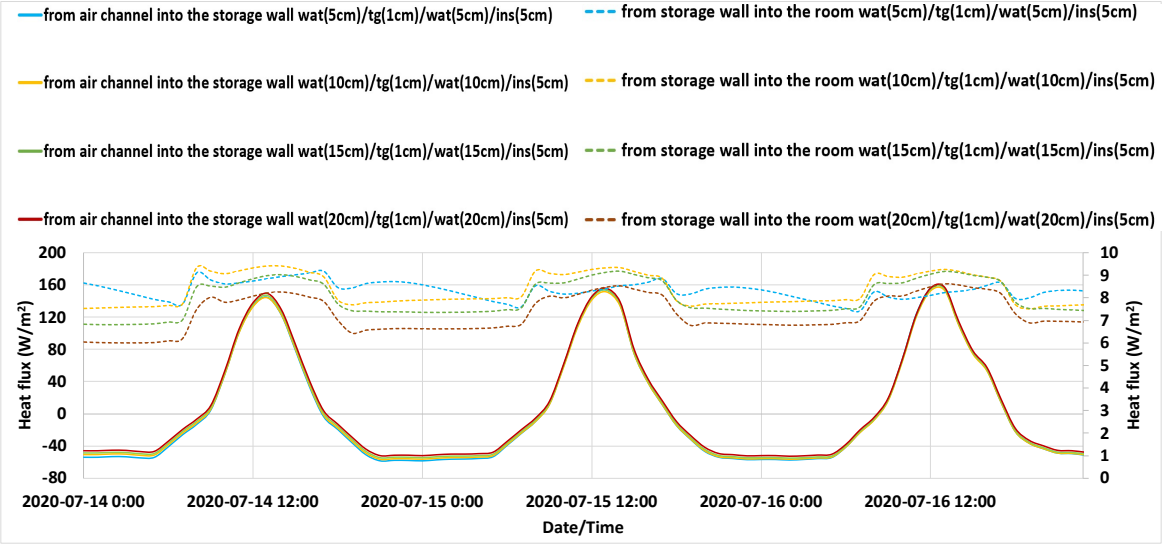

Figure B.26. Heat transferred from the air channel to the storage wall and from the storage wall to the air channel normalized by floor area (W/m^2) in a Trombe wall shown in Figure 3.1 consisting of a water storage wall of varying thickness with tinted glass at its midplane and transparent insulation at its inner surface during summer on July 14, July 15, and July 16, 2020, in Toronto, Ontario

B.7.3. Hourly cooling load for the case of the water Trombe wall with tinted glass at its center and insulation at its inner surface over three consecutive summer days

Figure B.27 shows the hourly cooling load for three consecutive days (July 14, 15, and 16) in a Trombe wall consisting of a water storage wall of varying thicknesses with tinted glass at its midplane and insulation at its inside surface. The results show that the zone cooling load during peak hours decreases with an increase in the Trombe wall thickness. For example, on July 14th at around 8 am the zone cooling load is around 46 W/m^2 when the wall thickness is 11 cm, whereas the cooling load on the same day and time is about 43 W/m^2 when the wall thickness is 41 cm. Similarly, the cooling load in the evening on July 14th at 5 pm is calculated to be around 32 W/m^2 for an 11 cm thick wall. On the other hand, the cooling load during the same day/time is reduced to around 29 W/m^2 when the wall thickness increases to 41 cm.

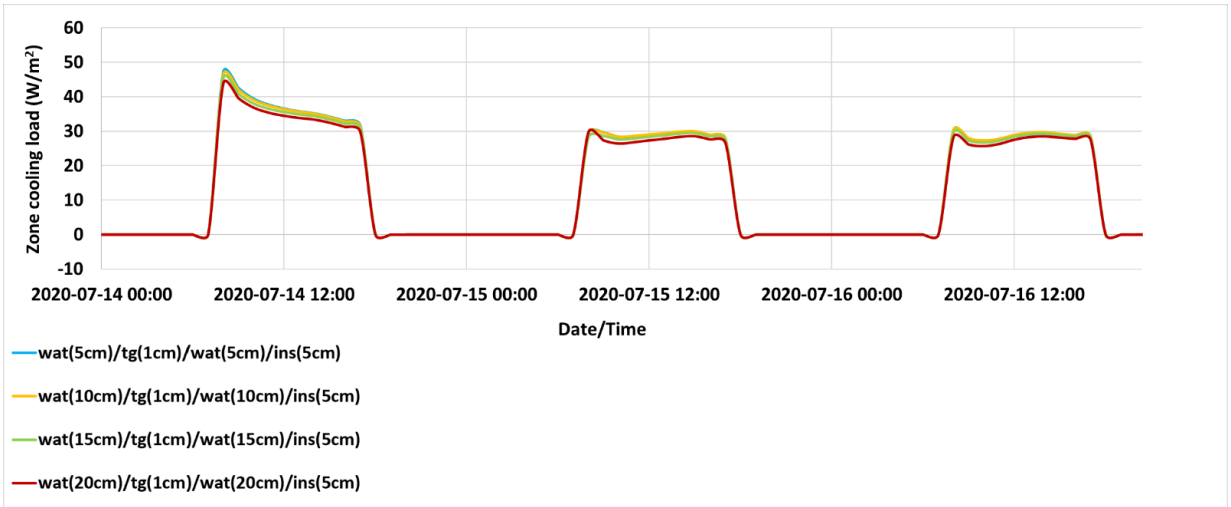

Figure B.27. Hourly cooling load normalized by floor area (W/m^2) for three consecutive days (July 14, 15, and 16) for the model building shown in Figure 3.1 for the case when the Trombe wall consists of a storage wall made of water of varying thickness with tinted glass at its midplane and transparent insulation at its inner surface during summer, 2020, in Toronto, Ontario

B.7.4. Total cooling load for the case of the water Trombe wall with tinted glass at its center and insulation at its inner surface over three consecutive summer days

Figure B.28 shows the total cooling load for three consecutive days (July 14, 15, and 16) in a Trombe wall equipped with a water storage wall with tinted glass at its midplane and insulation on its inner surface. The results show that the total cooling load decreases slightly as the thickness of the storage wall increases. For example, the total cooling load when the storage wall thickness is 41 cm is 5.2 % less than the cooling load that occurs when the storage wall is 11 cm thick.

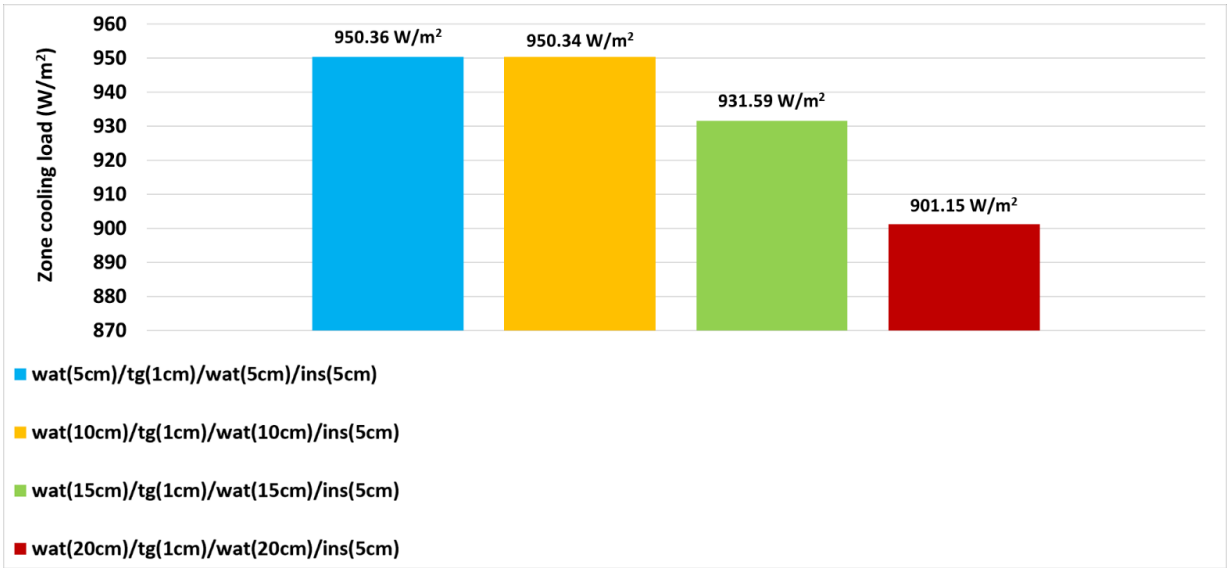

Figure B.28. Total cooling load normalized by floor area (W/m^2) for three consecutive days (July 14, 15, and 16) for the model building shown in Figure 3.1 for the case when the Trombe wall consists of a water wall of varying thickness with tinted glass at its midplane and transparent insulation at its inner surface during summer in Toronto, Ontario

B.8. Simulation results for a water Trombe wall with tinted glass at its center and insulation at both sides under summer weather conditions

B.8.1. Thermal energy stored in a water Trombe wall with tinted glass at its center and insulation at both sides

Figure B.29 shows the thermal energy stored in a Trombe wall consisting of a water storage wall with a tinted glass layer at its midplane and insulation on both sides. For the cases considered, the maximum thermal energy stored within the inner and outer portions of the water wall is achieved when the thickness of the wall is 51 cm, whereas the minimum thermal energy storage is stored at 21 cm thickness. For example, on July 15th the maximum thermal energy stored in the inner and outer portions of the 51 cm thick wall is around 315 MJ and 286 MJ, respectively. The energy stored when the wall thickness is 21 cm is around 75 and 77 MJ for the inner and outer portions of the wall, respectively.

The maximum temperature (T_M) and ΔT of the outer wall increase with an increase in the thickness of the wall. For example, there is an 0.52 ^oC increase in the temperature (T_M) and 0.62

°C increase in the ΔT value on July 15th when the thickness increases from 21 cm to 51 cm for the outer portions of the wall. On the other hand, the maximum temperature (T_M) and ΔT of the inner wall decrease with an increase in the thickness of the wall. For example, there is an 0.45 °C decrease in the temperature (T_M) and 1.45 °C decrease in the ΔT value on July 15th when the thickness increases from 21 cm to 51 cm for the inner portions of the wall.

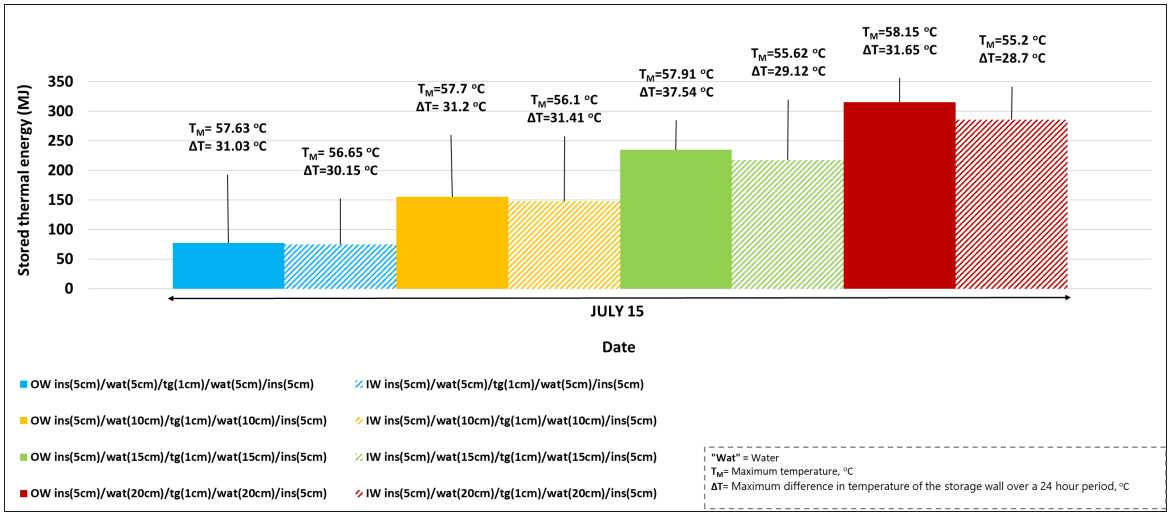

Figure B.29. Thermal energy stored in a Trombe wall consisting of storage wall of varying thickness made of transparent insulation (layer1), water of varying thickness (layer 2), tinted glass (layer 3), water of varying thickness (layer 4), and transparent insulation (layer5) during summer on July 14, July 15, and July 16, 2020, in Toronto, Ontario

B.8.2. Heat transferred through the surfaces of the room and water storage wall with tinted glass at its center and insulation at both sides during summer conditions

Figure B.30 shows heat transferred from the air channel to the storage wall for the case when the storage wall is a water wall with varying thickness with tinted glass at its midplane and insulation on both of its surfaces. There is no significant change in the heat entering the storage wall due to a change in its thickness. Also, a maximum heat transfer of around 23 W/m^2 entering the storage wall occurs during the peak sunshine hours between 12:00 to 1:00 pm on July 14th.

The heat transferred from the storage wall into the room is also shown as the dashed lines in Figure B.30. The amount of heat transferring from the storage wall into the room decreases as the thickness of storage wall increases. For example, on July 15th the maximum heat flux is around

5.9 W/m^2 at around 3 pm when the thickness is 21 cm. However, the maximum heat flux amount decreases to approximately 4 W/m^2 when the wall thickness is increased to 51 cm.

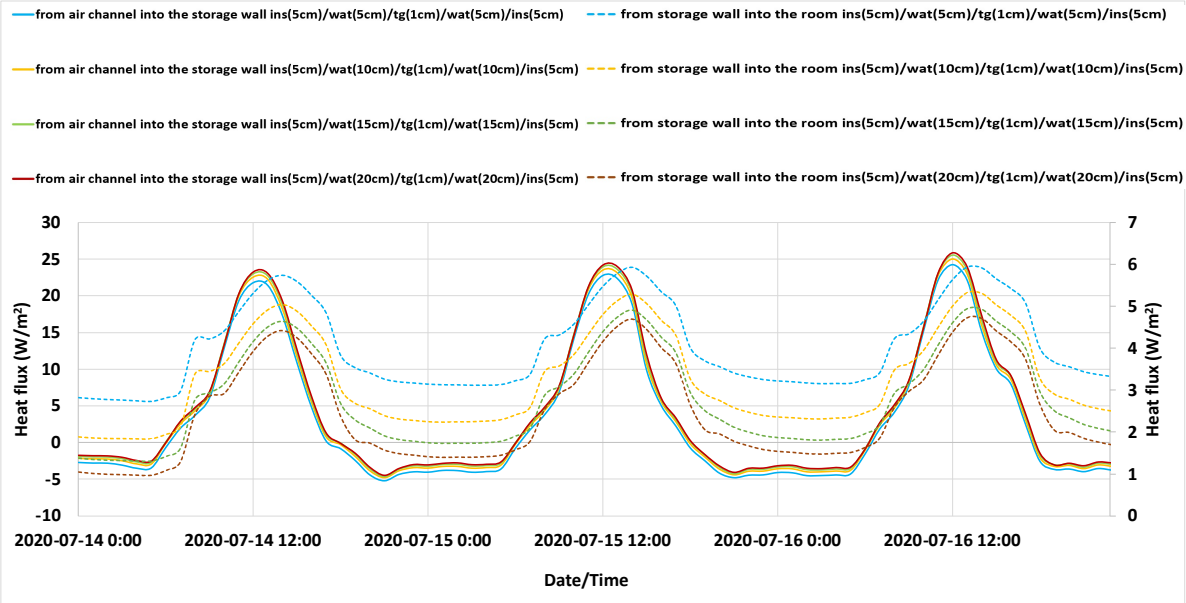

Figure B.30. Heat transferred from the air channel to the storage wall (solid lines) and from the storage wall to the room (dashed lines) normalized by floor area (W/m^2) for the case when the Trombe wall model shown in Figure 3.1 consists of a storage wall made of transparent insulation (layer 1), water of varying thickness (layer 2), tinted glass (layer 3), water of varying thickness (layer 4), and transparent insulation (layer 5), during summer on July 14, July 15, and July 16, 2020, in Toronto, Ontario

B.8.3. Hourly cooling load for the case of the water Trombe wall with tinted glass at its center and insulation at both sides over three consecutive summer days

Figure B.31 shows the hourly cooling load for three consecutive days (July 14, 15, and 16) for the building shown in Figure 3.1 for the case when the Trombe wall is comprised of a water storage wall of varying thickness with tinted glass at its midplane and insulation on both of its surfaces. The results show the zone cooling load during peak hours decreases slightly as the Trombe wall thickness increases. For example, on July 14th at 8 am the zone cooling load is around 35 W/m^2 when the wall thickness is 11 cm, whereas the cooling load on the same day and time is about 32 W/m^2 when the storage wall thickness is 41 cm.

Similarly, the cooling load in the evening on July 14th around 5 pm is recorded to be around 25 W/m^2 when the Trombe wall is 11 cm thick. On the other hand, the cooling load on the same day/time is reduced to around 23 W/m^2 when the thickness of the storage wall is 41 cm.

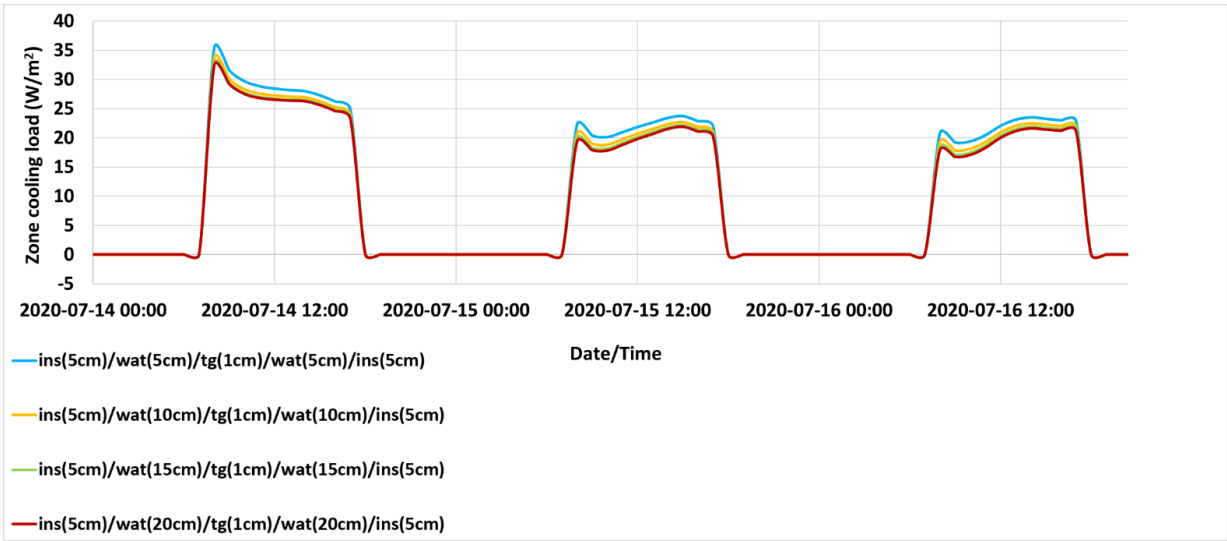

Figure B.31. Hourly cooling load normalized by floor area (W/m^2) for three consecutive days (July 14, 15, and 16) in a Trombe wall model consisting of a storage wall made of transparent insulation (layer 1), water of varying thickness (layer 2), tinted glass (layer 3), water of varying thickness (layer 4), and transparent insulation (layer 5), during summer in Toronto, Ontario

B.8.4. Total cooling load for the water Trombe wall with tinted glass at its center and insulation on both sides over three consecutive summer days

Figure B.32 shows the total cooling load for three consecutive days (July 14, 15, and 16) in a Trombe wall consisting of a water storage wall of varying thickness with tinted glass at its midplane and insulation on both sides. The results show that the total cooling load decreases with an increase in the Trombe wall thickness. For example, the total cooling load when the thickness is 41 cm is 8.5 % less than the cooling load when the storage wall thickness is 11 cm.

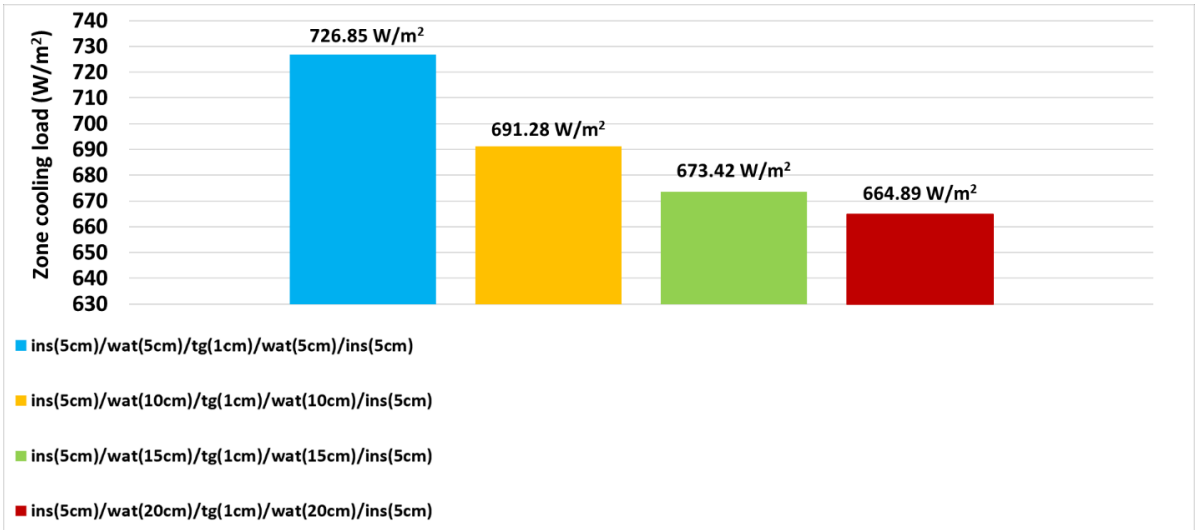

Figure B.32. Total cooling load normalized by floor area (W/m^2) for three consecutive days (July 14, 15, and 16) in a Trombe wall model consisting of a storage wall made of transparent insulation (layer 1), water of varying thickness (layer 2), tinted glass (layer 3), water of varying thickness (layer 4), and transparent insulation (layer 5), during summer in Toronto, Ontario

B.9. Simulation results for a sand Trombe wall under summer weather conditions

B.9.1. Thermal energy stored in a sand Trombe wall under summer conditions

Figure B.33 shows the thermal energy stored in a Trombe wall model consisting of a sand storage wall of varying thickness. As expected, the results show that the total thermal energy stored in the Trombe wall increases with an increase in the thickness of the wall. The maximum thermal energy stored in the wall is achieved when the thickness of the wall is 40 cm whereas the minimum amount of thermal energy stored occurs when the wall thickness is 5 cm. For example, for the case when the thickness of the storage wall is 40 cm, on July 15th the maximum thermal energy stored in the storage wall is around 130MJ. However, the minimum energy stored for the case when the thickness is 5 cm is around 22 MJ.

On the other hand, the maximum temperature (T_M) and ΔT decrease as the thickness of the wall increases up to 20 cm. For example, on July 15th there is a 3.73 ^oC decrease in T_M and ΔT values with an increase in the thickness from 5 cm to 40 cm.

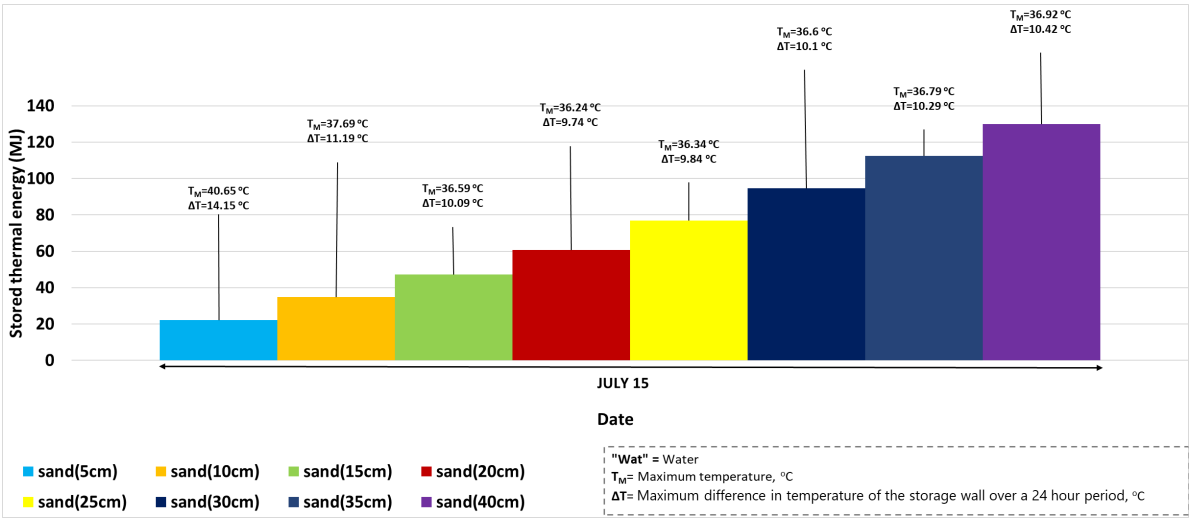

Figure B.33. Thermal energy stored in a Trombe wall consisting of storage wall of varying thickness made of granite sand during summer on July 14, July 15, and July 16, 2020, in Toronto, Ontario during summer on July 14, July 15, and July 16, 2020, in Toronto, Ontario

B.9.2. Heat transferred through the surfaces of the sand storage wall under summer conditions

Figure B.34 shows the heat transferred from the air channel to a sand storage wall (solid lines). There is no significant change in the heat entering the storage wall due to a change in the thickness of the storage wall. Moreover, on July 14th a maximum heat flux of around 192 W/m^2 occurs during the peak sunshine hours between 12:00 to 1:00 pm. The heat flux from the storage wall to the room is also shown by the dashed lines in Figure B.34.

When the thickness of the wall is 25 cm or greater, the maximum heat flux is around 98 W/m^2 at 5:00 pm on July 14th. When the sand storage wall thickness is between 10 cm to 20 cm, the maximum heat flux is approximately 122 W/m^2 at 5:00 pm on July 14th. When the water storage wall is 5 cm the maximum heat transfer rate from the storage wall into the room is about 157 W/m^2 at 3:00 pm on July 14th.

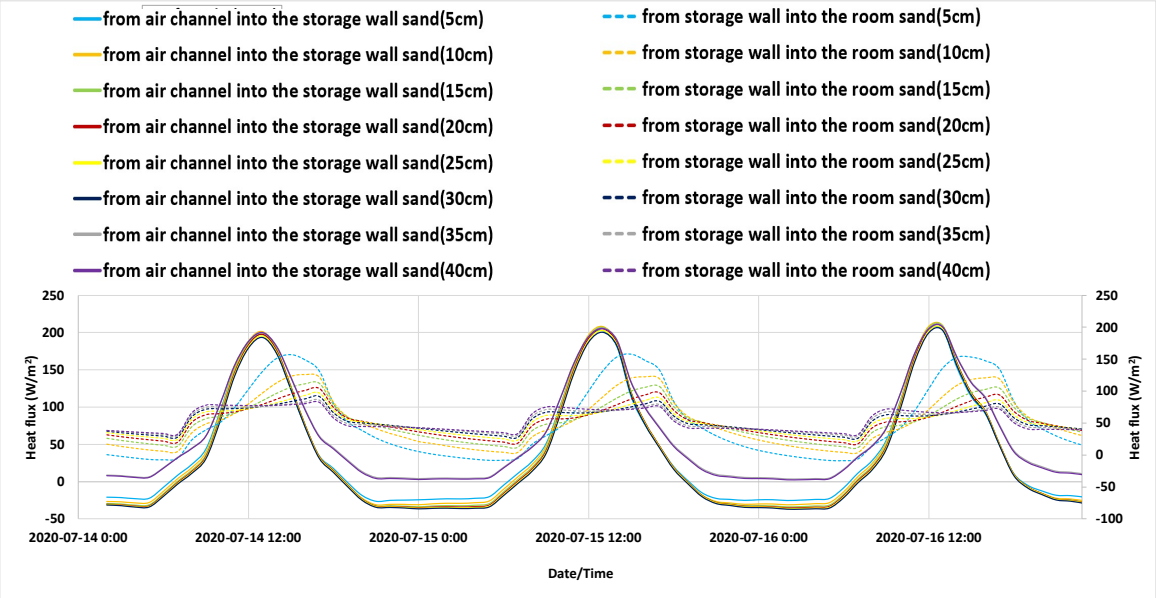

Figure B.34. Heat transferred from the air channel to the storage wall and from the storage wall into the room normalized by floor area (W/m^2) in a Trombe wall shown in Figure 3.1 consisting of a storage wall of varying thickness made of granite sand during summer on July 14, July 15, and July 16, 2020, in Toronto, Ontario

B.9.3. Hourly zone cooling load for the case of the sand Trombe wall under summer conditions

Figure B.35 shows the hourly cooling load for three consecutive days (July 14, 15, and 16) for the single room building shown in Figure 3.1 for the case when the Trombe wall has a sand storage wall of varying thickness.

The results show that the zone cooling load is higher later in day around 3:00 pm when the storage wall thickness is the thinnest. For example, on July 14th at around 8:00 am the zone cooling load is around 116 W/m^2 when the wall is 5 cm thick, and it increases up to 142 W/m^2 at around 3:00 pm on the same day. On the other hand, the cooling load is the highest in the morning when sun first comes out for increased wall thickness from 15 cm to 40 cm. For example, the cooling load on July 14th at around 8:00 am is around 140 W/m^2 when the wall thickness is 40 cm, and it is reduced to 116 W/m^2 at around 3 pm on the same day.

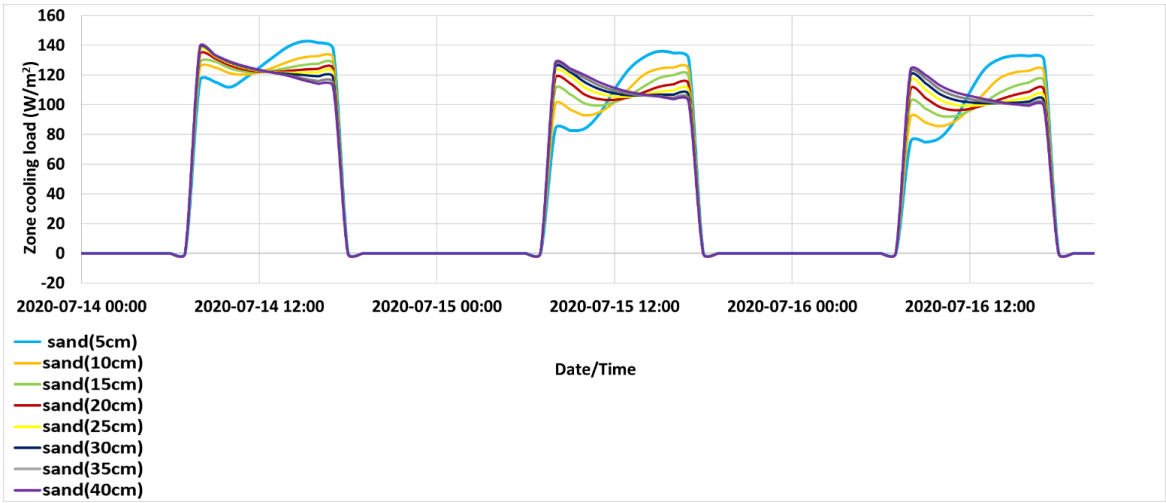

Figure B.35. Hourly cooling load normalized by floor area (W/m^2) for three consecutive days (July 14, July 15, and July 16, 2020) in a Trombe wall model consisting of storage wall of varying thickness made of granite sand during summer in Toronto, Ontario

B.9.4. Total cooling load in the sand Trombe wall for three consecutive days under summer conditions

Figure B.36 shows the total cooling load for the building shown in Figure 3.1 when the Trombe wall is made of a sand storage wall of varying thickness over three consecutive days (July 14, 15, and 16). The results show the total cooling load decreases with an increase in the sand wall thickness up to 15 cm. The cooling load increases as the Trombe wall thickness increases from 20 cm to 40 cm. For example, when the sand wall thickness is 5 cm the cooling load is about 3470 W/m^2, and the cooling load is approximately 3400 W/m^2 and 3388 W/m^2 when the water wall thickness is 10 cm and 15 cm, respectively. When the water wall thickness is 40 cm the cooling load is around 3437 W/m^2.

Figure B.36. Total cooling load normalized by floor area (W/m^2) for three consecutive days (July 14, July 15, and July 16, 2020) in a Trombe wall model consisting of a storage wall of varying thickness made of granite sand during summer in Toronto, Ontario

The results shown in Figures B9 to B12 show that the performance of the Trombe wall with a water wall integrated with tinted glass is very close to the case when the Trombe wall has a storage medium made of sand. The tinted glass effectively absorbs most of the sunlight which results in heating the adjacent water, which acts as a good TES medium, especially considering its high heat capacity. This section has shown the performance of a water-based Trombe wall can be very close to that of a sand-based Trombe wall under winter conditions. Thus, there is not a big disadvantage to using a water-based Trombe wall during winter conditions. The results in the next section are used to evaluate the benefits of using a water-based Trombe wall during the summer season.

APPENDIX C: CALCULATIONS OF THERMAL ENERGY STORED AND THERMAL EFFICIECNY

C.1. Experimental methods for determining the effects of integrating tinted glass at front side and clear plexiglass sheet at back side in water-based Trombe walls on their energy storage efficiency

C.1.1. Case 1: Water as a TES medium with clear plexiglass sheet integrated at the back side of the Trombe wall:

$$Q_i = Intensity \times area\ of\ acrylic\ plexi\ sheet$$

$$Q_i = \frac{44.35\ mW}{cm^2} \times 2467.74\ cm^2$$

$$Q_i = 109{,}444.269\ mW = 109.4\ W$$

$$Q_i = 109.4\ \frac{J}{s} \times 18000\ s$$

$$Q_i = 1.97\ MJ$$

$$Q_{TES} = m \times c_p \times \Delta_T$$

$$= v \times \rho \times c_p\ (T_2 - T_1)$$

$$T_{avg,top\ water,1x} = \frac{T_{top} + T_{middle}}{2}$$

$$T_{avg,bottom\ water,1x} = \frac{T_{middle} + T_{bottom}}{2}$$

$$T_{avg,top\ water,1x} = \frac{47\ ℃ + 35\ ℃}{2}$$

$$T_{avg,top\ Water,1x} = 41\ ℃$$

$$T_{avg,bottom\ water,1x} = \frac{35\ ℃ + 32\ ℃}{2}$$

$$T_{avg,bottom\ water,1x} = 33.5\ ℃$$

$$Q_{TES,top\ water,1x} = 0.009\ m^3 \times 990\ \frac{kg}{m^3} \times 4190\ \frac{J}{kg.°C}(41\ ℃ - 21.9\ ℃) = 0.71\ \text{MJ}$$

$$Q_{TES,bottom\ water,1x} = 0.009\ m^3 \times\ 990\ \frac{kg}{m^3} \times\ 4190\ \frac{J}{kg.°C}(33.5\ ℃ - 21.9\ ℃) = 0.43\ \text{MJ}$$

$$Q_{TES,water,1x} =\ 0.71\ \text{MJ} + 0.43\ \text{MJ}$$

$$Q_{TES,water,1x} = 1.14\ MJ$$

$$\eta_{exp,water,1x} = \frac{Thermal\ energy\ stored\ (Q_{TES})}{incident\ solar\ gain\ (Q_i)}$$

$$\eta_{exp,water,1x} = \frac{1.14\ MJ}{1.97\ MJ}$$

$$\eta_{exp,water,1x} = 57.87\ \%$$

C.1.2. Case 2: Water as a TES medium with a tinted acrylic sheet at its front side

$$T_{avg,top\ water,tg,1x} = \frac{T_{top} + T_{middle}}{2}$$

$$T_{avg,bottom\ water,tg,1x} = \frac{T_{middle} + T_{bottom}}{2}$$

$$T_{avg,top\ \ water,tg,1x} = \frac{56\ ℃ + 39\ ℃}{2}$$

$$T_{avg,top\ water,tg,1x} =\ 47.5\ ℃$$

$$T_{avg,bottom\ water,tg,1x} = \frac{39\ ℃ + 33\ ℃}{2}$$

$$T_{avg,bottom\ water,tg,1x} =\ 36\ ℃$$

$$Q_{TES,water,top\ tg,1x} = 0.009\ m^3 \times\ 990\ \frac{kg}{m^3} \times\ 4190\ \frac{J}{kg.°C}(47.5\ ℃ - 20.9℃) = 0.99\ \text{MJ}$$

$$Q_{TES,water,bottom\ tg,1x} = 0.009\ m^3 \times\ 990\ \frac{kg}{m^3} \times\ 4190\ \frac{J}{kg.°C}(36\ ℃ - 20.9℃) = 0.563\ \text{MJ}$$

$$Q_{TES,water,tg,1x} = 0.99 + 0.563$$

$$Q_{TES,water,tg,1x} = 1.55\ MJ$$

$$\eta_{exp,water,tg,1x} = \frac{Thermal\ energy\ stored\ (Q_{TES})}{incident\ solar\ gain\ (Q_i)}$$

$$\eta_{exp,water,tg,1x} = \frac{1.55\ MJ}{1.97\ MJ}$$

$$\eta_{exp,water,tg,1x} = 78.8\ \%$$

C.1.3. Case 3: Water as a TES medium with two clear plexiglass sheets at the rear side of the Trombe wall prototype:

$$Q_{TES} = m \times\ c_p\ \times\ \Delta_T$$

$$= v \times \rho \times\ c_p\ (T_2 - T_1)$$

$$T_{avg,top\ water,2x} = \frac{T_{top}+T_{middle}}{2}$$

$$T_{avg,bottom\ water,2x} = \frac{T_{middle} + T_{bottom}}{2}$$

$$T_{avg,top\ water,2x} = \frac{52\ ℃ + 35\ ℃}{2}$$

$$T_{avg,top\ water\ ,2x} = 43.5\ ℃$$

$$T_{avg,bottom\ water,2x} = \frac{35\ ℃ + 33\ ℃}{2}$$

$$T_{avg,bottom\ water\ ,2x} = 34\ ℃$$

$$Q_{TES,top\ water,2x} = 0.009\ m^3 \times\ 990\ \frac{kg}{m^3} \times\ 4190\ \frac{J}{kg.°C}(43.5\ ℃ - 22.82\ ℃) = 0.77\ \text{MJ}$$

$$Q_{TES,bottom\ water,2x} = 0.009\ m^3 \times\ 990\ \frac{kg}{m^3} \times\ 4190\ \frac{J}{kg.°C}(34℃ - 22.82\ ℃) = 0.42\ \text{MJ}$$

$$Q_{TES,water,2x} = 0.77 + 0.42$$

$$Q_{TES,water,2x} = 1.19\ MJ$$

$$\eta_{water,2x} = \frac{Thermal\ energy\ increase\ (Q_{TES})}{incident\ solar\ gain\ (Q_i)}$$

$$\eta_{exp,water,2x} = \frac{1.19\ MJ}{1.97\ MJ}$$

$$\eta_{exp,water,2x} = 60.27\ \%$$

C.1.4. Case 4: Water as a TES medium with a tinted acrylic sheet at the front side and with two clear plexiglass sheets at the rear side of the Trombe wall prototype:

$$T_{avg,top\ water,tg,2x} = \frac{T_{top} + T_{middle}}{2}$$

$$T_{avg,bottom\ water,tg,2x} = \frac{T_{middle} + T_{bottom}}{2}$$

$$T_{avg,top\ water,tg,2x} = \frac{56\ ℃ + 42\ ℃}{2}$$

$$T_{avg,top\ \ water,tg,2x} = 49\ ℃$$

$$T_{avg,bottom\ water,tg,2x} = \frac{42\ ℃ + 35.66\ ℃}{2}$$

$$T_{avg,bottom\ water,tg,2x} = 38.8\ ℃$$

$$Q_{TES,top\ water,tg,2x} = 0.009\ m^3 \times\ 990\ \frac{kg}{m^3} \times\ 4190\ \frac{J}{kg.°C}(49 - 22℃) = 1.01\ \text{MJ}$$

$$Q_{TES,bottom\ water,tg,2x} = 0.009\ m^3 \times\ 990\ \frac{kg}{m^3} \times\ 4190\ \frac{J}{kg.°C}(38.8 - 22℃) = 0.63\ \text{MJ}$$

$$Q_{TES,water,tg,2x} = 1.01 + 0.63$$

$$Q_{TES,water,tg,2x} = 1.64\ MJ$$

$$\eta_{exp,water,tg,2x} = \frac{Thermal\ energy\ stored\ (Q_{TES})}{incident\ solar\ gain\ (Q_i)}$$

$$\eta_{exp,water,tg,2x} = \frac{1.64\ MJ}{1.97\ MJ}$$

$$\eta_{exp,water,tg,2x} = 83.16$$

C.2. Average incident radiation:

To calculate the average incident radiant energy from the solar simulated light provided by the lamp, the plexiglass at the front of the Trombe wall prototype is considered to be divided into

equal areas in a 3 x 3 mesh. The incident light intensity is then measured at the centre of each of the nine areas in this mesh using a power meter (THORLABS, PM 100D), and the average of these measurements is taken as the average incident radiation.

C.2.1. First run

Table C.1. Average incident radiation (mw/cm^2) results from the first experimental run

	Incident radiation $(\frac{mw}{cm^2})$		
Top	43.38	54.42	32.85
Middle	65.18	81.2	53.7
Bottom	18.26	30.35	17.45

C.2.2. Second run

Table C.2. Average incident radiation (mw/cm^2) results from the second experimental run

	Incident radiation $(\frac{mw}{cm^2})$		
Top	40.51	51.89	35.07
Middle	66.14	78.6	53.81
Bottom	22.65	30.92	21.85

C.3. Energy balance: A rough energy balance was conducted to compare and check the energy flow in and out of the Trombe wall prototype. The incident energy from the lamp was compared to the sum of the thermal energy stored in the water, the energy of the light transmitted through the Trombe wall prototype, and the heat transferred through the front and rear faces of the Trombe wall prototype over the duration of the 5-hour charging phase. The heat losses through the

insulated surfaces of the Trombe wall prototype was estimated to be negligible. The results show that the energy inputs and outputs was balanced to within 10% for call cases. The energy balance calculations for all cases are shown in Table C.3. There were rough assumptions made while conducting the energy balance. These assumptions were:

- A convective heat transfer coefficient, h = 4 W/m^2·K was assumed for all air/plexiglass surfaces. This was selected because it minimized the discrepancy in the energy balance and because it is a reasonable h-value for an air/plexiglass interface.
- The difference in temperature between the inside and outside of the Trombe wall prototype at the 5-hour point of the experiment (just before the light was turned off) was used when calculating the heat loss through the front and rear sides of the prototype. The temperature difference at the 5-hour mark was assumed to be representative of the temperature difference during the entire charging period.
- Average temperatures were used for the water, and air inside and surrounding the Trombe wall prototype.

List of Symbols

Symbol		Units
E_I	Energy input	MJ
E_L	Energy losses	MJ
E_B	Energy balance	MJ
Q_i	Incident light	MJ
L_R	Light transmitted through rear window	MJ
Q_F	Heat transfer through front window	MJ
Q_R	Heat transfer through rear window	MJ

List of Acronyms

TES	Thermal energy stored
Wat,1x	Water and single window at back
Wat,2x	Water and double window at back
Wat/tg,1x	Water with tinted glass at front and single window at back
Wat/tg,2x	Water with tinted glass at front and double window at back

Table C.3. Energy balance calculations for all four cases of Trombe wall prototype model

Case	$E_I\ (MJ)$	TES (MJ)	$E_L\ (MJ)$			E_B	
	Q_i	TES	L_R	Q_F	Q_R	$E_I - TES - L_R - Q_F - Q_R$ (MJ)	$\frac{(E_I - TES - L_R - Q_F - Q_R)}{E_I} \times 100$
Case 1 Wat/tg,2x	1.97	1.64	0.01	0.33	0.07	-0.03	-3.1
Case 2 Wat/tg,1x	1.97	1.55	0.1	0.34	0.16	-0.09	-8.97
Case 3 Wat,2x	1.97	1.19	0.18	0.35	0.07	0.09	8.77
Case 4 Wat 1x	1.97	1.14	0.28	0.34	0.16	0.02	2.35